Supplementary wavelength calibration methods for SALT/RSS spectropolarimetric observations

Justin Cooper

B.Sc. (Hons) *cum laude*

Submitted in fulfillment of the requirements for the degree

Magister Scientiæ

in the Faculty of Natural and Agricultural Sciences

Department of Physics

University of the Free State

South Africa

Date of submission: October 2024

Supervised by: Prof. B. van Soelen, Department of Physics

Abstract

TODO:

- **Done last**
- **Flow from use of SALT and pipeline and basics of its science implementations into why a more streamlined wavelength calibration is an improvement.**
- **Give summary of results.**
- **Aim for a paragraph (~ 600) without going too in-depth into anything specific.**
- **Brian's comment: Abstract should summarize paper. Include results, conclusions, etc.**

Keywords: POLSALT, Polarimetric reductions for SALT, STOPS, Supplementary Tools for POLSALT Spectropolarimetry, SALT, Southern African Large Telescope, RSS, Robert Stobie Spectrograph, IRAF, Image Reduction and Analysis Facility, Python, Wavelength Calibration, Spectropolarimetry, Astrophysics, Astronomy **TODO: Add Keywords (especially for pipeline development and data reduction) → look up the astronomy journal keywords**

Acknowledgements

I hereby acknowledge and express my sincere gratitude to the following parties for their valuable contributions:

- **TODO: Add acknowledgements!**

Contents

Glossary

FITS extensions Extensions used in Flexible Image Transport System (FITS) files to store different types of data.

'BPM' The Bad Pixel Map extension in a FITS file.

'Primary' The Primary extension of a FITS file which contains the file Header.

'SCI' The Science data extension in a FITS file.

'VAR' The Variance data extension in a FITS file.

'WAV' The Wavelength extension in a FITS file.

Johnson-Cousins photometric system A widely-used system of broad-band photometry that uses a set of standard filters to measure the magnitudes of stars and other astronomical objects.

U The ultraviolet filter, typically centered around 3640 Å.

B The blue filter, typically centered around 4420 Å.

V The visual filter, designed to approximate human visual sensitivity and typically centered around 5400 Å.

R The red filter, typically centered around 6580 Å.

I The infrared filter, typically centered around 8060 Å.

List of Acronyms and Symbols

A-DC	Analog-to-Digital Converter
ADC	Atmospheric Dispersion Compensator
Ar	Argon
BAT	Burst Alert Telescope
CCD	Charged-Coupled Device
CLI	Command Line Interface
CMOS	Complementary Metal-Oxide-Semiconductor
CuAr	Copper-Argon
CRR	Cosmic Ray Rejection
EW	Equivalent Width
Fermi LCR	Fermi Light Curve Repository
Fermi-*LAT*	Fermi Large Area Telescope
FITS	Flexible Image Transport System
FORS	Focal Reducer and Low Dispersion Spectrograph
FWHM	Full Width at Half Maximum
GRB	Gamma-ray Burst
GUI	Graphical User Interface
HDU	Header and Data Unit
HEASA	High Energy Astrophysics South Africa
HET	Hobby-Eberly Telescope
HRS	High Resolution Spectrograph
IRAF	*Image Reduction and Analysis Facility*
L+45°	Linear +45° Polarized
L−45°	Linear −45° Polarized
LCP	Left Circularly Polarized
LHP	Linear Horizontally Polarized
LVP	Linear Vertically Polarized
HgAr	Mercury-Argon
Ne	Neon-Argon
NIR	Near Infra-Red
NIRWALS	Near Infra-Red Washburn Labs Spectrograph
POLSALT	*Polarimetric reductions for SALT*
PyPI	Python Package Index
RCP	Right Circularly Polarized
RMS	Root Mean Square
RSS	Robert Stobie Spectrograph

S/N	Signal-to-Noise Ratio
SAAO	South African Astronomical Observatory
SAC	Spherical Aberration Corrector
SALT	Southern African Large Telescope
SALTICAM	SALT Imaging Camera
SED	Spectral Energy Distribution
STOPS	*Supplementary Tools for* POLSALT *Spectropolarimetry*
Swift	Neil Gerhels Swift Observatory
ThAr	Thorium-Argon
UV	Ultraviolet
UVOT	Ultraviolet Optical Telescope
VLT	Very Large Telescope
VPH	Volume Phase Holographic
Xe	Xenon

Chapter 1

Introduction

TODO: Very short intro to Spectroscopy, Polarization, and Spectropolarimetry and their importance in astronomy

TODO: Focus on AGN implications and implementations such as the types of objects and a short history for each type of object, Blazar focus with specification on BL Lacs and FSRQs, the Unified Model, ~~The Blazar sequence~~.
Brian's comment: **Highlight importance of polarimetry for understanding emission and how that plays a role in AGN.**

TODO: Basics of modelling (Different energy/wavelength ranges used and what the models tell us about emission processes/structure) so that Hester's results can be noted for applications of the pipeline.

TODO: Problem Statement, VERY IMPORTANT, roughly a sentence but problem thoroughly fleshed out.

1.1 Outline

The layout of the rest of the thesis is as follows:

Chapter 2 lays a foundation for spectroscopy, polarimetry, and spectropolarimetry as well as the implementation of these principles through instrumentation, focusing specifically on principles as relating to the Southern African Large Telescope (*SALT*) Robert Stobie Spectrograph (RSS). These principles provide an understanding of spectropolarimetric data as well as describe the reduction and calibration processes to be completed for the acquisition of spectropolarimetric results.

Chapter 3 describes the existing *Polarimetric reductions for SALT* (POLSALT) (used for spectropolarimetric reductions) and *Image Reduction and Analysis Facility* (IRAF) (used for wavelength calibrations) software, the developed *Supplementary Tools for POLSALT Spectropolarimetry* (STOPS) software, and provides a general reduction process for spectropolarimetric data. The principles, application, and challenges faced when using

the existing software for spectropolarimetric data reductions are broadly described, with greater emphasis placed on the developed software, STOPS, which was designed to streamline the data reduction process and overcome the limitations of the existing software.

Chapter 4 provides the testing of the developed software and discusses its application within published articles and proceedings. Testing was conducted on a 'per-module' basis aligning with the usage of STOPS.

Chapter 5 concludes the thesis body and notes future work to improve and expand the STOPS software. **TODO: Revise once this chapter is complete**

Finally, the appendices, Appendix A, B, and C, contain a working reduction procedure (referred to in Chapter 3), the STOPS source code, and Proceedings produced from conferences (referred to in Chapter 4), respectively.

Chapter 2

Spectropolarimetry and the SALT RSS

This chapter gives an overview of the basics of spectropolarimetry (§ 2.3), and how it functions, following from the principles of both spectroscopy (§ 2.1) and polarimetry (§ 2.2). Further, it is discussed how these techniques are practically implemented for *SALT* (§ 2.4), using the RSS (§ 2.4.3), and how the spectropolarimetric reduction process is completed (§ 2.4.3).

2.1 Spectroscopy

Spectroscopy originated in its most basic form with Newton's examinations of sunlight through a prism (Newton and Innys, 1730) but came to prominence as a field of scientific study with Wollaston's improvements to the optics elements (Wollaston, 1802), Fraunhofer's use of a diffraction grating instead of a prism (der Wissenschaften, 1824), and Bunsen and Kirchoff's classifications of spectral features to their respective chemical elements (Kirchhoff and Bunsen, 1861).

The simplest spectrometer schematic, as shown in Figure 2.1, consists of incident light collected from the telescope's optics, labelled A, being focused onto a slit, B, and passed through a collimator, C. The collimator collimates the light allowing a dispersion element, D, to disperse the light into its constituent wavelengths. The resultant spectrum is focused by camera optics, E, onto a focal plane, F. Viewing optics are situated at the focal plane in the case of a spectroscope and a detector is situated at the focal plane in the case of a spectrograph.

2.1.1 Telescope Optics

The telescope optics refers simply to all the components of a telescope necessary to acquire a focal point at the spectrometer entrance, labelled B. The focal point in most traditional telescope designs is fixed relative to the telescope and so the spectrometer may be mounted at that point. In cases where the telescope is designed to have a moving focal point relative to the telescope (see Buckley et al., 2006; Cohen, 2009; Ramsey et al., 1998), the spectrometer, or a signal transfer method such as a fibre feed to the spectrometer, must also move along the telescope's focal path.

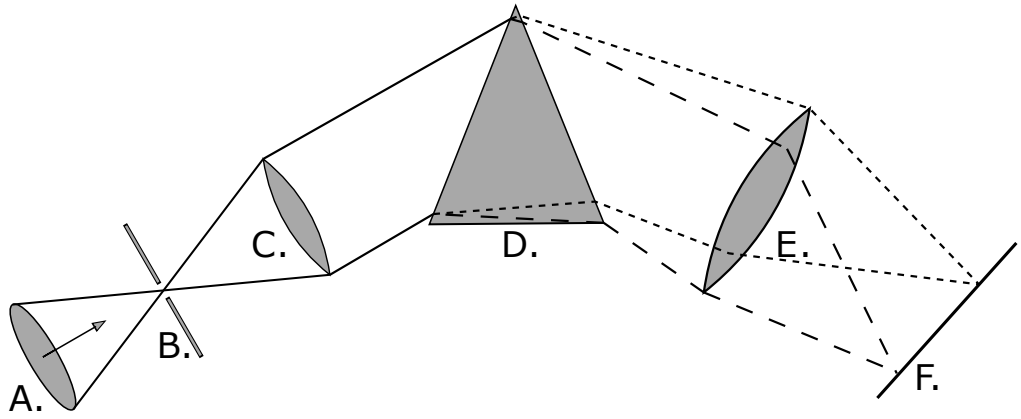

Figure 2.1: Layout depicting the light path through a spectrometer. Diagram adapted from Birney et al. (2006).

2.1.2 Slit

The slit's function is to control the amount of incident light entering a spectrometer and, along with the exposure time of the detector, prevents over-exposures of bright sources on highly sensitive detectors (Tonkin, 2013). If a source is spatially resolvable, or larger than the seeing conditions, the slit additionally acts to spatially limit the source to increase the spectral resolution, resulting in sharper features in the resultant spectrum. Without the slit the spectral resolution would be determined by the projected width of the source on the detector, or the seeing if the source was a star-like point source. Increasing the spectral resolution comes with the trade-off of decreasing the light collected from the source and thus acquiring a less intense resultant spectrum. Multiple spectra may be acquired simultaneously when the slit is positioned such that collinear sources lie along the slit.

The spectrometer is usually situated at the focal point. In cases where this is not feasible due to restrictions, for example restrictions of weight or size, a fibre feed may be situated behind the slit on the telescope. This allows the signal to be routed away from the telescope to a controlled environment with only miniscule losses.

2.1.3 Collimator

The collimators function is to collimate the focused light from the telescope, ensuring that all light rays run parallel before reaching the dispersion element. The focal ratio of the collimator (f_c/D_c, where f refers to the focal length and D refers to the diameter) should ideally match the focal ratio of the telescope (f_T/D_T).

2.1.4 Dispersion Element

Including a dispersion element in the optical path is what defines a spectrometer. As the name suggests, a dispersion element disperses the light incident on it into its constituent wavelengths and produces a spectrum. There are two types of dispersion elements, namely the prism and the diffraction grating, which operate on different principles, as discussed in § 2.1.7.

2.1.5 Camera Optics

The lens functions similarly to that of the telescope's optics but in this case focuses the dispersed light onto a receiver situated at the focal plane. As mentioned previously, an eye piece is fixed to the focal point for a spectroscope while a spectrograph employs a detector.

2.1.6 Detector

The two most prevalent detector types in spectroscopy are the Charged-Coupled Device (CCD) and Complementary Metal-Oxide-Semiconductor (CMOS) detectors. In astronomical spectroscopy however, sources are fainter and exposure times are much longer and so the CCD detectors are by far the preferred detector as their output has a higher-quality and lower-noise when compared to CMOS cameras under the same conditions (Janesick et al., 2006).

The CCD is a detector composed of many thousands of pixels which can store a charge so long as a voltage is maintained across the pixels. Each pixel detects incoming photons using photo-sensitive capacitors through the photoelectric effect and converts the photons to a charge (Buil, 1991). There are also thermal agitation effects which introduce noise to the charge accumulated by a pixel, further discussed in § 2.1.8. Once the exposure is finished the accumulated charge is read column by column, row by row, through an Analog-to-Digital Converter (A-DC) which produces a two-dimensional array of 'counts'.

2.1.7 Dispersion of Light

Light can be broken up into its constituent wavelengths through two different physical phenomena, namely dispersion and diffraction, which dispersive elements use to create spectra. Dispersive prisms and diffractive gratings each have their strengths and weaknesses and a wide spectrum of instruments exist which implement either, or both, concepts. Regardless of the specific element, dispersive elements all have a resolving power, R, and an angular dispersion. Generally, while the angular dispersion is a more involved process to determine, the resolving power of a spectrograph can be measured as:

$$R = \frac{\lambda}{FWHM}\,, \tag{2.1}$$

where λ is the wavelength of an incident monochromatic beam and Full Width at Half Maximum (FWHM) refers to the width of the feature on the detector at half of its maximum intensity.

Prism

The prism operates on the principle that the refractive index of light, n, varies as a function of its wavelength, λ. Prisms were the only dispersive elements available for early spectroscopic studies, but they were not without flaw. The angular dispersion of a prism is given by:

$$\frac{\partial\theta}{\partial\lambda} = \frac{B}{a}\frac{dn}{d\lambda}\,, \tag{2.2}$$

where θ is the angle at which the refracted light differs from the incident light, λ is the wavelength of the incident light, B is the longest distance the beam would travel through

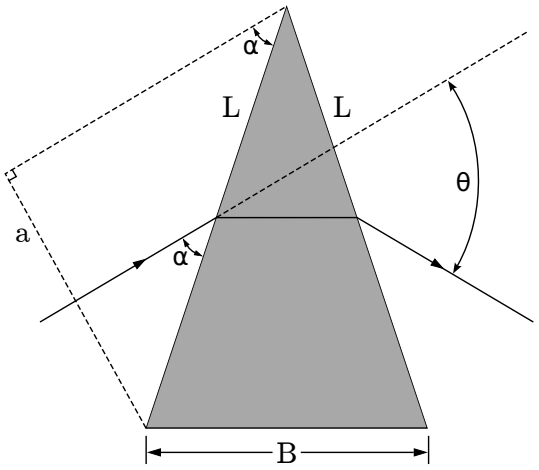

Figure 2.2: Geometry of a prism refracting an incident monochromatic beam at a minimum deviation angle. Diagram adapted from Birney et al. (2006).

the prism. $a = L\sin(\alpha)$ is the maximal beam width that would fit onto a prism with a transmissive surface of length L for a given angle, α, at which a beam would strike the transmissive surface, as shown in Figure 2.2.

The refractive index of a material as a function of its wavelength, $n(\lambda)$, can be approximated by Cauchy's equation:

$$n(\lambda) = A_C + \frac{B_C}{\lambda^2} + \frac{C_C}{\lambda^4} + \dots , \tag{2.3}$$

where A_C, B_C, C_C are the Cauchy coefficients and have known values for certain materials. Cauchy's equation is a much simpler approximation of the refractive index that remains very accurate at visible wavelengths (Jenkins and White, 1976). Taking only the first term of the derivative of the Cauchy equation allows us to approximate the angular dispersion of a prism,

$$\begin{aligned} \frac{\partial\theta}{\partial\lambda} &= -\frac{B}{a}\frac{2B_C}{\lambda^3} \\ &\propto -\lambda^{-3} , \end{aligned} \tag{2.4}$$

which shows that the angular dispersion of a prism is wavelength dependent and furthermore that longer wavelengths are dispersed less than shorter wavelengths (Birney et al., 2006; Hecht, 2017). The dependence of the angular dispersion, $d\theta/d\lambda$, on the wavelength, λ, is crucial for the formation of a spectrum but this cubic, non-linear, relation results in a non-linear spectrum. Since prisms rely on the refractive index of the material they are made of, they have low angular dispersions.

Multiple prisms can be used to increase the angular dispersion but as the dispersion is non-linear it becomes increasingly more difficult to calibrate. The more material and material boundaries the light must pass through, the more its intensity decreases due to attenuation effects and Fresnel losses. Even so, the transmittance of modern prisms for their selected wavelength range is generally very high due to improved manufacturing methods as well as improved transmitting materials.[1]

[1]See manufacturers technical specifications, THORLABS, or Edmund Optics for example.

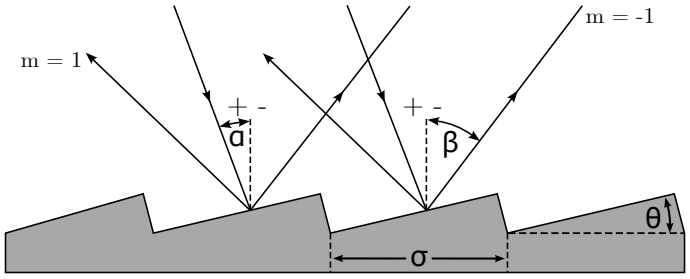

Figure 2.3: Geometry of a reflective blazed grating refracting an incident monochromatic beam. Diagram adapted from Birney et al. (2006).

Diffraction Grating

The alternative dispersing element is a diffraction grating, which operates on the principle that as light interacts with a grating where the groove size is comparable to the light's wavelength, the light is dispersed through constructive and destructive interference. This interference results in multiple diffracted beams m, called orders, either side of a central reflected, or transmitted, beam such that $m \in Z$, where $m = 0$ is the non-dispersed, or reflected, beam.

An example of a reflective blazed grating is illustrated in Figure 2.3. Here a monochromatic beam is incident on the grating at an angle of α from the grating normal. Due to the interference, a diffracted beam of wavelength λ is found at an angle of β from the grating normal. The relation between the incident and diffracted beams is given by the grating equation:

$$m\lambda = \sigma(\sin(\alpha) \pm \sin(\beta)) \,, \tag{2.5}$$

where σ is the groove spacing of the grating and m is the order of the diffracted beam being considered. The grating equation also applies to transmission gratings, though care should be taken for the signs of α and β.

Equation 2.5 also shows that different diffracted beams may share an angle of dispersion for beams not in the same order. The regions of an order that do not overlap with another order are called free spectral ranges. An order-blocking filter may be used to account for the overlaps and increase the free spectral range. A diffraction grating can also be blazed by an angle θ, as illustrated in Figure 2.3. Blazing refers to the fact that the grooves on the surface of the grating are not symmetrical. The asymmetry of the grooves diffracts the incident beam such that most of the beam's intensity is found in a reflected, zeroth order, beam. The wavelength at which a blazed spectrograph is most effective is called the blaze wavelength, λ_b, which is determined by:

$$\begin{aligned} m\lambda_b &= 2\sigma \sin(\theta)\cos(\alpha - \theta) \,, \text{ where} \\ 2\theta &= \alpha + \beta \,. \end{aligned} \tag{2.6}$$

Taking the derivative of Equation 2.5 with respect to λ while keeping α constant, allows us to determine the angular dispersion of a diffraction grating,

$$\frac{\partial\beta}{\partial\lambda} = \frac{m}{\sigma\cos(\beta)} \,. \tag{2.7}$$

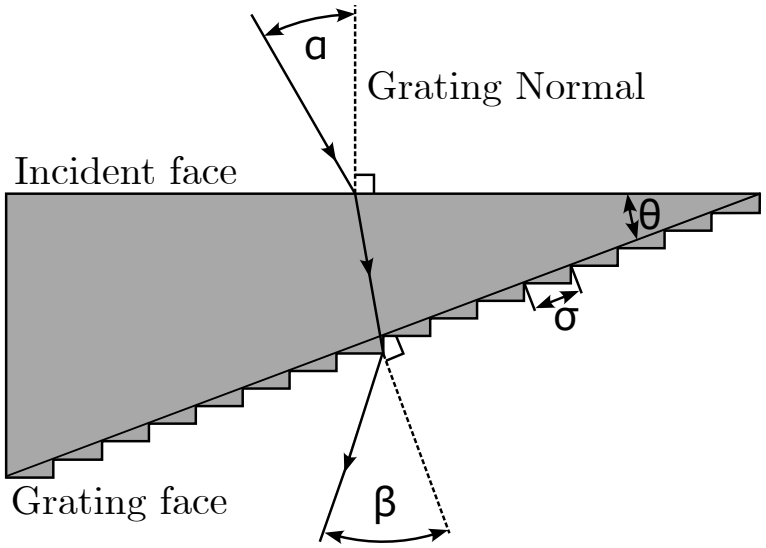

Figure 2.4: Diagram of a grism for an incident monochromatic beam of light and a diffracted beam of order $m = 1$. Diagram adapted from Birney et al. (2006).

Substituting m/σ with the grating equation results in

$$\begin{aligned} \frac{\partial\beta}{\partial\lambda} &= \frac{\sin(\alpha) + \sin(\beta)}{\lambda\cos(\beta)} \\ &\propto \lambda^{-1}\,. \end{aligned} \tag{2.8}$$

Similar to the dispersion of a prism, Equation 2.8 shows that the dispersion of a grating is wavelength dependent, but this dependence is only inversely proportional and thus more uniform across a wavelength range than that of a prism. Furthermore, shorter wavelengths are refracted less than longer wavelengths since there is no negative relation between the angular dispersion and the wavelength (Birney et al., 2006; Hecht, 2017).

Alternate Diffraction Elements

As mentioned before, multiple subgroups exist for both dispersive prisms and diffractive gratings. For prisms, along with the single and multiple prism setups mentioned, there also exists grisms and immersed gratings. A grism (Grating Prism), as shown in Figure 2.4, refers to a transmissive grating etched onto one of the transmissive faces of a prism and allows a single camera to capture both spectroscopic and photometric images without needing to be moved, with and without the grism in the path of the beam of light, respectively. An immersed grating refers to a grism modified such that the transmissive grating is coated with reflective material. The primary source of dispersion for both grisms and immersive gratings is the grating and any aberration effects from the prism are negligible in comparison.

Other types of gratings include the Volume Phase Holographic (VPH) grating as well as the echelle grating. The VPH grating consists of a photoresist, which is a light-sensitive material, sandwiched between two glass substrates. Diffraction is possible since the photoresist's refractive index varies near-sinusoidally perpendicularly to the gratings lines, as seen in Figure 2.5. This allows for sharper diffraction orders and low stray light scattering as compared to more traditional gratings but since blazing is not possible the

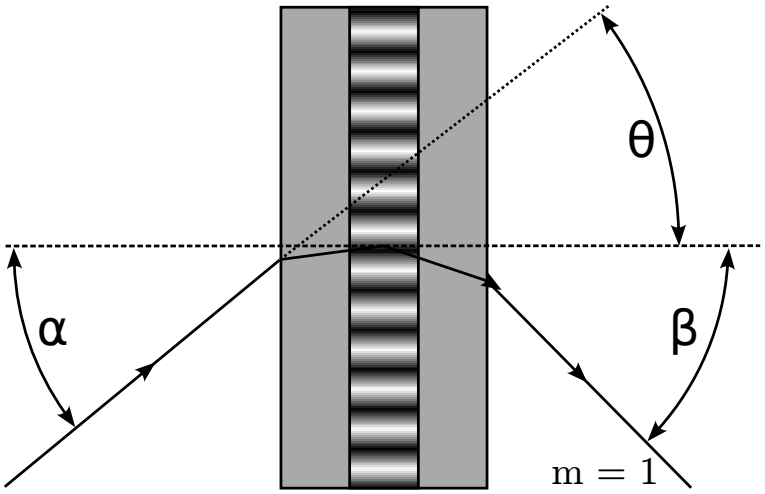

Figure 2.5: Diagram of a VPH grating for an incident monochromatic beam of light. Diagram adapted from Birney et al. (2006).

efficiency is decreased. An echelle grating refers to a diffraction grating with higher groove spacing which is optimized for use at high orders. The high order of the diffracted beam allows for greater angular dispersion which is most useful when combined with another dispersion element to cross-disperse a spectrum, resulting in a high resolution spectrum.

2.1.8 Detector and Spectroscopic Calibrations

Acquiring a spectrum from observations is more involved than simply reading out the data recorded on the CCD. A raw science image, which is the raw counts of the observed source read from the CCD with no calibrations applied, has on it a combination of useful science data as well as noise. The noise is a combination of random noise introduced through statistical processes and systematic noise introduced through the instrumentation and the observation conditions the source was observed under. This noise causes an uncertainty in the useful data and can be minimized, predominantly by calibrating for the systematic noise, but never fully removed (Howell, 2006).

The dominant source of noise in a raw image is detector noise. CCDs are manufactured to have a small base charge in each pixel, called the 'bias' current which allows the readout noise, a type of random noise, to better be sampled. There is also an unintentional additional charge which is linearly proportional to the exposure time and originates from thermal agitation of the CCD material, called the 'dark' current. The dark current can be minimized and possibly ignored if the CCD is adequately cooled. These types of noise add to the charge held by a pixel and are thus considered additive.

The CCD is not a perfect detector and the efficiency of it and the optics of the telescope also contribute noise to the image. The efficiency of a CCD is referred to as the Quantum Efficiency, and it is a measure of what percentage of light striking the detector is actually recorded and converted to a charge. The efficiency of the CCD and telescope optics is also wavelength dependent and so the noise that results from them is more complex than that of additive noise. This type of noise is referred to as multiplicative noise.

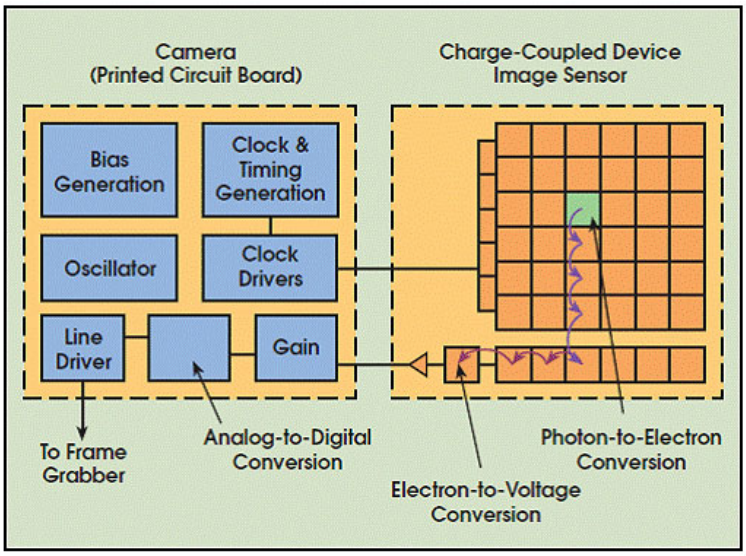

Figure 2.6: Diagram of the inner logic of a CCD. Figure adapted from Litwiller (2001).

Additive noise, such as bias and dark currents, is inherent to CCD images, and as such needs to be subtracted out first when performing calibrations. Bias currents can be found by taking a bias image or by adding an overscan region to each image. A bias image is an image where the charges on the CCD are reset and then immediately read off without exposing anything on the detector, effectively taking an image with zero exposure time. Alternatively, to save time during an observational run, overscan regions may be added to the images. An overscan region refers to adding a few cycles to the readout of each column of the CCD such that the base current is read out and appended to each image.

Dark currents can be found by taking an image with nothing exposed onto the detector for a certain exposure time. This resultant dark image can then be scaled to the science images exposure time since the dark current should be linearly proportional to exposure time. When the detector is capable of being held at precise temperatures, dark images may be taken over multiple hours during the day to produce a high quality master dark image that may then be scaled and subtracted from all subsequent images.

Next, multiplicative noise, such as a CCD's pixel-to-pixel response, should be accounted for. This pixel-to-pixel response should be uniform across the image and to achieve this an average response may be divided out. The average response is referred to as a 'flat' image or flat-field and may be acquired by observing a uniformly illuminated surface to determine the pixel-to-pixel response.

Dome flats are images taken of a relatively flat surface, usually the inside of a telescopes dome, and are used in both photometry and spectroscopy. The surface is uniformly and indirectly illuminated by a projector lamp, ideal for flat-field images. Alternate flat-fielding methods, such as night sky and twilight flats, are available but are suited solely for photometry.

Night sky flats are produced from science images containing mostly sky. The science images are combined using the 'mode' statistic which removes any celestial objects at the cost of a low Signal-to-Noise Ratio (S/N) flat-field.

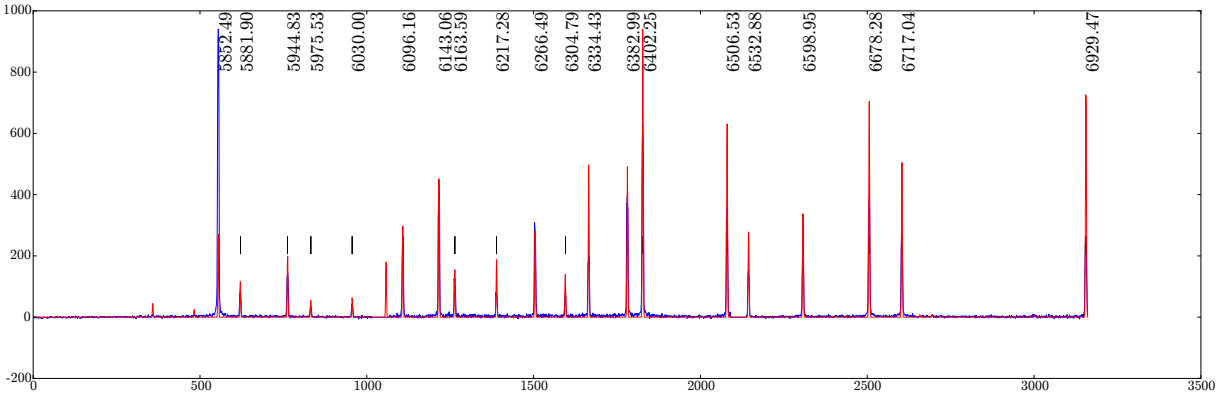

Figure 2.7: Example of an arc spectrum for NeAr taken with *SALT*'s RSS using the PG1800 grating at a grating angle of 34.625°, an articulation angle of 69.258°, and covering a wavelength range of $\sim 5600 - 6900$ Å. Plot adapted from *SALT*'s published Longslit Line Atlases, (2023).[2]

Twilight flats are produced from images of the twilight (or dawn) sky. They are taken when the Sun has just set, in the opposite direction, at $\sim 20°$ from zenith and provide a better S/N at the cost of careful timing of the images.

A flat-field must be normalized before being used to correct any science images since it only acts to account for the pixel-to-pixel response and not for the additive errors. A normalized spectroscopic flat image, $F^n_\lambda(x, y)$, can be calculated as:

$$F^n_\lambda(x,y) = \frac{F_\lambda(x,y) - B(x,y) - (\frac{t_S}{t_D})D(x,y)}{\text{med}_{lp}(F_\lambda(x,y) - B(x,y) - (\frac{t_S}{t_D})D(x,y))}\,, \tag{2.9}$$

where $F_\lambda(x, y)$ is the non-corrected flat image, $B(x, y)$ is the bias image, $D(x, y)$ is the dark image which is scaled by the exposure time of the science image, t_S, and the dark image, t_D. med_{lp} is a low-pass median filter which smoothes out any rapid changes in the pixel-to-pixel response, removing the illumination contribution.

The calibrated science image, $S^*_\lambda(x, y)$, which accounts for the bias and dark currents as well as the flat fielding can then be calculated as:

$$S^*_\lambda(x,y) = \frac{S_\lambda(x,y) - B(x,y) - (\frac{t_S}{t_D})D(x,y)}{F^n_\lambda(x,y)}\,. \tag{2.10}$$

When multichannel CCDs are used, which consist of multiple CCDs or a CCD with multiple output amplifiers, additional calibrations, specifically cross-talk corrections and mosaicking, are required. Cross-talk noise refers to contamination that occurs during readout in one channel from another channel with a high signal and occurs because the signals can not be completely isolated from one another. Cross-talk corrections therefore account for this signal contamination between channels being read out at the same time (Freyhammer et al., 2001). Mosaicking is necessary for multichannel CCDs since the digitized signal read out from the detector has no reference of the physical location of the pixel it was detected at. Mosaicking, therefore, correctly orients the data acquired from a multichannel detector so that a single correctly oriented image is produced.

[2] NeAr plot sourced from https://astronomers.salt.ac.za/data/salt-longslit-line-atlas/

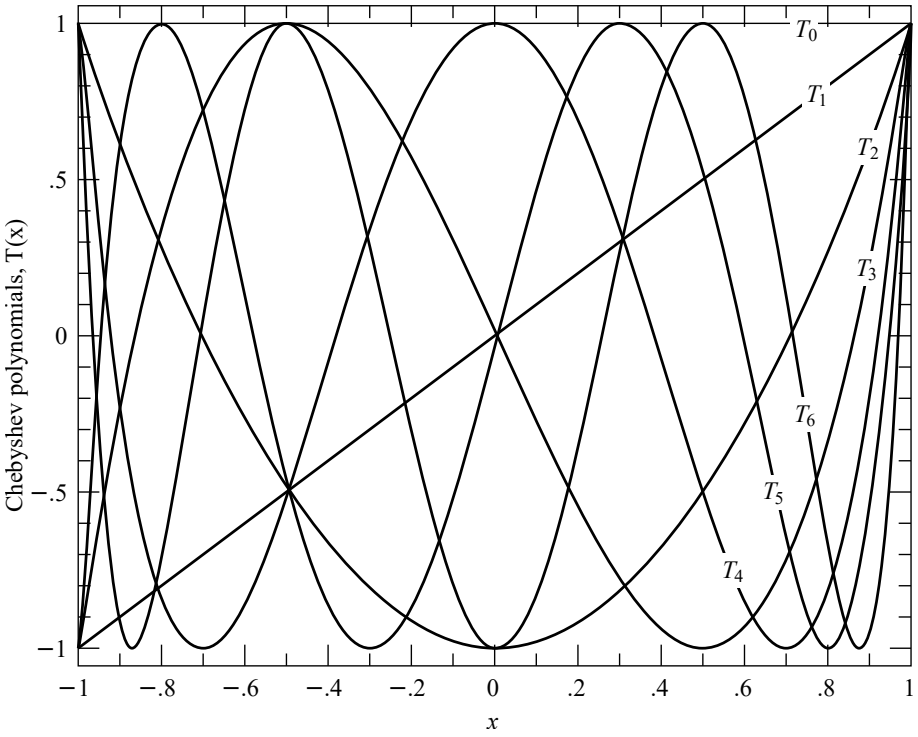

Figure 2.8: The first seven Chebyshev polynomials (T_0 through T_6) as defined by Equation 2.12 over the region $[-1, 1]$ for which they are orthogonal. Plot adapted from (Press et al., 2007) (2023)[3]

Wavelength Calibration

Finally, since the dispersion element breaks the incident light into its constituent wavelengths non-linearly (§ 2.1.7), the relation between the pixel on a detector and the wavelength of the light incident on it is unknown. Ideally, the spectrometer's optics would be modelled to produce a reliable pixel to wavelength calibration (see E.g. Liu and Hennelly, 2022), but this becomes increasingly more difficult for spectrometers with complex, non-sedentary, optical paths.

Alternatively, a source with well-defined spectral features, with said features evenly populating the wavelength region of interest, such as in Figure 2.7 may be observed. The observed frame is commonly referred to as an 'arc' frame, after the arc-lamps used to acquire the spectra, and should be observed alongside the science frames over the course of an observation run.

It is important that the arc frame is observed at the same observing conditions and parameters as the science frames since the optical path will vary over the course of an observing run and for different observing parameters, invalidating previously acquired arc frames. The wavelength calibrations then consist of defining a two-dimensional pixel-to-wavelength conversion function from the arc frame which may later be applied to calibrate the science frames. The two most common approximations for wavelength calibrations are the Chebyshev and Legendre polynomial approximations.

[3]Excellent resources on Chebyshev and Legendre polynomials are available digitally at www.numerical.recipes/book.

Chebyshev Polynomials The Chebyshev polynomials are defined explicitly as:

$$T_n(x) = \cos(n \cos^{-1}(x)) \,, \tag{2.11}$$

or recursively as:

$$\begin{aligned} T_0(x) &= 1 \,, \\ T_1(x) &= x \,, \text{ and} \\ T_{n+1}(x) &= 2xT_n(x) - T_{n-1}(x) \,, \text{ for } n \geq 1 \,, \end{aligned} \tag{2.12}$$

where T is a Chebyshev polynomial of order n.[4] An important property of Chebyshev polynomials is that they are orthogonal polynomials. This means that the inner product of any two differing Chebyshev polynomials, $T_i(x)$ and $T_j(x)$, over the range $[-1, 1]$ is zero, as shown by:

$$\int_{-1}^{1} T_i(x) T_j(x) \frac{1}{\sqrt{1-x^2}} \, dx = \begin{cases} 0, & i \neq j \\ \pi/2, & i = j \neq 0 \\ \pi, & i = j = 0 \end{cases} , \tag{2.13}$$

where $1/\sqrt{1-x^2}$ is the weighting factor for Chebyshev polynomials. This property is important because it means that the coefficients in the Chebyshev polynomial expansion are independent of one another, allowing for a unique solution when approximating an unknown function (Arfken and Weber, 1999; Press et al., 2007). A Chebyshev approximation of an unknown wavelength calibration function is given by:

$$f(x) \approx \sum_{i=0}^{N} c_i T_i(u) \,, \text{ or} \tag{2.14}$$

$$F(x, y) \approx \sum_{i=0}^{N} \sum_{j=0}^{M} c_{ij} T_i(u) T_j(v) \,, \tag{2.15}$$

for a one- or a two-dimensional wavelength surface function, respectively. Here N and M are the desired x and y orders, and c_i and c_{ij} are the Chebyshev polynomial coefficients (Florinsky and Pankratov, 2015; Leng, 1997). Since the orthogonality property of the Chebyshev polynomials only holds true over the range $[-1, 1]$, the $(x, y) \in ([0, a], [0, b])$ pixel coordinates must be remapped to $u, v \in [-1, 1]$ following the relation:

$$(u, v) = \frac{2(x, y) - a - b}{b - a} \,. \tag{2.16}$$

The Chebyshev polynomials are more suited for wavelength calibrations than standard polynomials since they are orthogonal and have minima and maxima located at $[-1, 1]$, as seen in Figure 2.8. This means that the Chebyshev approximation is exact when $x = x_n$, where x_n are the positions of the $n - 1$ x-intercepts of $T_N(x)$. These properties greatly minimize the error in the Chebyshev approximation, even at lower orders (Arfken and Weber, 1999).

[4] Chebyshev polynomials are denoted T as a hold-over from the alternate spelling of 'Tchebycheff'.

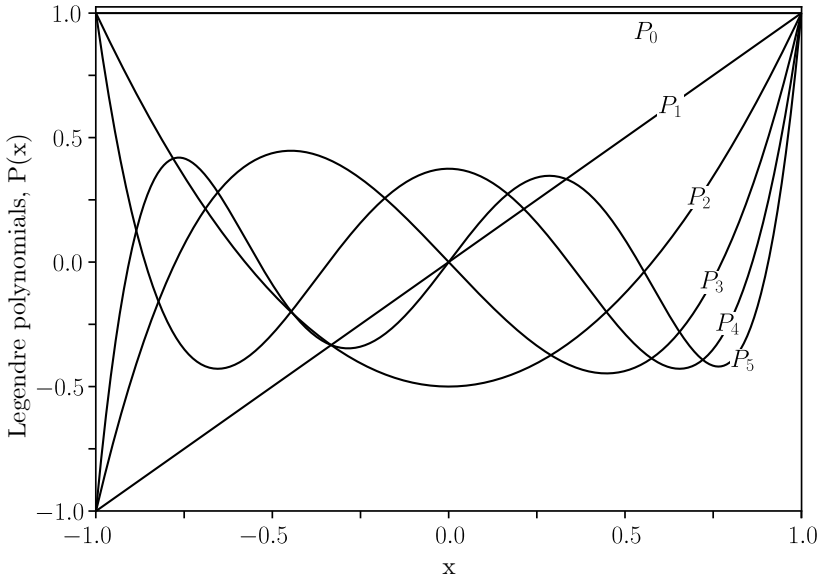

Figure 2.9: The first six Legendre polynomials (P_0 through P_5) as defined by Equation 2.20 over the region $[-1, 1]$ for which they are orthogonal. Plot adapted from Geek3, CC BY-SA 3.0, via Wikimedia Commons (2023).

Legendre Polynomials Similar to the Chebyshev polynomials, the Legendre polynomials may be defined explicitly as:

$$P_n(x) = \frac{1}{2^n n!} \frac{d^n}{dx^n}(x^2 - 1)^n \,, \tag{2.17}$$

or recursively as:

$$\begin{aligned} P_0(x) &= 1 \,, \\ P_1(x) &= x \,, \text{ and} \\ (n+1)P_{n+1}(x) &= (2n+1)xP_n(x) - nP_{n-1}(x) \,, \text{ for } n \geq 1 \,, \end{aligned} \tag{2.18}$$

where P is a Legendre polynomial of order n. Legendre polynomials also hold the property of orthogonality. This means that the inner product of any two differing Legendre polynomials, $P_i(x)$ and $P_j(x)$, over the range $[-1, 1]$ is zero, as shown by:

$$\int_{-1}^{1} P_i(x)P_j(x)\,dx = \begin{cases} 0, & i \neq j \\ \frac{2}{2n+1}, & i = j \end{cases} \,, \tag{2.19}$$

where a weight of 1 is the weighting factor for Legendre polynomials (Dahlquist and Björck, 2003; Press et al., 2007). A Legendre approximation of an unknown wavelength calibration function is given by:

$$f(x) \approx \sum_{n=0}^{N} a_n P_n(u) \,, \text{ or} \tag{2.20}$$

$$F(x, y) \approx \sum_{i=0}^{N} \sum_{j=0}^{M} a_{ij} P_i(u) P_j(v) \,, \tag{2.21}$$

for a one-dimensional wavelength function or a two-dimensional surface function, respectively. Here N and M are the desired x and y orders, u and v are the same mapping variable as in Equation 2.16, and a_{ij} are the Legendre polynomial coefficients.

Legendre polynomials benefit from having the orthogonality condition with no weight necessary ($w = 1$) which makes their coefficients computationally easier to compute but increases the error in a Legendre approximation when compared to that of the error in a Chebyshev approximation for functions of the same order, N (Ismail, 2005).

Regardless of which method of polynomial approximation is chosen, the polynomials are fit by varying the relevant coefficients using the least squares method. The resultant minimized function may then be used to convert the science frames from an (x-pixel, y-pixel) coordinate system to a (λ, y-pixel) coordinate system.

2.2 Polarimetry

Both Huygens and Newton came to the conclusion that light demonstrates transversal properties (Huygens, 1690; Newton and Innys, 1730), which was later further investigated and coined as 'polarization' by Malus (Malus, 1809). Malus also investigated the polarization effects of multiple materials including some of which were birefringent, such as optical calcite, which he referred to as Iceland spar after Bartholinus' investigations of the material (Bartholinus, 1670).

Fresnel built on Malus' work showing that two beams of light, polarized at a right angle to one another, do not interfere, conclusively proving that light is transversal in nature, opposing the widely accepted longitudinal nature of light due to the prevalent belief in the ether. He later went on to correctly describe how polarized light is reflected and refracted at the surface of optical dielectric interfaces, without knowledge of the electromagnetic nature of light. Fresnel's equations for the reflectance and transmittance, R and T, are defined as:

$$\begin{aligned} R_s &= \left| \frac{Z_2 \cos\theta_i - Z_1 \cos\theta_t}{Z_2 \cos\theta_i + Z_1 \cos\theta_t} \right|^2 , \\ R_p &= \left| \frac{Z_2 \cos\theta_t - Z_1 \cos\theta_i}{Z_2 \cos\theta_t + Z_1 \cos\theta_i} \right|^2 , \\ T_s &= 1 - R_s \,, \text{ and} \\ T_p &= 1 - R_p \,, \end{aligned} \tag{2.22}$$

where s and p are the two polarized components of light perpendicular to one another, Z_1 and Z_2 are the impedance of the two media, and θ_i, θ_t, and θ_r are the angles of incidence, transmission, and reflection, respectively (Fresnel, 1870).

Nicol was the first to create a polarizer, aptly named the Nicol prism, where the incident light is split into its two perpendicular polarization components, namely the ordinary and extraordinary beams. Faraday discovered the phenomenon where the polarization plane of light is rotated when under the influence of a magnetic field, known as the Faraday effect. Brewster calculated the angle of incidence, $\theta_B = \arctan n_2/n_1$, at which incident polarized light is perfectly transmitted through a transparent surface, with refractive indexes of n_1 and n_2, while non-polarized incident light is perfectly polarized when reflected and partially polarized when refracted.

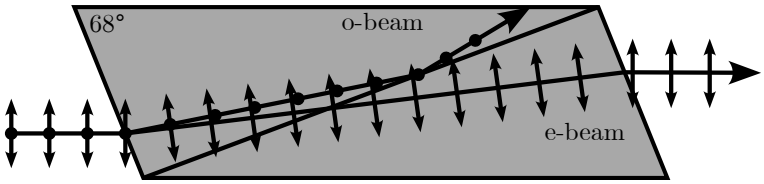

Figure 2.10: Diagram of a Nicol prism for incident non-polarized light. Diagram adapted from Fred the Oyster, CC BY-SA 4.0, via Wikimedia Commons (2023).

Stokes' work created the first consistent description of polarization and gave us the Stokes parameters which describe an operational approach to measuring polarization (discussed further in § 2.2.1) (Stokes, 1852). Hale was the first to apply polarization to astronomical observations, using a Fresnel rhomb and Nicol prism as a quarter-wave plate and polarizer, respectively (Hale, 1908, 1979). Wollaston also created a prism, similarly named the Wollaston prism, which allowed simultaneous observation of the ordinary and extraordinary beams due to the smaller deviation angle (Wollaston, 1802). Finally, Chandrasekhar's work furthered our understanding of astrophysical polarimetry by explaining the origin of polarization observed in starlight as well as mathematically modeling the polarization of rotating stars, which came to be named Chandrasekhar polarization (Chandrasekhar, 1950).

2.2.1 Polarization

Maxwell's equations for an electromagnetic field propagating through a vacuum are given as:

$$\begin{aligned} \nabla \cdot \mathbf{E} &= 0\,, \\ \nabla \cdot \mathbf{B} &= 0\,, \\ \nabla \times \mathbf{E} &= -\frac{1}{c}\frac{\partial \mathbf{B}}{\partial t}\,, \text{ and} \\ \nabla \times \mathbf{B} &= \frac{1}{c}\frac{\partial \mathbf{E}}{\partial t}\,, \end{aligned} \tag{2.23}$$

where $\mathbf{E}$ and $\mathbf{B}$ are the electric and magnetic field vectors, and c is the speed of light. In a right-handed (x, y, z) coordinate system, a non-trivial solution of an electromagnetic wave following Maxwell's Equations propagating along the z-axis, towards a hypothetical observer, is described by:

$$\begin{aligned} \mathbf{E} &= E_x \cos(kz - \omega t + \Phi_x)\hat{\boldsymbol{x}} + E_y \cos(kz - \omega t + \Phi_y)\hat{\boldsymbol{y}}\,, \text{ and} \\ \mathbf{B} &= \frac{1}{c}E_y \cos(kz - \omega t + \Phi_y)\hat{\boldsymbol{x}} + \frac{1}{c}E_x \cos(kz - \omega t + \Phi_x)\hat{\boldsymbol{y}}\,, \end{aligned} \tag{2.24}$$

where E_x, E_y, Φ_x, and Φ_y are all parameters describing the amplitude and phase of the electric field vector in the (x, y) plane, and with the magnetic field vector proportional and perpendicular to the electric field vector (Griffiths, 2005).

Considering only the electric field component and rewriting Equation 2.24 using complex values allows us to simplify the form of the solution to:

$$\mathbf{E} = \Re(\mathbf{E}_0 e^{-i\omega t})\,, \tag{2.25}$$

where we only consider the real part of the equation, and where $\mathbf{E}_0$ is defined as:

$$\mathbf{E}_0 = E_x e^{i\Phi_x}\hat{\boldsymbol{x}} + E_y e^{i\Phi_y}\hat{\boldsymbol{y}}\,, \tag{2.26}$$

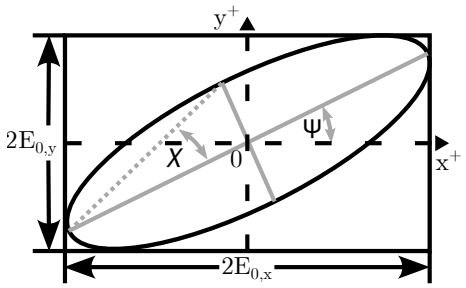

Figure 2.11: The polarization ellipse for an electric field vector propagating through free space. Diagram adapted from Inductiveload, PDM 1.0, via Wikimedia Commons (2023).

and is referred to as the polarization vector since it neatly contains the parameters responsible for the polarization properties (Degl'Innocenti, 2014).

For an electric field vector with oscillations in some combination of the x and y axes, the tip of the vector sweeps out an ellipse, as depicted in Figure 2.11. This ellipse is referred to as the polarization ellipse and has the form:

$$\left(\frac{\mathbf{E}_x}{\mathbf{E}_{0,x}}\right)^2 + \left(\frac{\mathbf{E}_y}{\mathbf{E}_{0,y}}\right)^2 - \frac{2\mathbf{E}_x\mathbf{E}_y}{\mathbf{E}_{0,x}\mathbf{E}_{0,y}}\cos\Phi = \sin^2\Phi\,, \tag{2.27}$$

where $\Phi = \Phi_x - \Phi_y$ is the phase difference between the x and y phase parameters. The degree of polarization for the polarization ellipse is related to the eccentricity of the ellipse and the angle at which it is rotated relates to the polarization angle. Since $\mathbf{E}_{0,x}$, $\mathbf{E}_{0,y}$, Φ_x, and Φ_y describe the wave, the polarization ellipse that results from these parameters is fixed as the wave continues to propagate.

Since observations consist of images taken over a desired exposure time, time averaging of Equation 2.27 over the exposure time is necessary. Given the periodical nature and high frequencies of the fields, the time averaging may be found over a single oscillation using:

$$\langle \mathbf{E}_i\mathbf{E}_j\rangle = \lim_{dt\to\infty}\frac{1}{T}\int_0^T \mathbf{E}_i\mathbf{E}_j\,dt\,, \quad \text{for } i,j \in (x,y)\,, \tag{2.28}$$

where T is the total averaging time over the electric field vectors $\mathbf{E}_i$ and $\mathbf{E}_j$ (Collett, 2005). Applying the time averaging to Equation 2.27 and simplifying results in:

$$(E_{0x}^2 + E_{0y}^2)^2 - (E_{0x}^2 - E_{0y}^2)^2 - (2E_xE_y\cos\Phi)^2 = (2E_xE_y\sin\Phi)^2\,. \tag{2.29}$$

The expressions inside the parentheses can be found through observation and may also be represented as:

$$\mathbf{S} = \begin{pmatrix} S_0 \\ S_1 \\ S_2 \\ S_3 \end{pmatrix} = \begin{pmatrix} I \\ Q \\ U \\ V \end{pmatrix} = \begin{pmatrix} E_{0x}^2 + E_{0y}^2 \\ E_{0x}^2 - E_{0y}^2 \\ 2E_{0x}E_{0y}\cos\Phi \\ 2E_{0x}E_{0y}\sin\Phi \end{pmatrix}\,, \tag{2.30}$$

where S_0 to S_3 are referred to as the Stokes (polarization) parameters. The parameters describe the: S_0, total intensity (often normalized to 1); S_1, ratio of the Linear Horizontally Polarized (LHP) to Linear Vertically Polarized (LVP) light; S_2, ratio of the Linear $+45°$ Polarized (L$+45°$) to Linear $-45°$ Polarized (L$-45°$) light; and S_3, ratio of the Right Circularly Polarized (RCP) (clockwise) to Left Circularly Polarized (LCP)

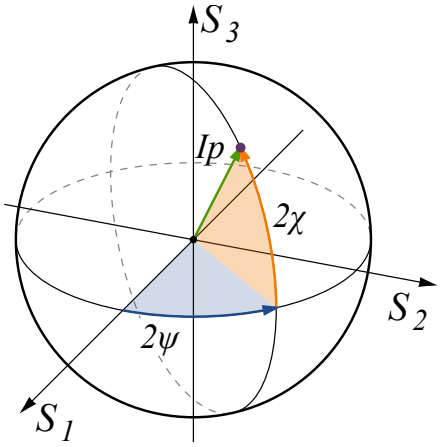

Figure 2.12: The Poincaré sphere describing the polarization properties of a wave-packet propagating through free space. Diagram adapted from Inductiveload, PDM 1.0, via Wikimedia Commons (2023).

(counter-clockwise) light. When the intensity is normalized, the Stokes parameters range from 1 to -1, based on the dominating component of the parameter (Chandrasekhar, 1950; Stokes, 1852).

From Equation 2.29 and 2.30, the polarization parameters are related by:

$$I^2 = Q^2 + U^2 + V^2 \,, \tag{2.31}$$

for entirely polarized light. Only beams of completely polarized light could be accounted for before Stokes' work on polarization. Using the Stokes parameters, we can now account for partially polarized light such that:

$$I^2 \geq Q^2 + U^2 + V^2 \,, \tag{2.32}$$

where $I, Q, U,$ and V are the normalized polarization parameters, often symbolized as

$$\bar{Q} = \frac{Q}{I} \,, \quad \bar{U} = \frac{U}{I} \,, \quad \text{and} \quad \bar{V} = \frac{V}{I} \,. \tag{2.33}$$

Similar to the polarization ellipse, the Stokes parameters may be depicted using the Poincaré sphere in spherical coordinates $(IP, 2\Psi, 2\chi)$, such that:

$$\begin{aligned} I &= S_0 \,, \\ P &= \frac{\sqrt{S_1^2 + S_2^2 + S_3^2}}{S_0} \,, \text{ for } 0 \leq P \leq 1 \,, \\ 2\Psi &= \arctan \frac{S_3}{\sqrt{S_1^2 + S_2^2}} \,, \text{ and} \\ 2\chi &= \arctan \frac{S_2}{S_1} \,, \end{aligned} \tag{2.34}$$

where I denotes the total intensity, P denotes the degree of polarization, or the ratio of polarized to non-polarized light in the wave-packet, χ denotes the polarization angle, and Ψ denotes the ellipticity angle of the polarization ellipse.

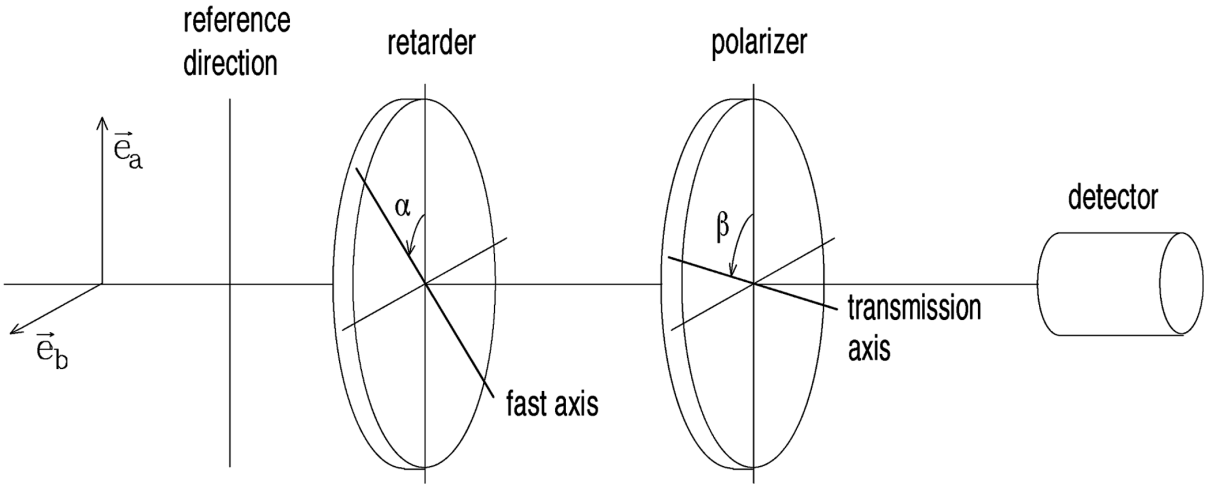

Figure 2.13: A diagram of an ideal polarimeter. Diagram adapted from Degl'Innocenti and Landolfi (2004).

2.2.2 Polarization Measurement

Except for polarimetry in the radio-wavelength regime, the polarization of a beam can not be directly measured. The polarization properties may, however, be recovered from the beam through the manipulation of the four parameters given in Equation 2.24. This so-called manipulation is achieved by passing the beam through optical elements which vary the beam for differing amplitudes and phases. These matrix operations may be represented by their corresponding Mueller matrices.

For ideal components, the resultant beam $\mathbf{S}'$ after passing through an optical element is given by $\mathbf{S}' = \mathbf{MS}$, where $\mathbf{S}$ is the beam incident on the optical element and $\mathbf{M}$ represents the 4×4 Mueller matrix representing the optical element. Mueller matrices are especially useful when dealing with paths through optical elements as they observe the 'train' property (Priebe, 1969). This means that an incoming beam $\mathbf{S}$ passing, in order, through elements with known Mueller matrices $(\mathbf{M}_0, \ldots, \mathbf{M}_N)$ results in an outgoing beam $\mathbf{S}'$ such that:

$$\mathbf{S}' = \mathbf{M}_N \ldots \mathbf{M}_0 \mathbf{S}\,. \tag{2.35}$$

Some Mueller Matrices are given below with angles related to those in Figure 2.13, measured counter-clockwise in a right-handed coordinate system.

General Rotation The Mueller matrix for coordinate space rotations about the origin by an angle θ,

$$\mathbf{R}(\theta) = \begin{bmatrix} 1 & 0 & 0 & 0 \\ 0 & \cos 2\theta & \sin 2\theta & 0 \\ 0 & -\sin 2\theta & \cos 2\theta & 0 \\ 0 & 0 & 0 & 1 \end{bmatrix}\,. \tag{2.36}$$

General Linear Retardance The Mueller matrix for retardance where α is the angle between the incoming vector and fast axis, and δ is the retardance introduced by the retarder,

$$\mathbf{W}(\alpha,\delta) = \begin{bmatrix} 1 & 0 & 0 & 0 \\ 0 & \cos^2 2\alpha + \sin^2 2\alpha \cos\delta & \cos 2\alpha \sin 2\alpha(1-\cos\delta) & \sin 2\alpha \sin\delta \\ 0 & \cos 2\alpha \sin 2\alpha(1-\cos\delta) & \cos^2 2\alpha \cos\delta + \sin^2 2\alpha & -\cos 2\alpha \sin\delta \\ 0 & -\sin 2\alpha \sin\delta & \cos 2\alpha \sin\delta & \cos\delta \end{bmatrix}. \quad (2.37)$$

The retarder is often referred to by this retardance, e.g. if the retardance is $\delta = \pi$ or $\pi/2$, the retarder is referred to as a half- or quarter-wave plate, respectively.

General Linear Polarization The Mueller matrix for linear polarization where β is the angle between the incoming vector and transmission axis,

$$\mathbf{P}(\beta) = \frac{1}{2}\begin{bmatrix} 1 & \cos 2\beta & \sin 2\beta & 0 \\ \cos 2\beta & \cos^2 2\beta & \cos 2\beta \sin 2\beta & 0 \\ \sin 2\beta & \sin 2\beta \cos 2\beta & \sin^2 2\beta & 0 \\ 0 & 0 & 0 & 0 \end{bmatrix}. \quad (2.38)$$

These matrices in combination with Equation 2.35 allow us to describe how the incoming Stokes parameters would change when passing through the various optical elements. For a setup similar to Figure 2.13, the detected Stokes parameters can be described by:

$$\begin{aligned} S'(\alpha,\beta,\gamma) \propto \frac{1}{2}\{ & I + [Q\cos 2\alpha + U \sin 2\alpha]\cos(2\beta - 2\alpha) \\ & - [Q \sin 2\alpha + U \cos 2\alpha]\sin(2\beta - 2\alpha)\cos\gamma \\ & + V \sin(2\beta - 2\alpha)\sin\gamma\}, \end{aligned} \quad (2.39)$$

where the retandance angle, α, polarization angle, β, for a wave plate with a relative phase difference, γ, may be varied to acquire a system of equations that can be solved to retrieve the Stokes polarization parameters (Bagnulo et al., 2009).

Several or more frames taken under differing configurations may be used to reduce a system of equations to extract all four Stokes polarization parameters, but it is possible to extract the I, Q and U polarization parameters using only four frames, or two dual-beam frames, for well-chosen configurations and assuming ideal components. This ideal configuration varies the retarder angle such that $\Delta\alpha = \pi/8$ while keeping the polarizer stationary. More frames for additional retarder angles are advisable and often necessary, however, as they correct for any differences in sensitivity, such as may arise in a polarized flat field and which is further discussed in § 2.2.3 (Patat and Romaniello, 2006). From Equation 2.39 we see that the linear retarder element is the driving element of a polarizer as the first three Stokes parameters (S_{0-2}, or I, Q, and U) may be found by changing only the angle of retardance, α.

Wave Plates Wave plates, also commonly referred to as retarders, are generally made from optically transparent birefringent crystals. A wave plate has a fast and slow axis, which are perpendicular to one another and both perpendicular to an incident beam. Due to the birefringence of the wave plate medium, the phase velocity of the beam polarized

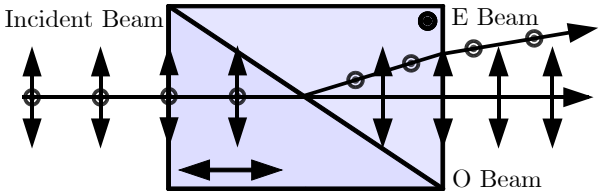

Figure 2.14: Diagram of a Rochon prism. Included in the diagram are the optical axes of the differing sections of the birefringent material as well as polarizing directions of the incident beam, denoted using the ↔ and ⊙ symbols, for the *O*- and *E*-beams, respectively. Figure adapted from ChrisHodgesUK, CC BY-SA 3.0, via Wikimedia Commons (2023).

parallel to the fast axis, namely the extraordinary beam, slightly increases while that of the beam polarized parallel to the slow axis, namely the ordinary beam, remains unaffected. This difference in the perpendicular component's phase velocities introduces a relative phase difference between the two beams, γ, which is given by:

$$\gamma = \frac{2\pi\Delta n L}{\lambda_0} \tag{2.40}$$

where Δn and L refer to the birefringence and thickness of the wave plate medium, respectively, and λ_0 refers to the vacuum wavelength of the beam (Hecht, 2017).

This relative phase difference determines the name of the wave plate, such that the $\gamma = m(\pi/2)$ and $\gamma = m(\pi/4)$ phase differences, for $m \in Z^+$, refer to the half- and quarter-wave plates (which are the most common wave plate phases), respectively. Phase differences with an integer multiple of one another relate to the same phase difference and are referred to as multiple-order wave plates, while wave plates with a phase difference less than an integer multiple are referred to as zero-order wave plates. Several multiple-order wave plates can be combined by alternatively aligning the fast axis of one to the slow axis of another to create a compound zero-order wave plate (Hale and Day, 1988).

Polarizers Polarizers are typically made from two prisms, of a birefringent material, cemented together with an optically transparent adhesive. The actual effect of separating the perpendicular polarization components is achieved using varying effects, namely through:

- absorption of one of the polarized components, such as in Polaroid polarizing filters,
- total internal reflection of a single polarized component, such as in a Nicol prism (Figure 2.10),
- Refraction of a single polarized component, such as in a Rochon prism (Figure 2.14), or
- Refraction of both polarization components in differing directions, such as in a Wollaston prism (Figure 2.15).

Wollaston Prisms The Wollaston prism consists of two right-angle prisms consisting of a birefringent monoaxial material, cemented together with an optically transparent adhesive along their hypotenuses with their optical axes orthogonal, as seen in Figure 2.15. The Wollaston prism is a common optical polarizing element in astrophysical polarimetry which separates an incident beam into two linearly polarized *O*- and *E*-beams, orthogonal to one another, and deviated from their common axis equally. The deviation angle of the

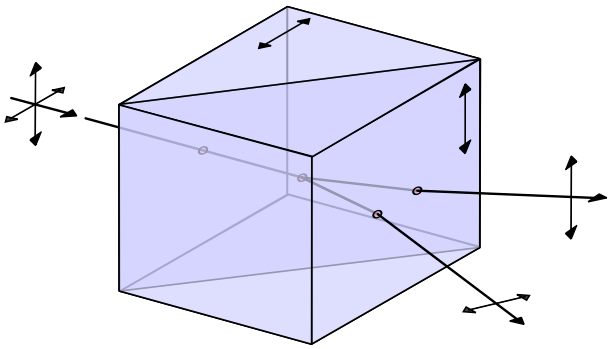

Figure 2.15: Diagram of a Wollaston prism. Included in the diagram are the optical axes of the differing sections of the birefringent material as well as polarizing directions of the incident beam, denoted using the ↔ and ↕ symbols, for the *O*- and *E*-beams, respectively. Diagram adapted from fgalore, CC BY-SA 3.0, via Wikimedia Commons (2023).

polarized beams is determined by the wedge angle which is defined as the angle from the common hypotenuse to that of the outer transmission face of either prism.

Wollaston prisms benefit over simpler elements (such as those listed in the polarizer paragraph) since a single frame allows for the observation of both orthogonal polarization components. This halves the observational time required to collect enough data to calculate the Stokes parameters, at the cost of an increase in calibration and reduction difficulty (Simon, 1986).

2.2.3 Polarimetric Calibrations

The raw science images acquired during polarimetric observations contain a combination of useful science data as well as noise. Corrections and calibrations related to the detector remain unchanged from those described in § 2.1.8, while those related to correcting for the optical elements relate to corrections for spurious polarization effects.

Flat Fielding

Once the CCD calibrations have been completed, the polarization intrinsic to the optical elements needs to be accounted for such that the pixel-to-pixel response is made uniform. Flat-fielding is, once again, used to correct for this. The flats taken for polarimetry, however, introduce an additional challenge as the targets for conventional flats are polarized, such as twilight and dome flats which are polarized by light scattering in the atmosphere and the reflective surface of the dome, respectively.

If no unpolarized flat images can be taken for flat field calibrations then, when possible due to the polarimeter design, the wave plate may be constantly rotated to act as a depolarizing element; this is effective so long as the wave plate rotation period is much faster than the flat's exposure time. Alternatively, polarized flats may be taken at the same set of half-wave plate angles used for science observations and averaged together to achieve a similar depolarizing effect.

Observing additional 'redundant' exposures for the science and flat images increases the depolarizing effect up to the maximum of 16 half-wave plate positions, where exposures with a half-wave plate angle differing by $\pi/4$ from another are considered redundant due to the *O*- and *E*-beams swapping between the related exposures.

Increasing the amount of redundant observations proportionally increases the time needed to observe all the exposures, which in turn introduces time-dependent effects such as fringing or intensity variations of the flat source. As such, a middle ground must be found for the amount of redundant frames observed. (Patat and Romaniello, 2006; Peinado et al., 2010).

Dual-Beam Extraction and Alignment

After calibrations for the CCD and light path are accounted for, the O- and E-beams can be extracted and further reduced. The extraction depends heavily on the layout of the polarimeter but often a simple cropping of the differing sections is enough to separate the two images.

After extracting the O- and E-beams for a specific half-wave plate angle, the images need to be aligned such that the sources present in them overlap. The Wollaston prism needs to be corrected for as it introduces a beam deviation which differs across both images. The aligning of the O- and E-beams is crucial as the comparison of the dual images is what allows for the calculation of the polarization properties.

Sky Subtraction

The polarization introduced by the sky introduces a difference in the intensity of the background sky and needs to be removed as it will influence the polarization results of the target source. Thankfully, the background polarization is an additive type of noise and may be subtracted out across the frames. This subtraction is done independently for both beams in a frame and for each frame since the background intensity of all observed polarimetric beams will differ based on the observational parameters.

2.3 Spectropolarimetry

As the name suggests, spectropolarimetry is the measurement of the polarization of light for a chosen spectral range and provides polarimetric results as a function of wavelength. As spectropolarimetry is so closely reliant on both spectroscopy and polarimetry, advancements in spectropolarimeters have always been gated by the advancements of spectrometers and polarimeters (as described in § 2.1 and § 2.2).

The most notable historical contributions of spectropolarimetry are those of spectropolarimetric studies instead of instrumental developments. Spectropolarimetry provides further insights into a materials physical structure, chemical composition, and magnetic field, allowing spectropolarimetry to be useful across multiple disciplines. In astronomy in particular, spectropolarimetry has been used to study the magnetic field, chemical composition, and underlying structure and emission processes of multiple types of celestial objects (see for example Antonucci and Miller, 1985; Donati et al., 1997; Wang and Wheeler, 2008).

Along with common points of consideration when developing any instrumentation for observational astronomy, such as resolution and sensitivity, spectropolarimeters need also consider the spectral response of the polarimetric components as well as the polarization

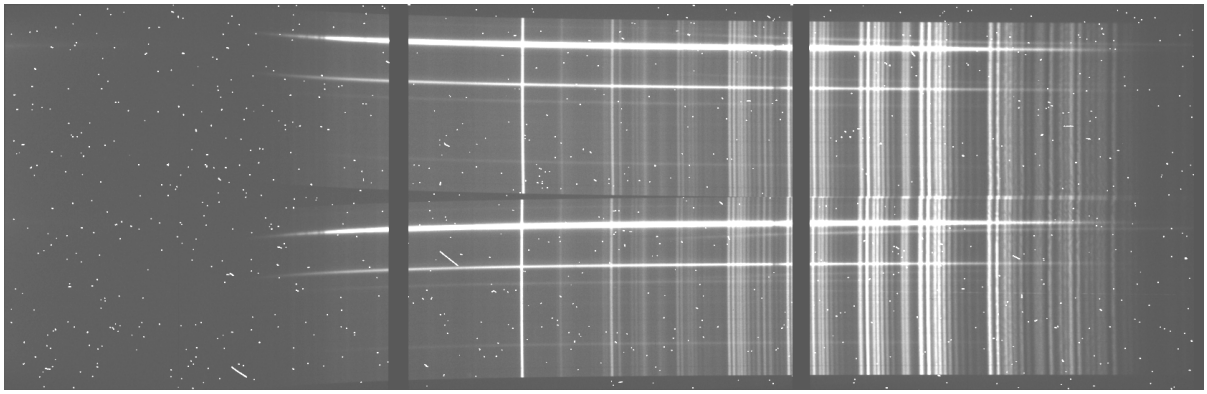

Figure 2.16: A spectropolarimetric target exposure as observed by the *SALT* RSS in spectropolarimetry mode.

response of the spectroscopic components as both are simultaneously in the light-path during observations and have noticeable affects on one another. Time is another constraint for spectropolarimetry as the incident light is separated both by wavelength and by polarization states. This division of the incident light results in increased exposure times for both target observations and observations necessary for calibrations.

Figure 2.16 illustrates a typical science image taken with a spectropolarimeter. The image contains the O- and E-beams which are both dispersed into their spectra. Spectropolarimetric results are acquired from measurements and calibrations of these images alongside any necessary calibration images.

2.3.1 Spectropolarimetric Measurement

The derived relations given in § 2.2.1, such as the Stokes parameters, describe polarization in general and are valid for both polarimetry and spectropolarimetry. Due to the time averaging of the observed light (Equation 2.28), any minor temporal variation, partial polarization, or monochromatic nature of the spectropolarimetric polarization parameters are accounted for.

For linear spectropolarimetry using a dual-beam polarizing element, an exposure measures the O- and E-beam wavelength dependent intensities, $f_{O,i}(\lambda)$ and $f_{E,i}(\lambda)$, for a given wave plate angle θ_i at angle i. These intensities thus relate to the wavelength dependent Stokes parameters as:

$$\begin{aligned} f_{O,i}(\lambda) &= \frac{1}{2}[I(\lambda) + Q(\lambda)\cos(4\theta_i) + U(\lambda)\sin(4\theta_i)]\,, \text{ and} \\ f_{E,i}(\lambda) &= \frac{1}{2}[I(\lambda) - Q(\lambda)\cos(4\theta_i) - U(\lambda)\sin(4\theta_i)]\,. \end{aligned} \tag{2.41}$$

At least four linear equations are required to solve for three variables in a system of linear equations and thus at least two exposures must be taken to solve for the linear ($I(\lambda)$, $Q(\lambda)$, and $U(\lambda)$) polarization parameters (Degl'Innocenti et al., 2006; Keller, 2002).

The first Stokes parameter, $I(\lambda)$, may be recovered for each dual-beam exposure using

$$I_i(\lambda) = f_{O,i}(\lambda) + f_{E,i}(\lambda)\,. \tag{2.42}$$

By calculating the $I_i(\lambda)$ Stokes parameter for each wave plate position i, the variation of the target over the course of observation may be corrected for, resulting in the $I(\lambda)$ Stokes parameter.

Next, the $Q(\lambda)$ and $U(\lambda)$ Stokes parameters are found by first defining the normalized difference in relative intensities, $F_i(\lambda)$, as:

$$F_i(\lambda) \equiv \frac{f_{O,i}(\lambda) - f_{E,i}(\lambda)}{f_{O,i}(\lambda) + f_{E,i}(\lambda)}\,, \tag{2.43}$$

which allows Equation 2.41 to be written, as

$$F_i(\lambda) = \bar{Q}(\lambda)\cos(4\theta_i) + \bar{U}(\lambda)\sin(4\theta_i) = P\cos(4\theta_i - 2\chi)\,, \tag{2.44}$$

in terms of the normalized Stokes parameters, or, alternatively, the degree of polarization, P, and polarization angle, χ (as described in Equation 2.33 and 2.34).

The optimal change in wave plate angle is $\Delta\theta_i = \pi/8$ as it allows the normalized Stokes polarization parameters to be calculated as:

$$\begin{aligned} \bar{Q}(\lambda) &= \frac{2}{N}\sum_{i=0}^{N-1} F_i(\lambda)\cos\left(\frac{\pi}{2}i\right)\,, \text{ and} \\ \bar{U}(\lambda) &= \frac{2}{N}\sum_{i=0}^{N-1} F_i(\lambda)\sin\left(\frac{\pi}{2}i\right)\,, \end{aligned} \tag{2.45}$$

where N is the number of exposures taken, limited such that $N \in [2, 16]$ (Patat and Romaniello, 2006).

2.3.2 Spectropolarimetric Calibrations

Just as the elements of a spectropolarimeter are an amalgamation of both a spectrometer and polarimeter, it naturally follows that the calibrations necessary to reduce spectropolarimetric data are a combination of the calibrations needed for spectroscopy and polarimetry, discussed further in § 2.1.8 and § 2.2.3. Even though the spectrometer and polarimeter components both have an effect on an incident beam following the light-path through the spectropolarimeter, the calibration procedures for both methods remain mostly independent of one another and as such need not be repeated here.

Spectropolarimetric calibrations are, however, more involved when compared to the same calibrations for either spectroscopy or polarimetry. Minor deviations in the calibrations across both the spectra and the polarized beam compound, especially when dealing with the wavelength calibration, resulting in poor Signal-to-Noise Ratio (S/N)'s. Generally, more exposures over longer timespans are required to acquire enough redundancy and signal for the calculation of the Stokes parameters on top of the time necessary for calibrations to be completed. It should therefore be noted just how important the calibrations are when dealing with spectropolarimetry.

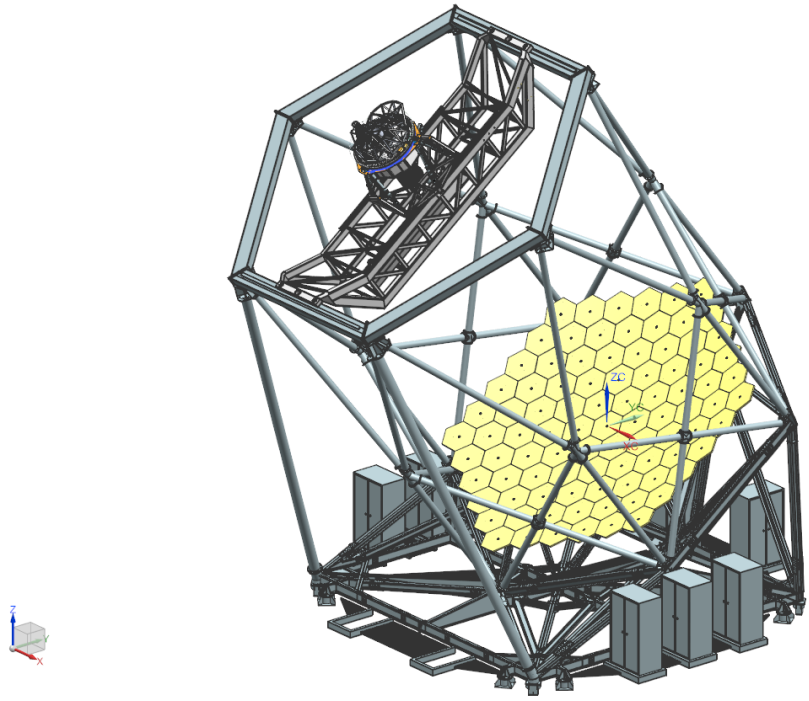

Figure 2.17: The tracker, supporting structure, and primary mirror of SALT. Figure adapted from the SALT call for proposals (2022).[5]

2.4 The Southern African Large Telescope

Southern African Large Telescope (*SALT*) is a 10 m class optical/near-infrared telescope situated at the South African Astronomical Observatory (*SAAO*) field station near Sutherland, South Africa (Burgh et al., 2003). The operational design was based on the Hobby-Eberly Telescope (*HET*) situated at McDonald Observatory, Texas, which limits the pointing of the telescope's primary mirror to a fixed elevation (37° from zenith in the case of SALT) while still allowing for full azimuthal rotation (Ramsey et al., 1998). Both SALT and HET utilize a spherical primary mirror which is stationary during observations and a tracker housing most of the instrumentation that tracks the primary mirrors spherically shaped focal path. Figure 2.17 depicts *SALT*'s tracker (top left), supporting structure, and primary mirror (bottom right).

2.4.1 The Primary Mirror

The primary mirror is composed of 91 individual 1 m hexagonal mirrors which together form an 11 m segmented spherical mirror. Each mirror segment can be adjusted by actuators allowing the individual mirrors to approximate a single monolithic spherical mirror. The fixed elevation means that SALT's primary mirror has a fixed gravity vector allowing for a lighter, cost-effective supporting structure when compared to those of a more traditional altitude-azimuthal mount but with the trade-off that the control mechanism and tracking have increased complexity (Buckley et al., 2006).

[5] http://pysalt.salt.ac.za/proposal_calls/current/ProposalCall.html

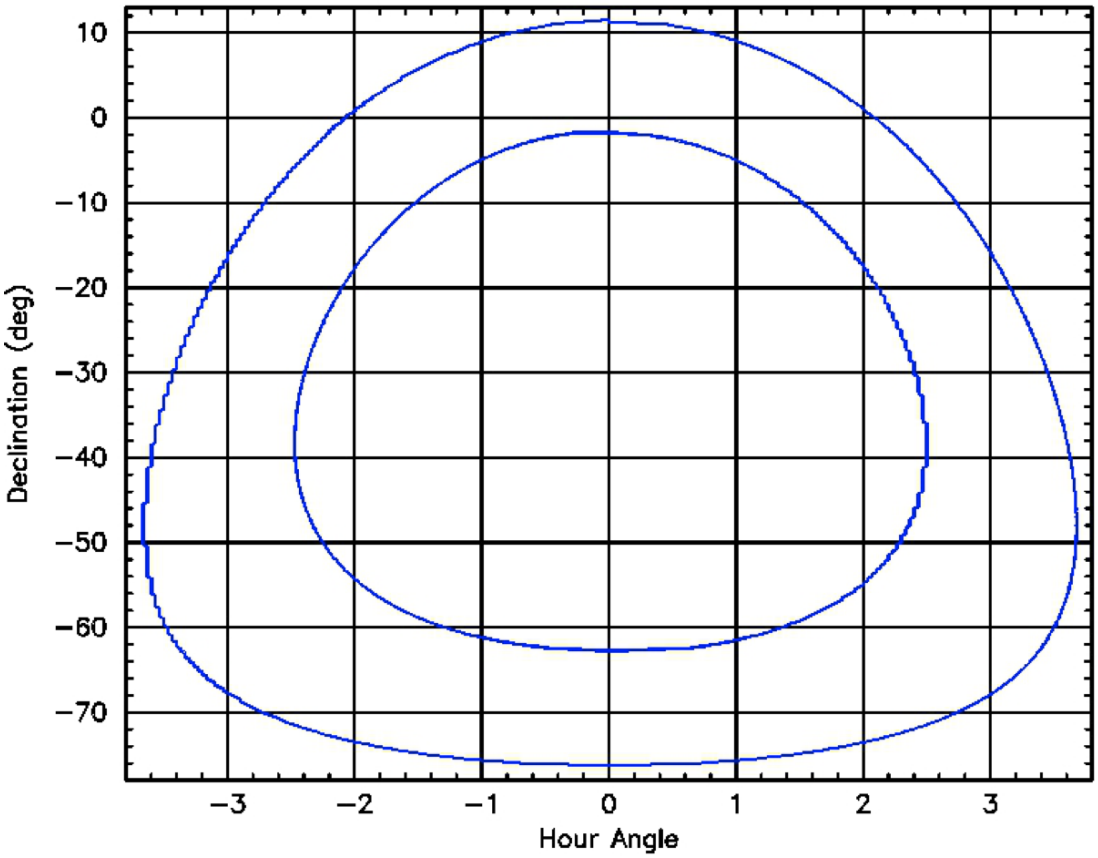

Figure 2.18: The visibility annulus of objects observable by SALT. Figure adapted from the SALT call for proposals (2013).[6]

2.4.2 Tracker and Tracking

During observations the primary mirror is stationary and the tracker tracks celestial objects across the sky by moving along the primary focus. The tracker is capable of 6 degrees of freedom with an accuracy of ~ 5 μm and is capable of tracking $\pm 6^\circ$ from the optimal central track position. Targets at declinations from 10.5° to -75.3°, as shown in Figure 2.18 are accessible during windows of opportunity. As the tracker moves along the track the effective collecting area varies and thus SALT has a varying effective diameter of ~ 7 m to 9 m when the tracker is furthest and closest to the optimal central position, respectively.

The tracker is equipped with a Spherical Aberration Corrector (SAC) (O'Donoghue, 2000), and an Atmospheric Dispersion Compensator (ADC) (O'Donoghue, 2002), which corrects for the spherical aberration caused by the geometry of the primary mirror and allows access to wavelengths as short as 3200 Å. These return a corrected flat focal plane with an $8'$ diameter field of view at prime focus on to the science instruments, with a $1'$ annulus around it used by the tracker in a closed-loop guidance system. The tracker also houses the calibration system which contains the Ar, CuAr, HgAr, Ne, ThAr, and Xe wavelength calibration lamps (Buckley et al., 2008).

[6] https://pysalt.salt.ac.za/proposal_calls/2013-2/

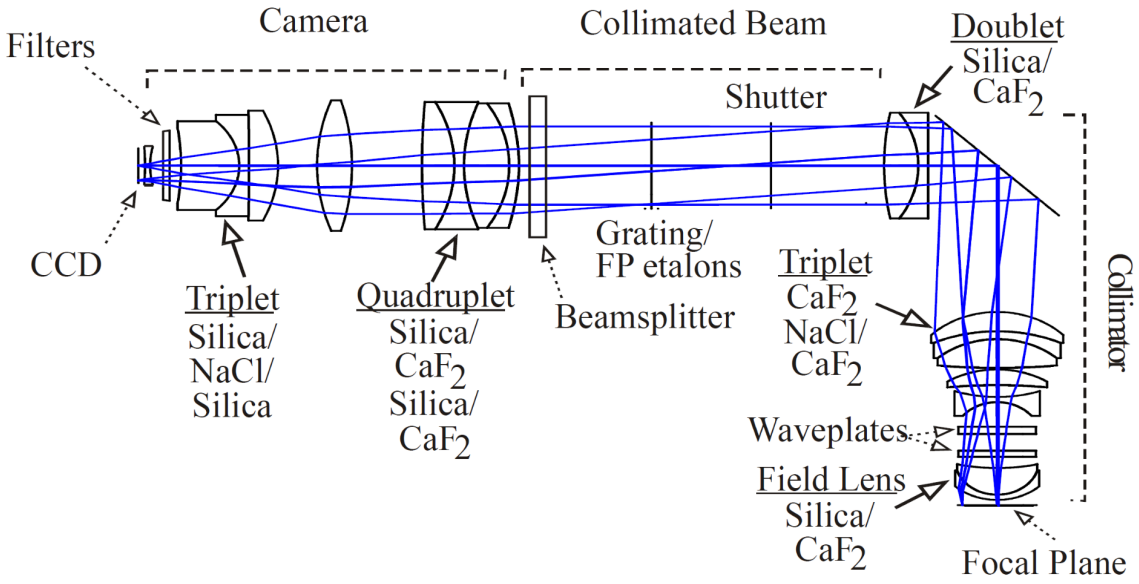

Figure 2.19: The optical path of the *SALT* RSS. Figure adapted from the SALT call for proposals (2023).[7]

2.4.3 SALT Instrumentation

SALT is equipped with the SALT Imaging Camera (SALTICAM) and the RSS science instruments onboard the tracker, and the High Resolution Spectrograph (HRS) and Near Infra-Red Washburn Labs Spectrograph (NIRWALS) science instruments which are fibre-fed from the tracker to their own climate controlled rooms. The RSS is currently the only instrument used for spectropolarimetry.

NIRWALS

The Near Infra-Red Washburn Labs Spectrograph (NIRWALS) is currently being commissioned and will have a wavelength coverage of 8000 to 17000 Å, providing medium resolution spectroscopy at R = 2000 to 5000 over Near Infra-Red (NIR) wavelengths (Brink et al., 2022; Wolf et al., 2022). NIRWALS is fibre-fed from its integral field unit, containing 212 object fibers, along with a separate sky bundle, containing 36 fibers, housed in the *SALT* fibre instrument feed. It is ideally suited for studies of nearby galaxies.

HRS

The High Resolution Spectrograph (HRS) echelle spectrograph was designed for high resolution spectroscopy at R = 37000 - 67000 covering a wavelength range of 3700 - 8900 Å and consists of a dichroic beam splitter and two VPH gratings (Nordsieck et al., 2003). This instrument is capable of stellar atmospheric and radial velocity analysis.

[7] https://pysalt.salt.ac.za/proposal_calls/current/ProposalCall.html

Table 2.1: Gratings available for use with the RSS. Table adapted from the *SALT* call for proposals (2023).

Grating Name	Wavelength Coverage (Å)	Usable Angles (°)	Bandpass per tilt (Å)	Resolving Power (1.25″ slit)
PG0300[8]	3700 – 9000		3900/4400	250 – 600
PG0700[8]	3200 – 9000	3.0 – 7.5	4000 – 3200	400 – 1200
PG0900	3200 – 9000	12 – 20	∼ 3000	600 – 2000
PG1300	3900 – 9000	19 – 32	∼ 2000	1000 – 3200
PG1800	4500 – 9000	28.5 – 50	1500 – 1000	2000 – 5500
PG2300	3800 – 7000	30.5 – 50	1000 – 800	2200 – 5500
PG3000	3200 – 5400	32 – 50	800 – 600	2200 – 5500

SALTICAM

The SALT Imaging Camera (SALTICAM) functions as the acquisition camera and simple science imager with various imaging modes, such as full-mode and slot-mode imaging, and supports low exposure times, down to 50 ms (O'Donoghue et al., 2006). This enables photometry of faint objects, especially at fast exposure times.

RSS

The Robert Stobie Spectrograph (RSS) functions as the primary spectrograph on *SALT* and can operate in long-slit spectroscopy and spectropolarimetry modes, a narrowband imaging mode, and multi-object and high resolution spectroscopy modes (for an in-depth discussion on operational modes see Kobulnicky et al., 2003, or the latest call for proposals).

The Detector The RSS detector consists of a mosaic of 3 CCD chips with a total pixel scale of 0.1267″ per unbinned pixel with varying readout times depending on the binning and readout mode. The mosaicking results in a characteristic double 'gap' in the frames and resultant spectra taken with the RSS, as seen in Figure 2.16.

The Available Gratings The RSS is equipped with a rotatable magazine of six VPH gratings, as listed in Table 2.1. Observations may be planned using simulator tools provided by *SALT* and are performed in the first order only. The RSS has a clear filter, as well as three Ultraviolet (UV) (with differing lower filtering ranges) and one blue order blocking filter available, used in conjunction with the various gratings to block out contamination from the second order.

RSS Spectropolarimetry Spectropolarimetry using the RSS is currently commissioned for long-slit linear spectropolarimetry, (I, Q, U), where observations are taken following the waveplate pattern lists as in Table 2.2. Circular, (I, V), and all-Stokes, (I, Q, U, V), spectropolarimetry modes are in commissioning with observations including redundant half-wave plate pairs to be commissioned thereafter.[9]

[8]The PG0300 surface relief grating has been replaced with the PG0700 VPH grating as of November 2022 but has been included here as observations using the PG0300 are used in later sections.

[9]Commission status sourced from the latest 'Polarimetry Observers Guide' (2024).

Table 2.2: Spectropolarimetry waveplate patterns defined for the RSS. The stated angles refer to the angle of the half (½ -) and quarter (¼ -) waveplate's optical axis from the perpendicular of the dispersion axis. Table adapted from the *SALT* call for proposals (2023).

Linear (°)		Linear-Hi (°)		Circular (°)		Circular-Hi (°)		All Stokes (°)	
½	¼	½	¼	½	¼	½	¼	½	¼
0	-	0	-	0	45	0	45	0	0
45	-	45	-	0	−45	0	−45	45	0
22.5	-	22.5	-			22.5	−45	22.5	0
67.5	-	67.5	-			22.5	45	67.5	0
		11.25	-			45	45	0	45
		56.25	-			45	−45	0	−45
		33.75	-			67.5	−45		
		78.75	-			67.5	45		

Chapter 3

Existing and Developed Software:
An Overview of POLSALT, IRAF, and STOPS

This chapter contains an overview of POLSALT and the limitations faced during POLSALT wavelength calibrations (§ 3.1), a brief overview of the IRAF tasks relevant for spectropolarimetric wavelength calibrations (§ 3.2), and an overview of STOPS, the software developed to supplement the POLSALT reduction process (§ 3.3). Finally, a discussion of the updated reduction process, an example of which may be found in Appendix A, is included (§ 3.4).

3.1 POLSALT - *Polarimetric reductions for SALT*

The POLSALT (*Polarimetric reductions for SALT*) pipeline is the official reduction pipeline for spectropolarimetric data taken using the *SALT* RSS.[1] The newest version of the software, aptly named the 'beta version' ('version' 23 January 2020), was the version adapted in this study. It includes a GUI, depicted in Figure 3.1, which allows for limited interactivity during key steps in the reduction process.[2] The POLSALT pipeline is written in Python 2, and it is suggested that a Python environment manager, such as `anaconda` (Anaconda), is installed.

The steps that make up the POLSALT reduction pipeline include raw image reductions, wavelength calibrations, background subtraction and spectral extraction, raw Stokes calculations, final Stokes calculations, and visualization of the results. Accurate reductions at each step are crucial for accurate results and are thus briefly discussed below. Further details for the reduction process may be found at the POLSALT GitHub wiki.[3]

[1] POLSALT is made freely available via the POLSALT GitHub repository, available at `https://github.com/saltastro/polsalt`. It is strongly advised to follow the wiki for installation instructions.

[2] Installation files and instructions for the 'beta version' utilizing the GUI are available at `http://www.saao.ac.za/~ejk/polsalt/code/` in a TAR GZIP file.

[3] The GitHub wiki for POLSALT is available at `https://github.com/saltastro/polsalt/wiki`.

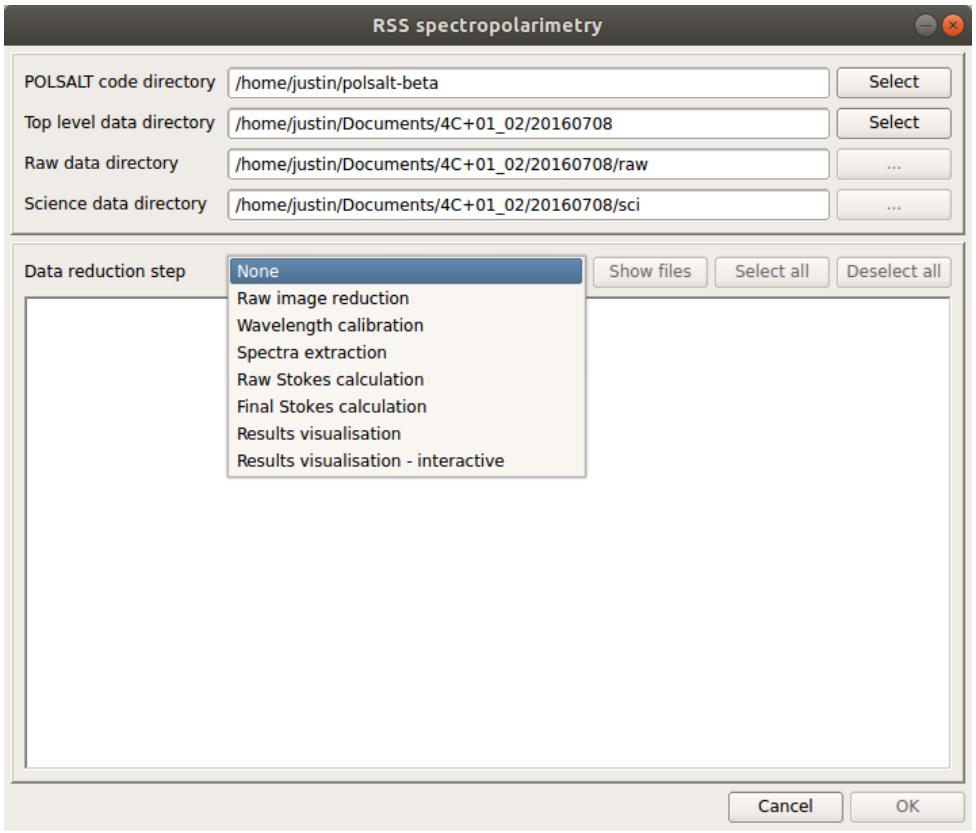

Figure 3.1: The layout of the POLSALT Graphical User Interface (GUI), including the contents of the reduction steps accessible via the dropdown menu. Note that there is no trailing forward slash after the 'Top level data directory'. Figure created from a local instance of the POLSALT GUI.

3.1.1 Raw Image Reductions

Raw image reductions are run via **imred.py** and apply the necessary basic reductions to the raw data before any calibrations are applied. These reductions include overscan subtractions, gain corrections, crosstalk corrections, and mosaicking as well as attaching the bad pixel maps and pixel variance information. Files with raw image reductions performed have "mxgbp" prepended to their names. As of February 2022, raw image reductions are automatically run for all RSS spectropolarimetric observations as part of the default SALT basic reduction pipeline that is run daily.

3.1.2 Wavelength Calibrations

Wavelength calibration and cosmic-ray rejection is performed via **specpolwavmap.py** and separately calibrates the *O*- and *E*-beams, based on the arc frames, and applies a simple cosmic-ray rejection for all science frames. This step is interactive and allows the user to individually fit wavelength calibration maps to each beam. The importance of an accurate correlation between both beams has been touched on previously (§ 2.3.2) and will be further discussed in § 3.1.8. The wavelength calibrated results are saved as an additional 'WAV' wavelength extension to each science FITS file, which are prefixed with a "w", and the *O*- and *E*-beams of the extensions are split into their own sub-extensions.

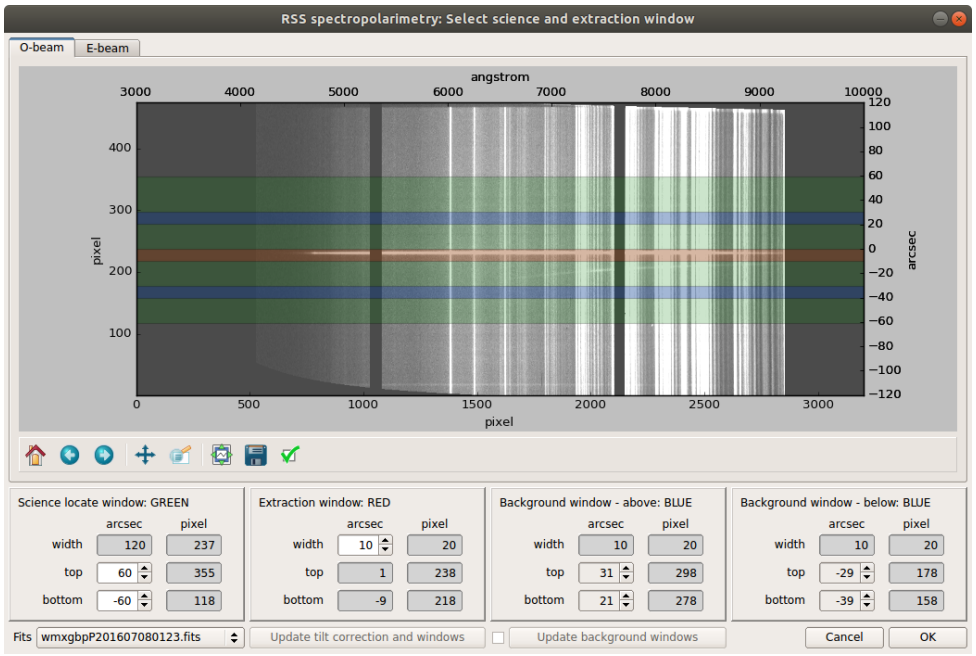

Figure 3.2: The layout of the interactive POLSALT `spectra extraction` GUI after selecting the 'update tilt correction and windows' button along the bottom border of the window. Figure created from a local instance of the POLSALT GUI.

3.1.3 Spectral Extraction

Background subtraction and spectral extraction is run via **specpolextract_dev.py** which corrects for the beam-splitter distortion and tilt, performs sky subtraction, and extracts a one dimensional wavelength dependent spectrum for each beam sub-extension. This step is interactive with Figure 3.2 showing the interactive window used for spectral extraction. The user, using the brightest trace in the image as a reference, defines regions which span the wavelength axis which define the background and trace regions for the sky subtraction and spectral extraction. Files with background and geometric corrections applied are saved with "c" prepended to their names and files which contain the extracted one dimensional spectrum have "e" further prepended to their names.

3.1.4 Raw Stokes Calculations

The raw Stokes calculations are performed via **specpolrawstokes_dev.py** and identify waveplate pairs for which the intensity, I, and a 'raw Stokes' signal, S, are calculated as:

$$I = \frac{1}{2}(O_1 + O_2 + E_1 + E_2)\,, \text{ and} \tag{3.1}$$

$$S = \frac{1}{2}\left[\left(\frac{O_1 - O_2}{O_1 + O_2}\right) - \left(\frac{E_1 - E_2}{E_1 + E_2}\right)\right]\,. \tag{3.2}$$

The raw Stokes signal is calculated as the normalized difference of the O- and E-beams, for a waveplate pair, taken perpendicular to one another. The created files contain the raw Stokes information and use a very specific naming style; most notably the indexes of the related waveplate pairs, from Table 2.2, are included in the file names.

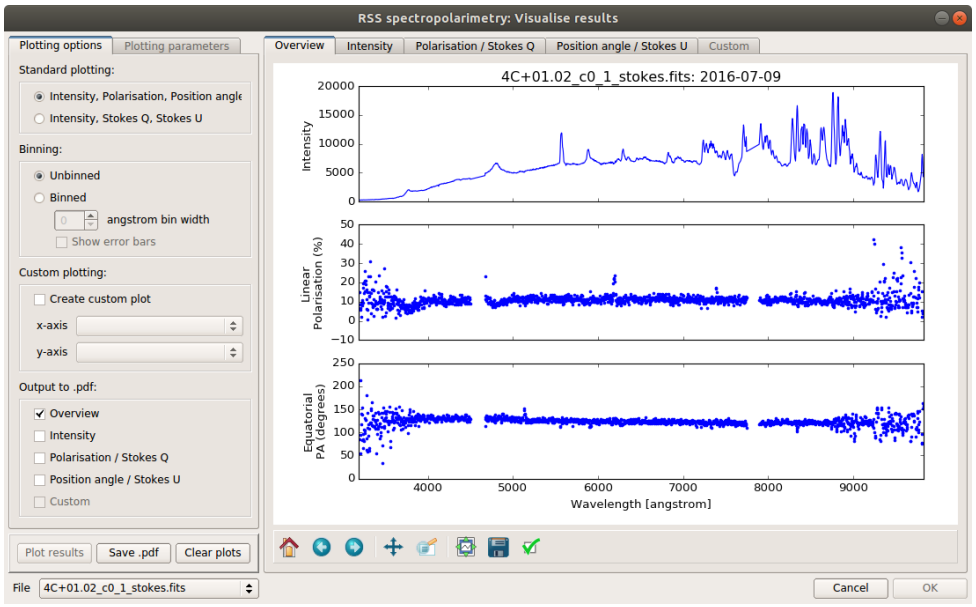

Figure 3.3: The layout of the interactive POLSALT `visualization` GUI after selecting the 'Plot results' button along the bottom border of the window. Figure created from a local instance of the POLSALT GUI.

3.1.5 Final Stokes Calculations

The Final Stokes calculations are performed via **specpolfinalstokes.py** and, using the waveplate pattern along with the raw Stokes signals, calibrates for the polarimetric zero-point and waveplate efficiency, and calculates the final Stokes parameters. Before the final Stokes calculations are performed, and if a sufficient number of redundant exposures were taken, the raw Stokes signals are culled to eliminate outlier signals which may arise from, for example, temporary atmospheric conditions affecting the signal. The culling is performed by comparing observation cycles against one another, comparing the deviation of the signal means which estimate the baseline systematic polarization fluctuations (due to imperfections in repeatability), and performing a χ^2 analysis to eliminate any statistical outliers.

3.1.6 Visualization

Plotting the results of the spectropolarimetric reduction process is done using **specpolview.py**, which generates a plot of the Intensity, Linear Polarization (%), and Equatorial Polarization Angle (°) against a shared wavelength axis, as seen in Figure 3.4. This step is interactive allowing the user control over various options, such as the wavelength range, binning, etc., with the GUI shown in Figure 3.3.

3.1.7 Post-Processing Analysis

Generally, the plot of the spectropolarimetric results is the stopping point for most reduction procedures as it contains or creates the desired results. However, additional tools exist which may be used after the polarization reductions, and which are not represented in the GUI, namely, flux calibration and synthetic filtering.

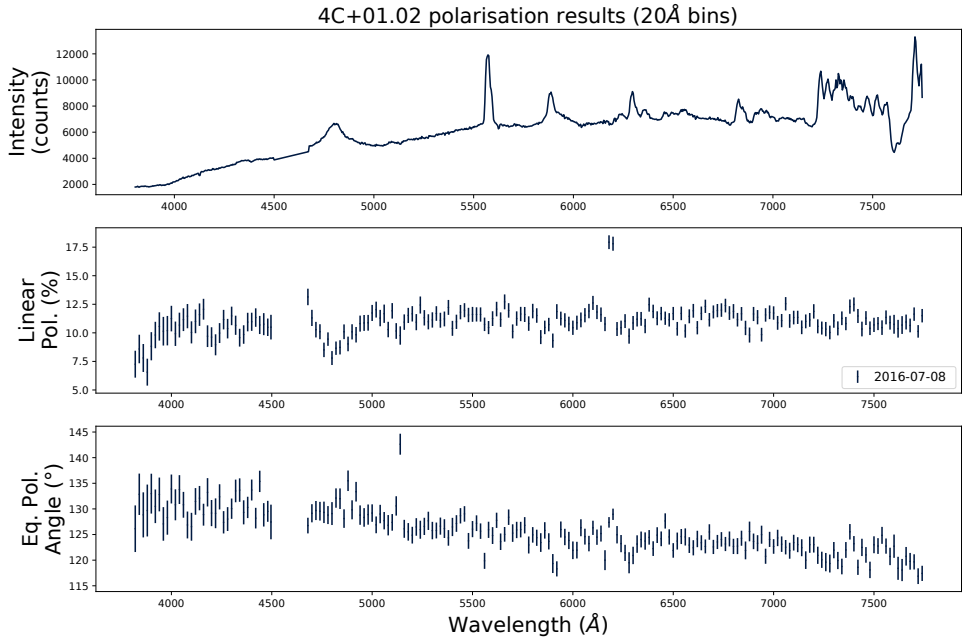

Figure 3.4: A typical plot resulting from the reduction process. Figure adapted from (Cooper et al., 2022).

Flux-calibrations are performed via **specpolflux.py** and are only intended for shape corrections of the spectrum. Additionally, a flux database file must exist for the observed standard and must be included in the working science directory.

Synthetic filtering is calculated via **specpolfilter.py** and computes the synthetically filtered polarization results. Any wavelength dependent throughput filter curve may be synthesized when defined by the user, but a few pre-defined filter curves are available, namely: the SALTICAMs U, B, V, R, and I Johnson-Cousins filter curves.

3.1.8 POLSALT Limitations and the Need for Supplementary Tools

The creation of supplementary tools for POLSALT spectropolarimetric reductions stemmed from the limitations of the wavelength calibration process and a need to compare wavelength solutions across the perpendicular O and E polarization beams. The process of calibrating wavelength solutions using the POLSALT pipeline is time-consuming for the average user, and often results in unexpected program crashes when receiving erroneous inputs or key presses. Due to the time-consuming process of recalibrating the wavelength solutions it is not feasible to perform the wavelength calibrations time and time again for anything larger than a handful of observations. This is particularly true for observations performed with the *SALT* PG0300 grating as the sparse spectral features of the Ar arc lamp are not handled well by the POLSALT pipeline.

Since PG0300 provided the widest wavelength range and highest throughput, it was almost exclusively used for observations of flaring blazars, resulting in a large backlog of unanalyzed data. The only arc available for the PG0300 grating with a close enough articulation and grating angle ($\sim 10.68°$ and $\sim 5.38°$, respectively), was the Ar arc lamp which displays sparse spectral features with large gaps over the wavelength range at these grating and articulation angles (Figure 3.5). This often led the POLSALT pipeline to create inconsistent wavelength solutions, or to fail to create a wavelength solution altogether,

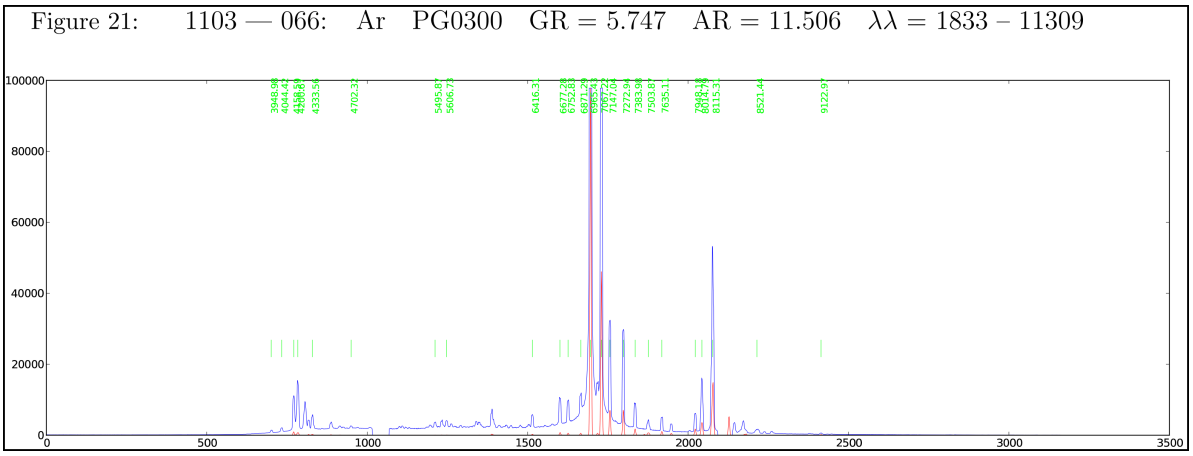

Figure 3.5: One of many Ar arc lamp spectra as provided by *SALT* for line identification. Plot adapted from *SALT*'s published Longslit Line Atlases (as of 2024), resized to fit within the document margins but otherwise unchanged.[4]

since minor deviations of identified spectral features resulted in large deviations in regions with no spectral features. To only further compound the difficulty of the wavelength calibrations, the spectrum of the Ar arc lamp contains a partial overlap of a higher order at longer wavelengths (§ 2.1.7, Equation 2.5).

The chosen solution to overcome the limitations of the wavelength calibration process was to use a well established wavelength calibration software which allowed for rapid recalibrations and provided a familiar interface. IRAF provides this familiar environment and reliability, in part thanks to its continued community development.

Unfortunately, IRAF is unable to natively parse the data structure implemented by POLSALT 'as is' and so the files must be restructured. This restructuring works both ways as once the IRAF reductions are complete the data structure must be restructured to match that of the POLSALT `wavelength calibration` output such that the reduction process may be completed in POLSALT.

3.2 IRAF - *Image Reduction and Analysis Facility*

The IRAF (*Image Reduction and Analysis Facility*) software is a collection of software designed specifically for the reduction and analysis of astronomical images and spectra (Tody, 1986, 1993). The software consists of many tasks which perform specific operations and which are grouped into relevant packages. Only a brief overview of the tasks will be provided here. Help documentation for any of the IRAF tasks may be found online or through the IRAF Command Line Interface (CLI) through the `?` or `:.help` 'cursor commands' when running interactive tasks, with more specific help documentation provided in the relevant section.[5]

Useful IRAF tasks that deserve a brief mention are: the `mkscript` task in the `system` package which allows a user to create and save a task along with the defined parameters

[4] The 'low resolution' Ar plot sourced from `https://astronomers.salt.ac.za/data/salt-longslit-line-atlas/`

[5] Online help for IRAF is available at `https://iraf.net/irafdocs/`

as a file which can later be called as a script,[6] the `implot` task in the `plot` package which allows the rows or columns of an image to be interactively displayed,[7] and the `eparam` task in the `language` package which allows the parameters of a task to be edited within the IRAF CLI.[8]

For the wavelength calibration of *SALT* spectropolarimetric data, the relevant tasks are the `identify` and `reidentify` tasks located in the `noao.onedspec` package, and the `fitcoords` and the (optional) `transform` tasks located under the `noao.twodspec.longslit` package. These tasks produce a two-dimensional wavelength solution which must be obtained separately for the *O*- and *E*-beam.

3.2.1 Identify

The `identify` task is used to interactively determine a one-dimensional wavelength function across a chosen row of an arc exposure by identifying features in the spectrum with known wavelengths.[9] The task creates the first approximation of the wavelength solution (see Figure 3.6) as well as a local database in which the solution is saved (see Listing 3.1). The initial solution is built on in subsequent tasks, and it is, therefore, imperative that the initial solution is well-fit to minimize errors further along the calibration process.

The execution of `identify` consists of identifying known features spanning the entire wavelength range and then removing any features which negatively impact the wavelength solution. A balance must be found between the number of identified features, the parameters of the fit, and the deviation of the fit from the known features.

3.2.2 Reidentify

The `reidentify` task is used to run the `identify` task autonomously and repeatedly across the entirety of the arc frame at defined (row) intervals.[11] The task uses the one-dimensional wavelength solution stored in the database created by the initial `identify` call and refits the positions of the relevant spectral features. The task may fail based on a number of conditions, most common of which is the loss of features as the task moves further from the row at which the user manually ran `identify`.

[6] Help documentation for the `mkscript` task may be found at https://astro.uni-bonn.de/~sysstw/lfa_html/iraf/system.mkscript.html.

[7] Help documentation for the `implot` task may be found at https://astro.uni-bonn.de/~sysstw/lfa_html/iraf/plot.implot.html.

[8] Help documentation for the `eparam` task may be found at https://astro.uni-bonn.de/~sysstw/lfa_html/iraf/language.eparam.html.

[9] Help documentation for the `identify` task may be found at https://astro.uni-bonn.de/~sysstw/lfa_html/iraf/noao.onedspec.identify.html.

[10] See also https://iraf.net/irafdocs/formats/identify.php for an explanation of the database contents.

[11] Help documentation for the `reidentify` task may be found at https://astro.uni-bonn.de/~sysstw/lfa_html/iraf/noao.onedspec.reidentify.html.

Listing 3.1: An example of the `identify` database contents.[10]

```
# Thu 15:19:16 13-May-2021
begin   identify arc00057[*,237]
    id  arc00057
    task        identify
    image       arc00057[*,237]
    units       Angstroms
    features    35
             53.61 5944.74989   5944.834  13.0 1 1 15257
           140.19 6029.9793    6029.997  13.0 1 1  4652
           185.30 6074.34644   6074.338  13.0 1 1 13396
           207.49 6096.15873   6096.161  13.0 1 1 21700
           255.23 6143.0493    6143.063  13.0 1 1 33330
           276.13 6163.56995   6163.594  13.0 1 1 11344
           330.89 6217.29293   6217.281  13.0 1 1 13705
           381.10 6266.51524   6266.495  13.0 1 1 21747
           420.21 6304.8113    6304.789  13.0 1 1 10226
           450.49 6334.45415   6334.428  13.0 1 1 36235
           500.18 6383.04826   6382.991  13.0 1 1 35824
           519.85 6402.26802   6402.248  13.0 1 1 70163
           626.70 6506.56147   6506.528  13.0 1 1 46165
           653.73 6532.91083   6532.882  13.0 1 1 21413
           721.60 6598.98642   6598.953  13.0 1 1 26396
           803.21 6678.31069   6678.277  13.0 1 1 51338
           843.15 6717.0732    6717.043  13.0 1 1 36780
          1099.95 6965.36335   6965.431  13.0 1 1  5618.4  ar
          1169.57 7032.38598   7032.413  13.0 1 1 100000
          1317.05 7173.89814   7173.938  13.0 1 1  5000    decrease
          1391.52 7245.11148   7245.167  13.0 1 1 73545
          1537.20 7383.93022   7383.981  13.0 1 1  5557.5  ar
          1595.02 7438.83545   7438.898  13.0 1 1 15000    decrease
          1663.64 7503.86263   7503.869  13.0 1 1 30000    ar; increase
          1697.46 7535.84584   7535.774  13.0 1 1  8000    increase
          1802.64 7635.07335   7635.106  13.0 1 1 20000    ar; decrease
          2209.19 8014.79559   8014.786  13.0 1 1  3000    ar; decrease
          2604.58 8377.66137   8377.607  13.0 1 1 14543
          2734.54 8495.41423   8495.359  13.0 1 1  8765
          2763.48 8521.52355   8521.442  13.0 1 1  4537.5  ar
          2840.92 8591.20799   8591.258  13.0 1 1  2000    decrease
          2889.39 8634.67334   8634.647  13.0 1 1  3059
          2911.42 8654.39264   8654.383  13.0 1 1  3000    decrease
          2926.56 8667.93501   8667.944  13.0 1 1   702.5  ar
          3135.72 8853.77575   8853.867  13.0 1 1  1820
    function legendre
    order 4
    sample *
    naverage 1
    niterate 0
    low_reject 3.
    high_reject 3.
    grow 0.
    coefficients        8
        2.
        4.
        53.60757446289061
        3135.715576171875
        7425.420339270724
        1457.513831286474
        -26.15751926622308
        -3.000903509842187
```

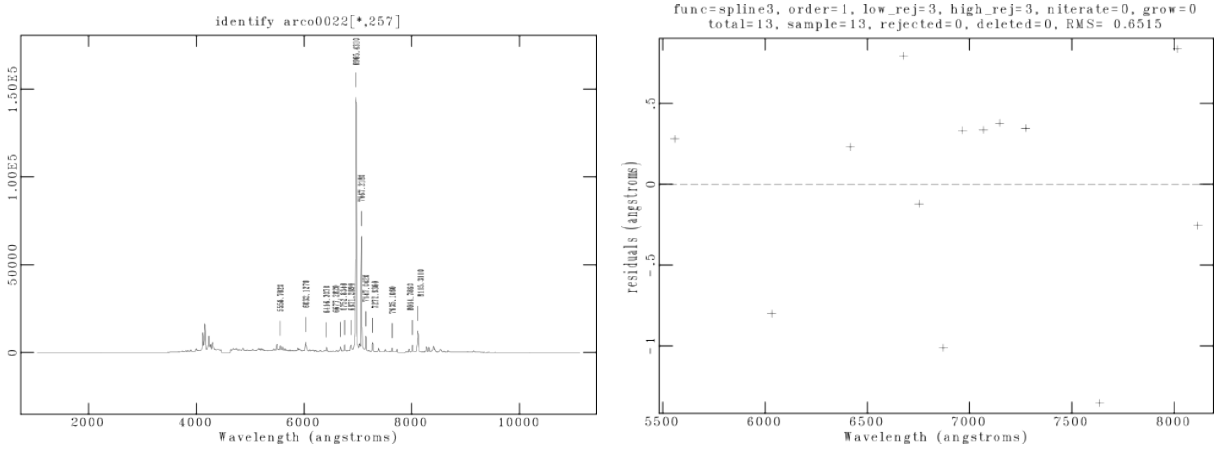

(a) Identified features.

(b) Root Mean Square (RMS) of the identified features.

Figure 3.6: A plot and the RMS of the identified features found using the IRAF `identify` task. Figures created using the IRAF `identify` task.

Listing 3.2: An example of the `fitcoords` database contents.[13]

```
# Thu 15:26:55 13-May-2021
begin   arc00057
        task    fitcoords
        axis    1
        units   angstroms
        surface 33
                1.
                5.
                5.
                1.
                1.
                3199.
                1.
                474.
                7419.096745914063
                1510.03933621895
                -21.10886852752348
                -2.079553916887794
                0.067726314205282 28
                0.7720164913117386
                -1.506773900054024
                0.1341878190232142
                -0.01659697703758917
                0.0251087019569153
                -3.318493303995171
                -0.3612632489821799
                0.003270665801371641
                -0.0157962041414068
                -0.003073690871589242
                0.007533453962924031
                0.02839687304474069
                -0.003233465769521899
                0.00174111456659807
                0.00645177595090841
                0.0105080093855621
                -0.01157827440314294
                -0.007789479002470706
                -0.006562085282926231
                -0.002321476801926803
```

When running `reidentify` non-interactively, it is recommended to set the `verbose` parameter to '`yes`' as this will provide immediate confirmation if the task quit early. Regardless of whether the task quit successfully, the newly defined wavelength solutions are appended to the local database following the `identify` task database format, an example of which is given in Listing 3.1.

3.2.3 Fitcoords

The `fitcoords` task is used to find a two-dimensional surface function from the one-dimensional wavelength solutions found for specific rows in the previous steps.[12] The usage of `fitcoords` is similar to that of `identify` and consists of examining the distribution of identified points and eliminating any points that `reidentify` may have misidentified (see Figure 3.7).

By eliminating outliers with bad residuals and modifying the two-dimensional surface function's type and degree, the overall error of the fit is decreased, aligning more closely to what the 'true' wavelength solution is. This surface function is the final two-dimensional wavelength solution for each two-dimensional spectrum. It is saved using the `fitcoords` database format, an example of which is given in Listing 3.2, as the list of parameters and function coefficients required to recreate the closest two-dimensional model. The IRAF wavelength solution is used by the STOPS `join` method to create the 'WAV' extension required by POLSALT, further described in § 3.3.2.

[12]Help documentation for the `fitcoords` task may be found at https://astro.uni-bonn.de/~sysstw/lfa_html/iraf/noao.twodspec.longslit.fitcoords.html.

[13]See also https://iraf.net/irafdocs/formats/fitcoords.php for an explanation of the database contents.

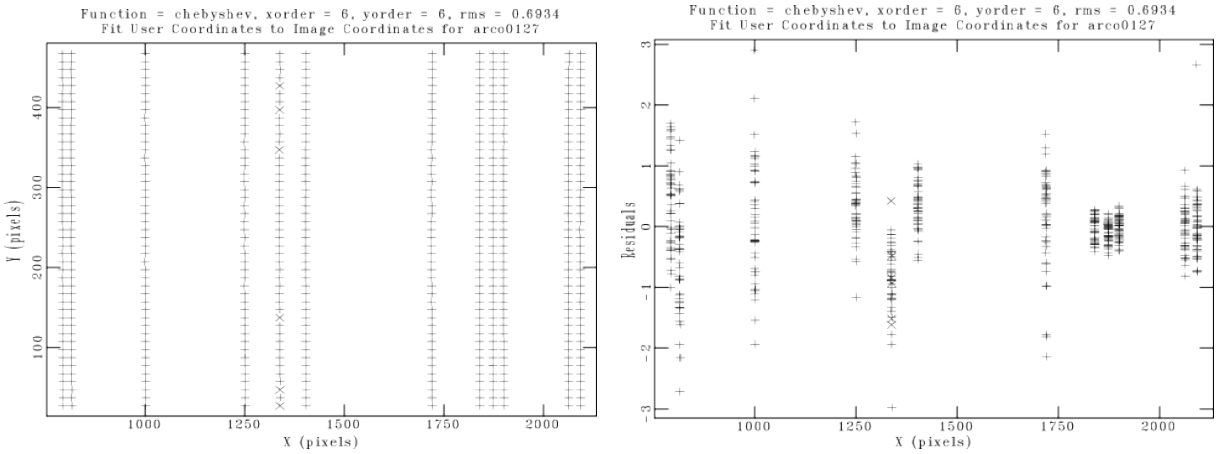

(a) Features identified across an exposure.

(b) RMS of the identified features.

Figure 3.7: A plot and the RMS of the features identified across the exposure using the IRAF `fitcoords` task. Figures created using the IRAF `fitcoords` task.

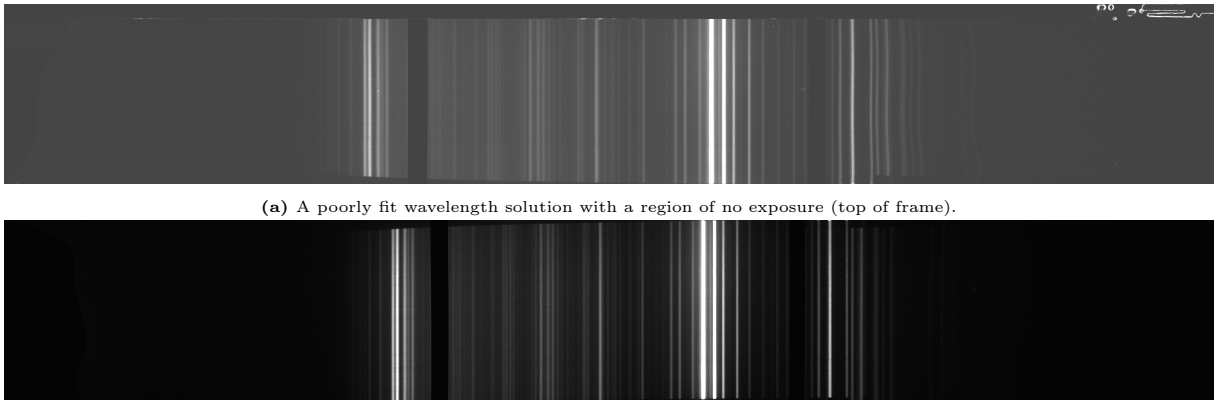

(a) A poorly fit wavelength solution with a region of no exposure (top of frame).

(b) A well-fit wavelength solution.

Figure 3.8: Examples of a poor fit (a) and well-fit (b) wavelength solution applied to the *O*- and *E*-beams of an arc image. The contrast of the figures were scaled to best capture any deviation of the arc lines. Figures created by the IRAF `transform` task.

3.2.4 Transform

The `transform` task is the optional final step in the IRAF wavelength calibration process.[14] Simply put, `transform` converts the (x_p, y_p) pixel units of an exposure to (λ, y_p) wavelength units which allows for an immediate check of whether the wavelength solution is consistent across the frame. Any general error in the wavelength solution may be spotted in the transformed images; ranging from minor errors, such as the arc lines or sky lines not being purely vertical across the frame, to more major errors, such as an incorrect wavelength solution skewing the exposure beyond recognition.

For example, Figure 3.8a shows a good fit to the wavelength solution, as after transformation all the sky lines run exactly vertical. Figure 3.8b, on the other hand, shows a seemingly good fit, but closer inspection reveals that the sky lines (especially towards the right of the frame) deviate from the vertical, indicating a poor fit to the wavelength solution.

[14]Help documentation for the `transform` task may be found at https://astro.uni-bonn.de/~sysstw/lfa_html/iraf/noao.twodspec.longslit.transform.html.

3.3 STOPS - *Supplementary Tools for POLSALT Spectropolarimetry*

Supplementary Tools for POLSALT Spectropolarimetry (STOPS) provides supplementary tools which convert the POLSALT and IRAF formats back and forth, allowing IRAF to be used for wavelength calibrations of *SALT* spectropolarimetric data. It also provides additional tools to check the accuracy of the wavelength calibration. STOPS is written in, and requires, Python 3 (3.11+) to run, as well as `Astropy` (6.0.0+) (Astropy Collaboration et al., 2013, 2018, 2022), `ccdproc` (2.4.1+) (Craig et al., 2017), `Matplotlib` (3.5.2+) (Hunter, 2007), `NumPy` (1.26.4+) (Harris et al., 2020), and `SciPy` (1.13.0+) (Virtanen et al., 2020).

The parsing of POLSALT data into an IRAF usable format and the reformatting of the IRAF wavelength calibrated data back into a POLSALT usable format, referred to as *splitting* and *joining*, is performed by the STOPS `split` and `join` methods, respectively.

Methods to verify the validity of the wavelength calibrations were also added to STOPS. The `skyline` method checks the sky line wavelength (x) positions across the frame as well as the variation of the sky lines across the positional (y) axis of the frame. The `correlate` method checks the correlation of the O- and E-beams either within a given FITS file or across multiple files (comparing only the O- and E-beams for each). With these two additional methods, a user is able to verify that the wavelength solutions do not conflict across the O- and E-beams and that no unexpected deviations are included in the wavelength solutions.

Help on the usage of STOPS in a CLI can be viewed by running:

```
$ python ~/STOPS --help
# OR
$ python ~/STOPS [split|join|correlate|skylines] --help
```

which retrieves and prints the help documentation to the CLI from Listing B.1 (in Appendix B), such as how to enable logging or increase the verbosity, or change default parameters of the various methods. Finally, help documentation for the specific STOPS methods may be found within this section (Listing 3.3 to 3.6) or in Appendix B.

3.3.1 Splitting

As mentioned previously, the format of the FITS file created by POLSALT after basic CCD reductions and the format expected by IRAF to be used for the wavelength calibrations are incompatible. Basic POLSALT CCD reductions return FITS files which contain a primary header along with extensions for the science, variance, and 'BPM' images. These extensions carry the image of the trace (see Figure 3.9), the variance of the image, and a map of the pixels to be masked out, split into sub-extensions for both polarimetry beams, respectively.

While IRAF is capable of dealing with multiple traces in an extension or lists of input files, it is not as capable when dealing with multiple wavelength solutions contained in a single extension (as expected by the POLSALT `wavelength calibration`) or extensions containing sub-extensions (as expected by the POLSALT `spectral extraction`).

Listing 3.3: The 'docstring' for **split.py**

```
The `Split` class allows for the splitting of `polsalt` FITS files based on the polarization beam.
The FITS files must have basic `polsalt` pre-reductions already applied (`mxgbp...` FITS files).

Parameters
----------
data_dir : str | Path
    The path to the data to be split
fits_list : list[str], optional
    A list of pre-reduced `polsalt` FITS files to be split within `data_dir`.
    (The default is None, `Split` will search for `mxgbp*.fits` files)
split_row : int, optional
    The row along which to split the data of each extension in the FITS file.
    (The default is SPLIT_ROW (See Notes), the SALT RSS CCD's middle row)
no_arc : bool, optional
    Decides whether the arc frames should be recombined.
    (The default is False, `polsalt` has no use for the arc after wavelength calibrations)
save_prefix : dict[str, list[str]], optional
    The prefix with which to save the  O & E beams. Setting `save_prefix` = `None` does not save the split O & E beams.
    (The default is SAVE_PREFIX (See Notes))

Attributes
----------
arc : str
    Name of arc FITS file within `data_dir`. `arc` = `""` if `no_arc` or not detected in `data_dir`.
o_files, e_files : list[str]
    A list of the `O`- and `E`-beam FITS file names. The first entry is the arc file if `arc` defined.
data_dir
fits_list
split_row
save_prefix

Methods
-------
split_file(file: os.PathLike) -> tuple[astropy.io.fits.HDUList]
    Handles creation and saving the separated FITS files
split_ext(hdulist: astropy.io.fits.HDUList, ext: str = 'SCI') -> astropy.io.fits.HDUList
    Splits the data in the `ext` extension along the `split_row`
crop_file(hdulist: astropy.io.fits.HDUList, crop: int = CROP_DEFAULT) -> tuple[numpy.ndarray]
    Crops the data along the edge of the frame, that is,
    `O`-beam cropped as [crop:], and
    `E`-beam cropped as [:-crop].
update_beam_lists(o_name: str, e_name: str) -> None
    Updates `o_files` and `e_files`.
save_beam_lists(file_suffix: str = 'frames') -> None
    Creates and writes (overwrites if exists) the `[o|e]_files` to files named `[o|e]_{file_suffix}`.
process() -> None
    Calls `split_file` and `save_beam_lists` on each file in `fits_list` for automation.

Other Parameters
----------------
**kwargs : dict
    keyword arguments. Allows for passing unpacked dictionary to the class constructor.

Notes
-----
Constants Imported (See utils.Constants):
    SAVE_PREFIX
    CROP_DEFAULT
    SPLIT_ROW
```

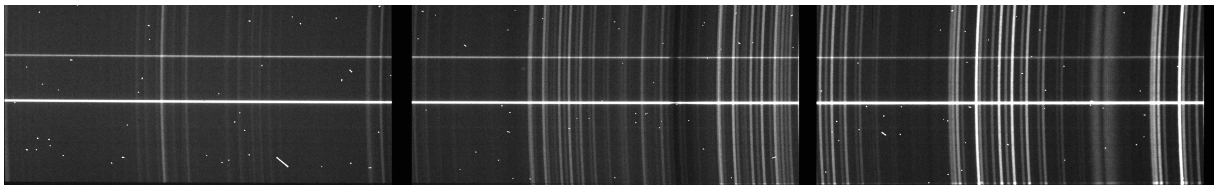

(a) The *O*-beam region of the FITS file.

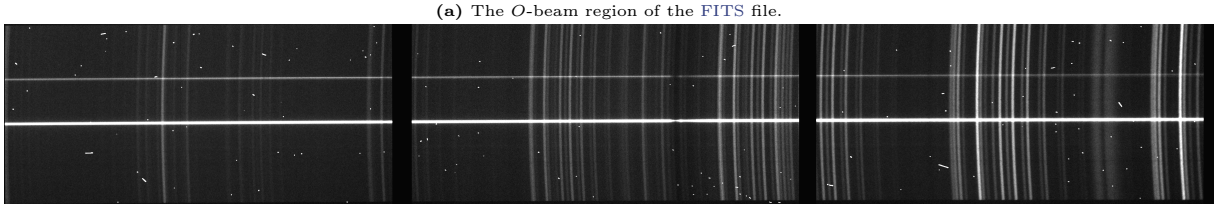

(b) The *E*-beam region of the FITS file.

Figure 3.9: The split *O*- (a) and *E*-beams (b) as handed to IRAF. Figure created from the STOPS `split` method output.

To simplify the IRAF reduction procedure it was decided to separate the perpendicular polarization beams into their own files.

The files with POLSALT pre-reductions applied, namely FITS files with an 'mxgbp' prefix (§ 3.1), are used as the starting point for the supplementary tool's `split` method. Running `split` finds all the FITS files for wavelength calibration within the working directory, creates two empty Header and Data Unit (HDU) structures for each FITS file (i.e. for both the *O*- and *E*-beam), and appends all header and science data necessary for wavelength calibration to the relevant HDU structure. Otherwise, defaults, such as which row to split the image along to separate the beams, were kept as close to the POLSALT pipeline as possible.

As the intent was always to parse the wavelength function back into POLSALT it was decided to keep these temporary FITS files as small as possible by only including the header and 'SCI' science extension. To aid the scripting of the IRAF wavelength calibration process, the `split` method also performs row cropping to exclude CCD regions which are not exposed to light, and creates files listing the split *O*- and *E*-beam FITS files which may be passed to the IRAF task inputs. Row cropping was decided on as IRAF does not handle rows with no exposure well, specifically when it comes to the autonomous `reidentify` task. The full STOPS `split` class docstring is given in Listing 3.3.

3.3.2 Joining

After the IRAF `fitcoords` task has been successfully run for both the *O*- and *E*-beams, the STOPS `join` method is used to extract and parse the wavelength solution from the IRAF database, and to create the wavelength calibrated FITS files required by the POLSALT pipeline. More specifically, the `join` method performs the following steps:

First, `join` parses the wavelength database file, described in § 3.2.3, for either a 'Chebyshev' or 'Legendre' solution, and calculates the wavelength at each (x_p, y_p) pixel position. This new image containing the corresponding wavelength values, seen in Figure 3.10, is appended to the wavelength calibrated FITS file as the 'WAV' extension.

Listing 3.4: The 'docstring' for **join.py**

```
The `Join` class allows for the joining of previously split files and the appending of
an external wavelength solution in the `polsalt` FITS file format.

Parameters
----------
data_dir : str | Path
    The path to the data to be joined
database : str, optional
    The name of the `IRAF` database folder.
    (The default is "database")
fits_list : list[str], optional
    A list of pre-reduced `polsalt` FITS files to be joined within `data_dir`.
    (The default is ``None``, `Join` will search for `mxgbp*.fits` files)
solutions_list: list[str], optional
    A list of solution filenames from which the wavelength solution is created.
    (The default is ``None``, `Join` will search for `fc*` files within the `database` directory)
split_row : int, optional
    The row along which the data of each extension in the FITS file was split.
    Necessary when Joining cropped files.
    (The default is 517, the SALT RSS CCD's middle row)
save_prefix : dict[str, list[str]], optional
    The prefix with which the previously split `O`- & `E`-beams were saved.
    Used for detecting if cropping was applied during the splitting procedure.
    (The default is SAVE_PREFIX (See Notes))
verbose : int, optional
    The level of verbosity to use for the Cosmic ray rejection
    (The default is 30, I.E. logging.INFO)

Attributes
----------
fc_files : list[str]
    Valid solutions found from `solutions_list`.
custom : bool
    Internal flag for whether `solutions_list` uses the `IRAF` or a custom format.
    See Notes for custom solution formatting.
    (Default (inherited from `solutions_list`) is False)
arc : str
    Deprecated. Name of arc FITS file within `data_dir`.
data_dir
database
fits_list
split_row
save_prefix

Methods
-------
get_solutions(wavlist: list | None, prefix: str = "fc") -> (fc_files, custom): tuple[list[str], bool]
    Parse `solutions_list` and return valid solution files and if they are non-`IRAF` solutions.
parse_solution(fc_file: str, x_shape: int, y_shape: int) -> tuple[dict[str, int], np.ndarray]
    Loads the wavelength solution file and parses keywords necessary for creating the wavelength extension.
join_file(file: os.PathLike) -> None
    Joins the files, attaches the wavelength solutions, performs cosmic ray cleaning, masks the extension,
    and checks cropping performed in `Split`. Writes the FITS file in a `polsalt` valid format.
check_crop(hdu: pyfits.HDUList, o_file: str, e_file: str) -> int
    Opens the split `O`- and `E`-beam FITS files and returns the amount of cropping that was performed.
process() -> None
    Calls `join_file` on each file in `fits_list` for automation.

Other Parameters
----------------
no_arc : bool, optional
    Deprecated. Decides whether the arc frames should be processed.
    (The default is False, `polsalt` has no use for the arc after wavelength calibrations)
**kwargs : dict
    keyword arguments. Allows for passing unpacked dictionary to the class constructor.

Notes
-----
Constants Imported (See utils.Constants):
    DATADIR,
    SAVE_PREFIX,
    SPLIT_ROW,
    CR_PARAMS

Custom wavelength solutions must be formatted containing:
    `x`, `y`, *coefficients...
where a solution are of order (`x` by `y`) and must contain x*y coefficients, all separated by newlines.
The name of the custom wavelength solution file must contain either "cheb" or "leg"
for Chebyshev or Legendre wavelength solutions, respectively.

Cosmic ray rejection is performed using lacosmic [1]_ implemented in ccdproc via astroscrappy [2]_.

References
----------
.. [1] van Dokkum 2001, PASP, 113, 789, 1420
       (article : https://adsabs.harvard.edu/abs/2001PASP..113.1420V)
.. [2] https://zenodo.org/records/1482019
```

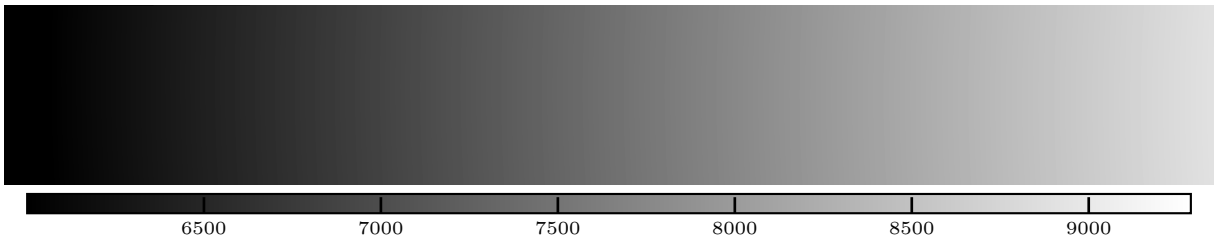

(a) The *O* polarimetric beam.

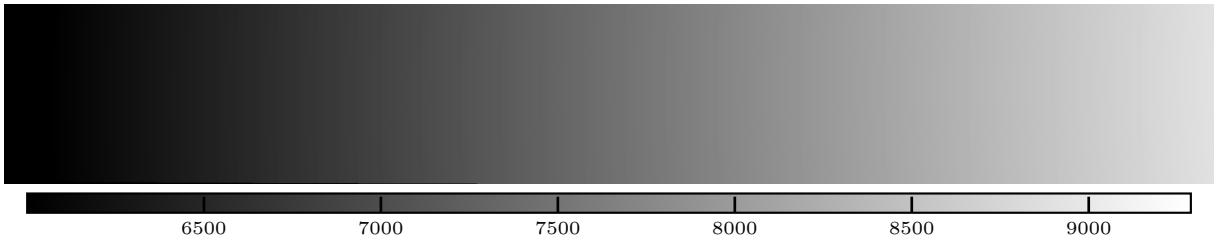

(b) The *E* polarimetric beam.

Figure 3.10: A representative 'WAV' extension of a FITS file, for the *O*- (a) and *E*-beam (b), ready to be processed by the POLSALT pipeline. The color bars show the wavelength in Å. Note that regions which fall outside the exposed region are masked by setting the corresponding pixel values of the wavelength and 'BPM' extensions to 0. Figure created from the STOPS `join` method output.

Second, cosmic-ray cleaning is performed on the 'SCI' extension using the `ccdproc` implementation of the `lacosmic` Python package which implements the L.A. Cosmic algorithm, based on Laplacian edge detection. The read noise and gain parameters used for cosmic ray cleaning were chosen based on the properties of the RSS, while the rest of the parameters were left as the default, following the publication and suggestions[15] by the algorithm's creator, as well as the implementation of the algorithm in the python `ccdproc` package (McCully et al., 2018; van Dokkum, 2001). The chosen parameters work well for most cosmic rays, as can be seen when comparing Figure 3.9 to Figure 3.11, but may be modified as needed.

Next, `join` updates the headers to be near-identical to those created by the POLSALT `wavelength calibration`, most notably updating the data shape, 'CTYPE3', and data type, 'BITPIX', keywords. The only difference in the header is the 'NAXIS2' keyword, due to the cropping performed by `split`. The cropped region could be reintroduced but would be masked out and further discarded in the following POLSALT `spectra extraction` process, making it redundant.

Finally, the 'WAV' extension is masked to remove any uncalibrated wavelength regions as well as masked for the skewing of the trace introduced by the wollaston element. The masking of the wollaston skewing is necessary since POLSALT introduces a wollaston correction in the `spectra extraction` process. The 'BPM' extension is masked to reflect the valid wavelength calibrated region, and the files are saved with the POLSALT wavelength calibrated 'wmxgbp' prefix. The full STOPS `join` class docstring is given in Listing 3.4.

Listing 3.5: The 'docstring' for **skylines.py**

```
Class representing the Skylines object.

Parameters
----------
data_dir : Path
    The directory containing the data files.
filenames : list[str]
    The list of filenames to be processed.
beam : str, optional
    The beam mode, by default "OE".
plot : bool, optional
    Flag indicating whether to plot the continuum, by default False.
save_prefix : Path | None, optional
    The prefix for saving the data, by default None.
**kwargs
    Additional keyword arguments.

Attributes
----------
data_dir : Path
    The directory containing the data files.
fits_list : list[str]
    The list of fits file paths.
beams : str
    The beam mode.
can_plot : bool
    Flag indicating whether to plot the continuum.
save_prefix : Path | None
    The prefix for saving the data.
wav_unit : str
    The unit of wavelength.

Methods
-------
checkLoad(self, path1: str) -> np.ndarray:
    Checks and loads the data from the given path.
transform(self, wav_sol: np.ndarray, spec: np.ndarray) -> np.ndarray:
    Transforms the input wavelength and spectral data based on the given wavelength solution.
rmvCont(self) -> np.ndarray:
    Removes the continuum from the spectrum.
process(self) -> None:
    Placeholder method for processing the data.

See Also
--------
matplotlib custom style:
    https://matplotlib.org/stable/users/explain/customizing.html

Notes
-----
Constants imported (see utils.Constants):
    SAVE_SKY:
        The default save name for the skylines plot.
    FIND_PEAK_PARAMS:
        The default parameters for finding peaks in the spectrum.
```

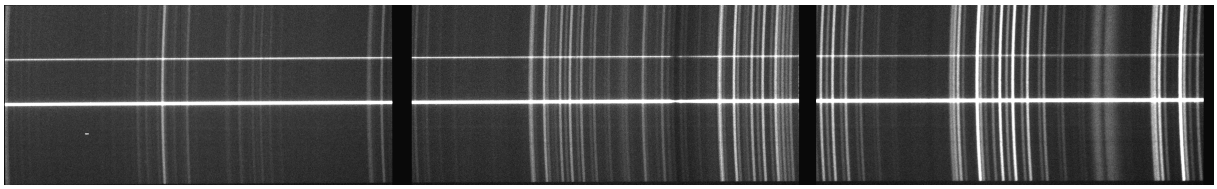

(a) The *O* polarimetric beam.

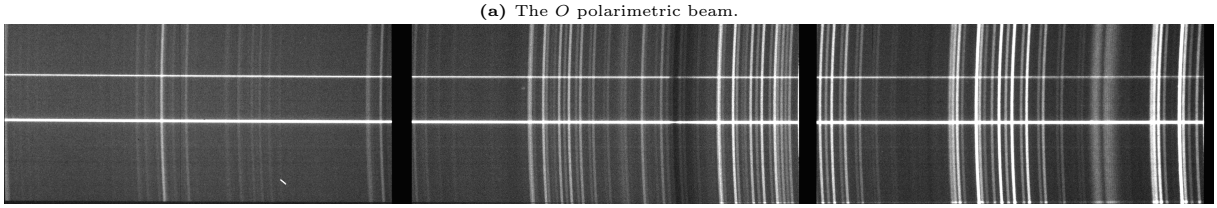

(b) The *E* polarimetric beam.

Figure 3.11: A representative 'SCI' extension of a FITS file, for the *O*- (a) and *E*-beam (b), ready to be processed by the POLSALT pipeline. The observed intensity is displayed via the grayscale value at each pixel. Figure created from the STOPSjoin method output.

3.3.3 Sky Lines

The `skyline` method has been implemented to compare the position of the sky lines on the 'SCI' extension, or arc lines in the arc exposure, to the known positions of the sky lines, or arc lines, as measured by *SALT*, respectively.[16] This provides an additional check of the accuracy of the wavelength solution across the frame. This method accepts both the IRAF `transform` FITS file or the 'wmxgbp' FITS files created by the `join` method as the input.

The `skyline` method loads the wavelength calibrated files, masks the traces present in the frames, transforms the frames from (x_p, y_p) pixel to (Å, y_p) wavelength units if the frame was not transformed by `transform`,[17] and compares the peak wavelength position of the sky lines to the reference sky lines as measured by *SALT*. Finally, a figure is created containing a plot of the background spectra (offset by the respective legend entries superscript) with the known sky lines marked with a vertical line, and a plot of the closest identified peaks of said spectra.

Minor variations in the comparison of the sky lines are expected, such as those seen in Figure 3.12, but any uniform trends, such as those in Figure 3.13 (bottom left), indicate an underlying poor fit across the horizontal axis of the wavelength solution. The full STOPS `skyline` class docstring is given in Listing 3.5.

3.3.4 Cross Correlation

The `skyline` method allows for confirmation of a single wavelength solution, but has no means for comparing how the wavelength solutions of two polarization beams differ from each other. As the Stokes results, and thus final polarization results, are determined by the difference between the *O*- and *E*-beams, a direct comparison is not appropriate.

[15] Suggested parameters for the `lacosmic` algorithm may be found at http://www.astro.yale.edu/dokkum/lacosmic/pars.html.

[16] Both sky and arc lines are available at https://astronomers.salt.ac.za/data/salt-longslit-line-atlas/ .

[17] The transformation applied by the `skyline` method uses linear interpolation and is thus less accurate at flux conservation than the transformation applied by the `transform` method.

Listing 3.6: The 'docstring' for **cross_correlate.py**

```
Cross correlate allows for comparing the extensions of multiple FITS files,
or comparing the $O$- and $E$-beams of a single FITS file.

Parameters
----------
data_dir : str | Path
    The path to the data to be cross correlated
filenames : list[str]
    The ecwmxgbp*.fits files to be cross correlated.
    If only one filename is defined, correlation is done against the two polarization beams.
split_ccd : bool, optional
    Decides whether the CCD regions should each be individually cross correlated.
    (The default is True, which splits the spectrum up into its separate CCD regions)
cont_ord : int, optional
    The degree of a chebyshev to fit to the continuum.
    (The default is 11)
plot : bool, optional
    Decides whether the continuum fitting should be plotted
    (The default is False, so no continua plots are displayed)
save_prefix : str, optional
    The name or directory to save the figure produced to. "." saves a default name to the current working.
    A default name is also used when save_prefix is a directory.
    (The default is None, I.E. The figure is not saved, only displayed)

Attributes
----------
data_dir
fits_list
beams : str
    The mode of correlation. 'OE' for same file, and 'O' or 'E' for different files but same extension.
ccds : int
    The number of CCD's in the data. Used to split the CCD's if split_ccd is True.
cont_ord : int
    The degree of the chebyshev to fit to the continuum.
can_plot : bool
    Decides whether the continuum fitting should be plotted
offset : int, DEPRECATED
    The amount the spectrum is shifted, mainly to test the effect of the cross correlation.
    (The default is 0, I.E. no offset introduced)
save_prefix
wav_unit : str
    The units of the wavelength axis.
    (The default is Angstroms)
wav_cdelt : int
    The wavelength increment.
    (The default is 1)
alt : Callable
    An alternate method of cross correlating the data.
    (The default is None)

Methods
-------
load_file(filename: Path) -> tuple[np.ndarray, np.ndarray, np.ndarray]
    Loads the data from a FITS file.
get_bounds(bpm: np.ndarray) -> np.ndarray
    Finds the bounds for the CCD regions.
remove_cont(spec: list, wav: list, bpm: list, plot_cont: bool) -> None
    Removes the continuum from the data.
correlate(filename1: Path, filename2: Path | None = None) -> None
    Cross correlates the data.
ftcs(filename1: Path, filename2: Path | None = None) -> None
    Cross correlates the data using the Fourier Transform.
plot(spec, wav, bpm, corrdb, lagsdb) -> None
    Plots the data.
process() -> None
    Processes the data.

Other Parameters
----------------
offset : int, optional
    The amount the spectrum is shifted, mainly to test the effect of the cross correlation.
    (The default is 0, I.E. no offset introduced)
**kwargs : dict
    keyword arguments.
    Allows for passing unpacked dictionary to the class constructor.
    ftcs : bool, optional
        Boolean whether to use Fourier Transform for cross correlation.

See Also
--------
scipy - correlation:
    https://docs.scipy.org/doc/scipy/reference/generated/scipy.signal.correlate.html

matplotlib custom style:
    https://matplotlib.org/stable/users/explain/customizing.html

Notes
-----
Constants Imported (See utils.Constants):
    SAVE_CORR:
        The default save name for the correlation plot.
    OFFSET:
        The vertical offset of spectra in the output plot.
```

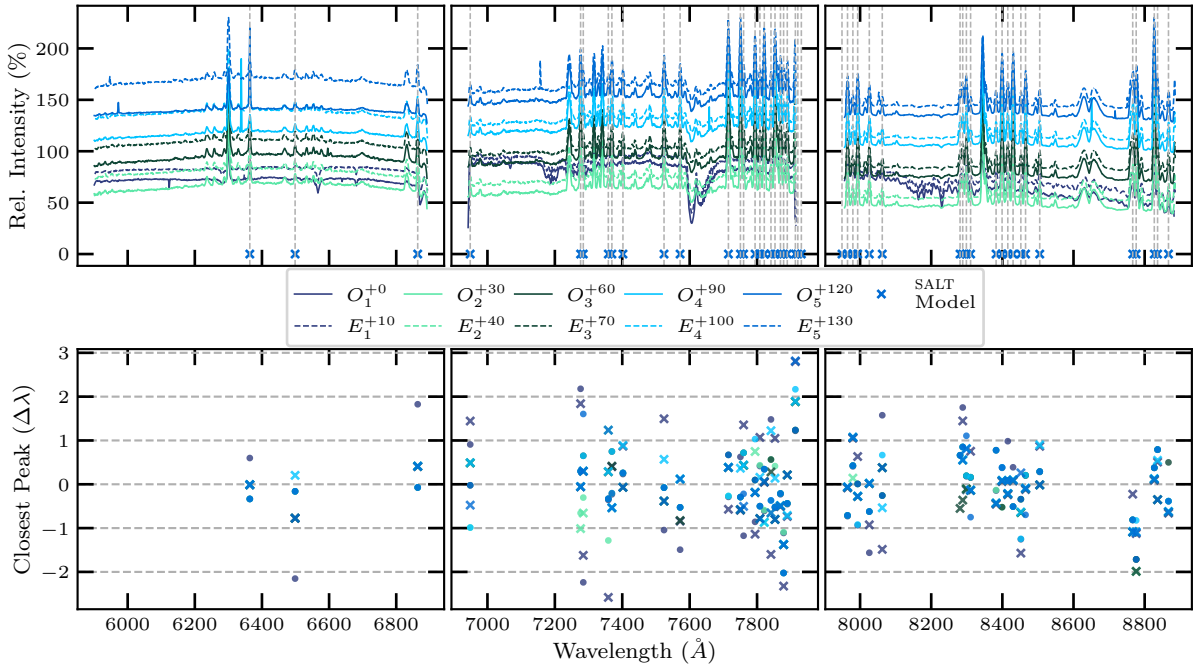

Figure 3.12: An example of a well calibrated wavelength solution, specifically shown for science images. Figure created via the STOPS `skyline` method.

Any observed unpolarized light, however, will reflect equally in both polarization beams and so the general trend of the two spectra may reasonably be expected to follow one another. The `correlate` method was created to allow for comparisons between the wavelength solutions of the *O*- and *E*-beams of a single exposure or the *O*- or *E*-beams of differing exposures by cross correlating the spectra.

The `correlate` method loads the POLSALT `spectra extraction` FITS files, removes the continuum and separates the CCD regions. The relevant CCD regions are cross correlated and the correlation peak is plotted and specified in the plot legend, as seen in Figure 3.14.

Sources under spectropolarimetric observation are generally expected to vary over time and, as such, the ratio of polarized to unpolarized light is also expected to vary. The accuracy of correlation may decrease as features with differences in the polarized component of the polarization beams change, and it is up to the user to determine the validity of the correlation result taking into consideration the two spectra being correlated. The differences in the features of the different spectra are often negligible when compared to the overall continuum of the spectra and are generally only reflected in a change in the intensity of said features when the continuum is removed. The full STOPS `split` class docstring is given in Listing 3.6.

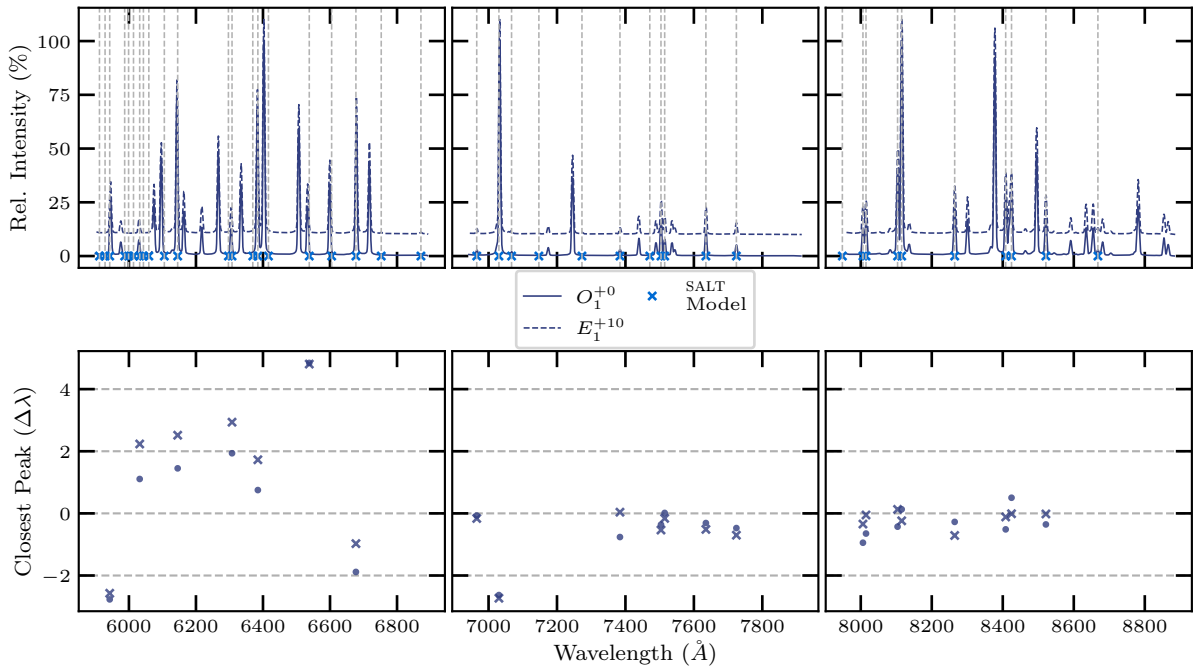

Figure 3.13: An example of a wavelength solution with a poor fit at shorter wavelengths (bottom left), specifically shown for an arc image. Arc lines are Figure created via the STOPS `skyline` method.

3.4 General Reduction Procedure

This section aims to provide a comprehensive discussion of the modified reduction procedure, an example of which is provided in Appendix A. As users all employ a variety of operating systems, language environments, and software setups, not much emphasis will be placed on how to get the software running or the managing of files; instead, the general order, seen in Figure 3.15, and commands necessary to complete each step of the reduction process are discussed, assuming that the software is running as intended.

3.4.1 Initial Setup

It is important to note that while POLSALT was developed in Python 2 (2.7), the STOPS supplementary tools were developed in, and require, Python 3 (3.11+), as well as the other requirements mentioned in § 3.3. While managing multiple versions of Python introduces some extra complication, it would not have been reasonable to develop STOPS in Python 2, as it has been deprecated, nor would it have been reasonable to update POLSALT to Python 3.

It is therefore recommended that the different versions of Python are managed using separate virtual environments. While the `anaconda` package manager was used in this study and is recommended, any package manager may be used. The `anaconda` environments are aliased '**salt**' for Python 2.7 and '**stops**' for Python 3.11. When Listings are provided (see for example Listing A.1 or the Listings in § 3.4.2 below), the `anaconda` environment is activated at the start of the Listing, otherwise it is assumed the previously specified environment is still active.

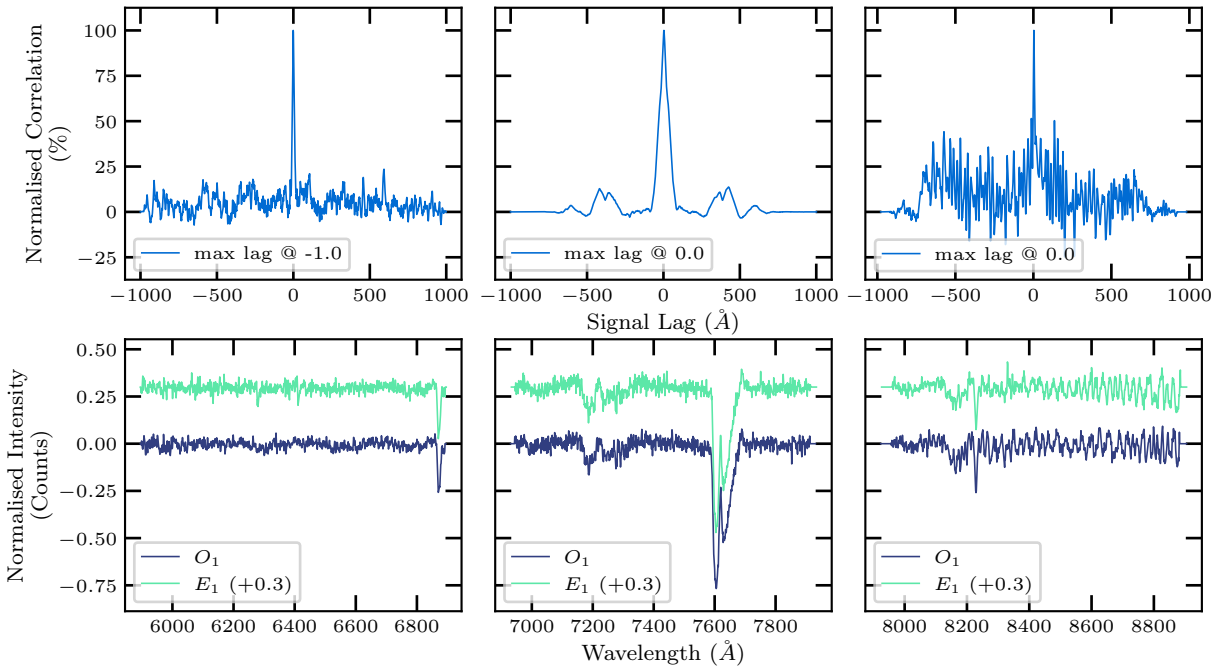

Figure 3.14: The resultant output plot of the STOPS `correlate` method. Figure created via the STOPS `correlate` method.

It is recommended to use POLSALT through the GUI as it provides a user-friendly environment while also sequentially listing each step of the reduction process in a dropdown menu, as seen in Figure 3.1. Reductions are possible, however, purely through the CLI using the POLSALT 'beta' scripts.

3.4.2 POLSALT Pre-Reductions

The POLSALT reduction process requires a file structure such that the raw data received from *SALT* is located in a folder named using the observing date with a sub-folder named raw, following the format `YYYYMMDD/raw/`. This directory structure allows POLSALT to create a 'working' directory following the format `YYYYMMDD/sci/` which contains all the files modified during the reduction process. Multiple reduction procedures using the same data may therefore be separated by simply renaming the `sci/` sub-folder.

The POLSALT GUI may be launched by opening a CLI and running the commands given in Listing A.1. Once the window, depicted in Figure 3.1, has launched, ensure that the first two paths at the top of the window point to the POLSALT and working directories, as seen in Figure 3.1. The 'raw image reduction' entry may then be selected from the dropdown menu and the pre-reductions run.

Alternatively, if the data already includes 'mxgbp' FITS files in the `YYYYMMDD/sci/` working directory, a CLI may be used to complete the initial pre-reductions using

```
$ cd <OBSDATE>/sci
$ conda activate salt
$ python ~/polsalt/scripts/reducepoldata_sc.py <OBSDATE>
```

which will start the full POLSALT reduction process. This process is quit once the POLSALT `wavelength calibration` GUI opens, and the alternate wavelength calibration procedure is followed.

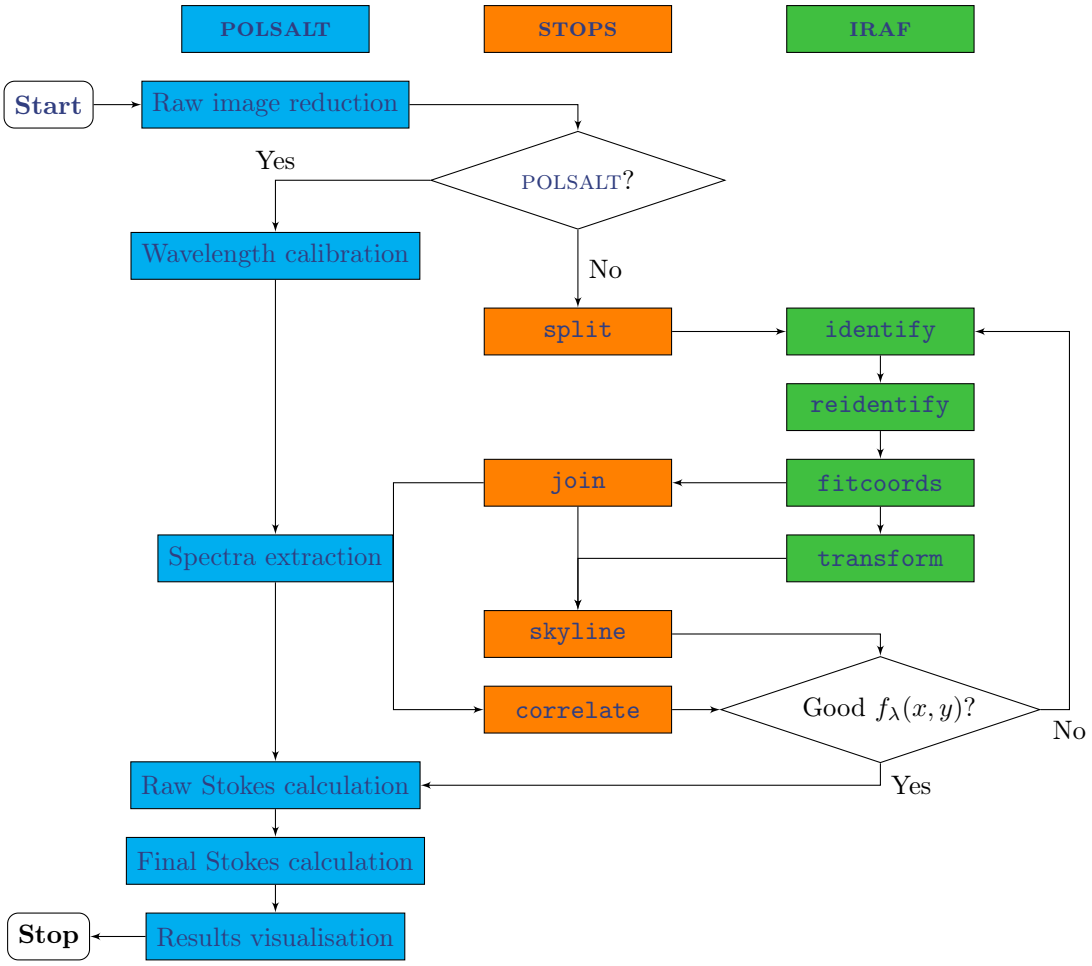

Figure 3.15: A general workflow for data reductions using a combination of POLSALT, IRAF, and STOPS. Diagram adapted from Cooper et al. (2022).

3.4.3 Wavelength Calibration

The wavelength calibrations may now be completed in IRAF. This section concerns the procedure for parsing the FITS files to and from both IRAF and POLSALT, as well as the relevant task names and methods to be run to complete the calibrations. A base working case of each of the tasks and methods are presented in Listing A.2 to A.8, but it should be noted that the art of wavelength calibration consists of modifying the parameters to achieve a well-fit calibration function.

Preparing the Data for IRAF

Splitting the data is presented in Listing A.2. The STOPS `split` method may take multiple parameters, as seen in § 3.3, but default parameters should be used wherever possible. The most notable parameters are the directory, which defaults to the current working directory of the CLI, the split row, which defaults to POLSALT's default center row, and the save prefix, which defaults to '`obeam`' and '`ebeam`'.

IRAF Wavelength Calibrations

The IRAF wavelength calibrations are performed using the tasks described in § 3.2, namely the `identify`, `reidentify`, `fitcoords`, and optionally `transform` tasks.

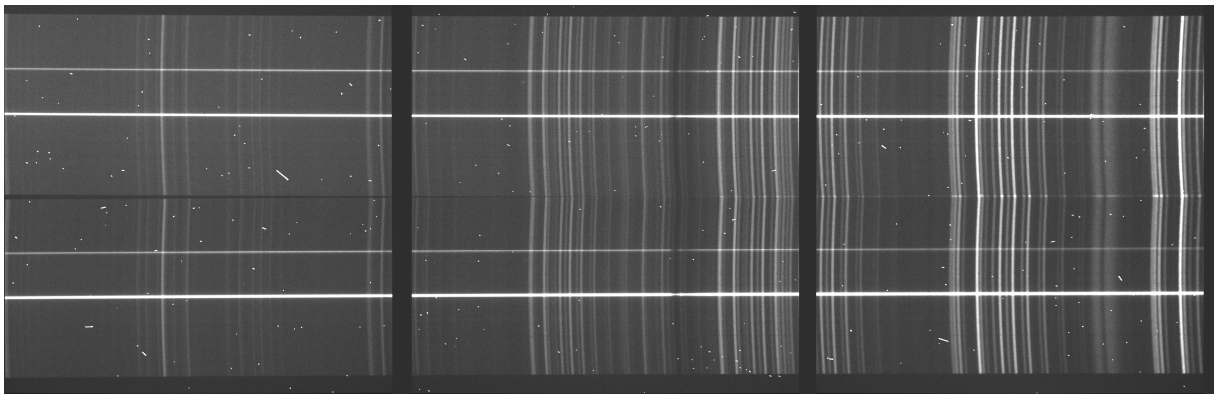

Figure 3.16: The 'SCI' extension of a typical spectropolarimetric FITS file taken with the *SALT* RSS, after basic POLSALT CCD reductions have been completed. Figure created from the STOPS `split` output.

In general, these tasks are run directly in the IRAF terminal using:[18]

```
cl> identify arc_files
cl> reidentify arc_ref arc_files
cl> fitcoords arc_files fit_2d
cl> transform files tr_file fit_2d
```

where 'arc_files' refers to a list or file containing the FITS files relevant to the task, 'arc_ref' refers to the FITS file previously identified, 'fit_2d' refers to the name to be used for the final two-dimensional wavelength solution, and 'tr_file' refers to the new name for the transformed input 'files'.

The interactive tasks take up the bulk of the reduction time as this is where the fine-tuning of the reduction is done, through the use of cursor (or colon) commands, which allow modification of the parameters mid-reduction. Task parameters may, however, be edited beforehand within the IRAF terminal using the `eparam` task, and optionally saved, and quit or run using a combination of `:w`, and `:q` or `:go` cursor commands, respectively.

The reduction process in Appendix A, namely Listing A.4 to A.7, describes how the tasks may be scripted and saved for posterity. It is recommended to create an IRAF Command Language (cl) script for each task to keep track of which parameters were used and for simple recalibrations. The scripts are created using the `mkscript` task which interactively asks for a task to script and parameters to use. Multiple tasks may be appended to an IRAF script, allowing for the parameters of both beams to be tracked.

Running an IRAF script may be done by running:

```
cl> cl < script_name.cl
```

but is not suggested for interactive scripts, which run best when simply copied from the `<.../>sci/script_name.cl` file to the IRAF terminal.

[18] Please see the IRAF help docs, available at https://astro.uni-bonn.de/~sysstw/lfa_html/iraf/iraf.html, on the relevant tasks for a comprehensive discussion of the parameters available.

Preparing the Data for POLSALT

After the wavelength calibrations have been completed, the wavelength solution is parsed back into the format expected by POLSALT. Joining the separate beams with their respective wavelength solutions is performed in the CLI following Listing A.8.

Similar to the `split` procedure, the `join` procedure has the same defaults defined. The onus of keeping track of any previously changed default parameters falls to the user, but logging is implemented in STOPS (see the discussion on help documentation in § 3.3) which allows for later reference of any changed parameters.

Sky Line Checks

The optional IRAF `transform` task and STOPS `skylines` method are used to confirm the wavelength solution across the frame (see § 3.3.3) by transforming and comparing known and observed sky line wavelength positions, respectively.

The `skyline` method is run in the CLI following Listing A.9. As with the rest of STOPS, default parameters describe the overplotting behavior for the *O*- and *E*-beams, the skylines provided by *SALT*, and the calculated variation of the wavelength axis of a frame.

Cross Correlation Checks

The `correlate` method is run in the CLI following Listing A.11. The input of the `correlate` method takes the output of the POLSALT `spectra extraction` and is thus only run thereafter, but is mentioned here as the completion of the POLSALT reductions is not discussed in much depth. If the user wishes to compare the *O*- and *E*-beams of a single file then only that image name is to be provided, otherwise it is assumed that the user wishes to compare the same polarization beam across each file provided.

Cleaning Up the IRAF and STOPS Output

Before the final POLSALT reductions, it is recommended that the user 'clean up' the `sci/` directory of all IRAF and STOPS files since the 'wmxgbp' FITS files are all that is expected by POLSALT. The POLSALT methods use wildcard file collection and as such any errant detections of files added by the user will result in unexpected crashes. It is suggested to move any additional files to a new subfolder following Listing A.10, but they may also be removed using:

```
$ rm beam*.fits arc*.fits frame* <any user created files>
```

3.4.4 POLSALT Reduction Completion

Reductions may now be completed using POLSALT. The reduction process consists of correcting for the wollaston tilt, extracting the spectra, creating the Stokes files, and displaying the results. The 'beta' version of POLSALT provides access to a GUI but may also be handled entirely through a CLI as scripts.

Listing 3.7: The modified `reducepoldata_sc.py` script file.

```
import os, sys, glob, shutil
poldir = '/home/justin/polsalt-beta/'                              # Will differ according to user

reddir=poldir+'polsalt/'
scrdir=poldir+'scripts/'
sys.path.extend((reddir,scrdir,poldir))

datadir = reddir+'data/'
import numpy as np
from astropy.io import fits as pyfits
from specpolview import printstokes
from imred import imred
from specpolwavmap import specpolwavmap
from specpolextract_sc import specpolextract_sc
from specpolrawstokes import specpolrawstokes
from specpolfinalstokes import specpolfinalstokes

print sys.argv
obsdate = sys.argv[1]
print obsdate
os.chdir(obsdate)
if not os.path.isdir('sci'): os.mkdir('sci')
shutil.copy(scrdir+'script.py','sci')
os.chdir('sci')

#basic image reductions
infilelist = sorted(glob.glob('../raw/P*fits'))
imred(infilelist, './', datadir+'bpm_rss_11.fits', crthresh=False, cleanup=True)

#basic polarimetric reductions
logfile='specpol'+obsdate+'.log'

                                                                   # The following lines may be removed or commented out as below
# #wavelength map
# infilelist = sorted(glob.glob('m*fits'))
# linelistlib=""
# specpolwavmap(infilelist, linelistlib=linelistlib, logfile=logfile)

#background subtraction and extraction
infilelist = sorted(glob.glob('wm*fits'))
extract = 10.   # star +/-5, bkg= +/-(25-35)arcsec:  2nd order is 9-20 arcsec away
locate = (-120.,120.)    # science target is brightest target in whole slit
#locate = (-20.,20.)

specpolextract_sc(infilelist,logfile=logfile,locate=locate,extract=extract)
#specpolextract_sc(infilelist,logfile=logfile,locate=locate,extract=extract,docomp=True,useoldc=True)

#raw stokes
infilelist = sorted(glob.glob('e*fits'))
specpolrawstokes(infilelist, logfile=logfile)

#final stokes
infilelist = sorted(glob.glob('*_h*.fits'))
specpolfinalstokes(infilelist, logfile=logfile)
```

POLSALT Beta in the GUI

The reduction process using the POLSALT GUI is completed by selecting and, when applicable, interactively modifying the reduction step through the interactive windows, one-by-one, from the GUI's dropdown menu, as explained in Appendix A (p. 90 onwards).[19]

POLSALT Beta through a CLI

Both GUI and CLI implementations of the POLSALT beta pipeline access the same script files. Although the GUI is more user-friendly, the CLI offers a more streamlined approach to the reduction process, allowing the reduction process to be automated once the IRAF wavelength solution is known and parsed into the 'wmxgbp' FITS file format. A modified version of the POLSALT beta `reducepoldata_sc.py` script (see Listing 3.7) is used to run the entire reduction process without needing to select which process to run next, using:

```
$ python reducepoldata_sc.py YYYYMMDD
```

where the only modification made to the `reducepoldata_sc.py` script file is the removal of a call to the `specpolwavmap` method.

[19] See the official POLSALT wiki or alternative online resources such as the *SALT* workshop slides.

The POLSALT beta `reducepoldata_sc.py` copies a `script.py` file into the science working directory, 'YYYYMMDD/sci/', which provides analysis scripts for analysis and modification of the POLSALT beta results. These tools consist of data culling for the final Stokes calculations, text and plot output, relative flux calibration corrections, and synthetic filtering of polarization results.

The POLSALT analysis scripts may be run using:

```
$ python script.py
```

followed by `specpolfinalstokes.py`, `specpolview.py`, `specpolflux.py`, or `specpolfilter.py`, for the different analysis modes, respectively.[20]

[20] Please see https://github.com/saltastro/polsalt/wiki/Linear-Polarization-Reduction.--Beta-version for a comprehensive discussion of the POLSALT beta analysis scripts.

Chapter 4

Testing and Application

This chapter contains an overview of the tests performed during the development of STOPS which includes the verification of the modified wavelength solutions (§ 4.1), as well as the application of STOPS on observations of both a spectrophotometric standard and science targets 4.2.

4.1 Testing STOPS

A fundamental requirement during the development of STOPS was ensuring that the software was compatible with both the POLSALT and IRAF file structures and that the 'reduction-specific' methods, namely the STOPS `split` and `join` methods, provided correct and consistent results. As development is an iterative process, STOPS was continually checked to ensure compatibility such that the varying STOPS method inputs were correctly parsed, and that their outputs were parsable by the relevant IRAF tasks or POLSALT methods.

To this end, observations which were verified to have been accurately reduced were duplicated for testing the 'reduction-specific' methods, allowing for continual checks of the STOPS pipeline to be made during the development process. The testing of the 'reduction-specific' methods are discussed in § 4.1.1 and § 4.1.2, respectively.

The secondary requirement during the development of STOPS was to provide a means to check the wavelength solutions. This was achieved through the 'check-specific' methods, namely the STOPS `correlate` and `skylines` methods, which were designed to validate the IRAF wavelength solutions, specifically after re-insertion of the wavelength solutions back into the POLSALT FITS file format. The file format distinction is necessary as IRAF provides immediate confirmation of the wavelength solutions during calibration through interactive RMS plots (see e.g. Figure 3.6, 3.7), as well as the transformation of the spectra through the `transform` IRAF task, while POLSALT only provides confirmation of the RMS for the interactive line identification during `wavelength calibration`.

The 'check-specific' methods were tested using synthetic spectra, which contained features with known and varying offsets introduced. The features refer to emission lines

Table 4.1: A comparison of the contents of a POLSALT pre-reduced FITS file to the STOPS `split` *O*- and *E*-beam FITS files. Table created using the '`Astropy`' `fitsinfo` CLI tool.

Filename	No.	Name	Type	Cards	Dimensions	Format
POLSALT	0	'Primary'	PrimaryHDU	161	-	-
	1	'SCI'	ImageHDU	19	(3199, 1028)	float32
	2	'VAR'	ImageHDU	8	(3199, 1028)	float32
	3	'BPM'	ImageHDU	8	(3199, 1028)	uint8
STOPS `split` '*O*'	0	'Primary'	PrimaryHDU	162	(3199, 474)	float32
STOPS `split` '*E*'	0	'Primary'	PrimaryHDU	162	(3199, 474)	float32

in the `correlate` related tests and absorption skylines in the `skylines` related tests. The testing of the 'check-specific' methods are discussed in § 4.1.3 and § 4.1.4, respectively.

4.1.1 Testing the `split` Method

The STOPS `split` method accepts any POLSALT pre-reduced ('mxgbp'- prefixed) FITS files as input and outputs IRAF compatible ('[arc|beam][O|E]'- prefixed) FITS file structures. As no 'split' FITS files are created during pure POLSALT reductions, the STOPS `split` method was tested by comparing the pre-reduced POLSALT files to the `split` method's output files, ensuring the correct structure and data integrity of the files handed off to IRAF.

Table 4.1 shows the contents of a FITS file before and after splitting. The split FITS files contain a single 'Primary' extension which holds the respective polarization beams' two-dimensional spectrum as well as a slightly modified copy of the 'Primary' header from the 'pre-split' file. The differences in the header and data are detailed below.

For the split FITS files, the header is left mostly untouched, and is only updated to represent the new data type and shape: the 'BITPIX' value is updated, from 8 to −32, and the 'NAXIS' value is updated, from 0 to 2; the 'NAXIS1' and 'NAXIS2' keywords are added, and their values are set to the new split 'SCI' data shape; and the 'EXTEND' keyword is removed.[1] This accounts for the discrepancy in the 'Cards' between the POLSALT and STOPS file header entries in Table 4.1.

After splitting it was confirmed that the split data was identical to the POLSALT 'pre-split' file by taking the difference between them, which showed a constant difference of zero. Each split FITS file, however, only includes half of the 'pre-split' data, for the relevant *O*- or *E*-polarization beam, with the data also being cropped at the top- and bottom-most rows of the POLSALT data, with the cropping defaulting to 40 pixels (see § 3.3.1). This accounts for the discrepancy in the 'Dimensions' between the POLSALT and STOPS files in Table 4.1.

This output file structure was chosen for IRAF compatibility, and was tested over multiple grating and articulation angles, as well as with various data sets to ensure that the `split` method was robust and reliable.

[1] The 'EXTEND' keyword indicates that the FITS file contains multiple extensions while the 'NAXIS1' and 'NAXIS2' keywords indicate the shape and size of the data stored in the relevant extension.

Table 4.2: A comparison of the POLSALT wavelength calibrated FITS file to the (IRAF wavelength calibrated) STOPS `join` FITS file. Table created using the `Astropy fitsinfo` CLI tool.

Filename	No.	Name	Type	Cards	Dimensions	Format
POLSALT	0	'Primary'	PrimaryHDU	161	-	-
	1	'SCI'	ImageHDU	21	(3199, 514, 2)	float32
	2	'VAR'	ImageHDU	10	(3199, 514, 2)	float32
	3	'BPM'	ImageHDU	10	(3199, 514, 2)	uint8
	4	'WAV'	ImageHDU	21	(3199, 514, 2)	float32
STOPS `join`	0	'Primary'	PrimaryHDU	161	-	-
	1	'SCI'	ImageHDU	21	(3199, 474, 2)	float32
	2	'VAR'	ImageHDU	10	(3199, 474, 2)	float32
	3	'BPM'	ImageHDU	10	(3199, 474, 2)	uint8
	4	'WAV'	ImageHDU	21	(3199, 474, 2)	float32

4.1.2 Testing the `join` Method

The `join` method requires both an IRAF database with wavelength solutions[2] for both polarimetric beams, and the POLSALT pre-reduced files as input, and outputs POLSALT `spectra extraction` compatible ('wmxgbp'- prefixed) FITS files. Ensuring that the output format was correct was paramount as the POLSALT `spectra extraction` method is unable to process the files otherwise, thus halting the reduction process. Thankfully, the `join` method output could be directly compared to the POLSALT `wavelength calibration` method output files, ensuring that any changes introduced by the STOPS pipeline are well characterized.

Table 4.2 shows the FITS file information for both the POLSALT and STOPS wavelength calibrated files. Other than the 'Dimensions' of each 'ImageHDU' extension, the FITS files have identical structures.[3]

Although the 'Cards' count is the same, minor differences across the headers are present. The 'HISTORY' keyword, which would have contained the POLSALT 'CRCLEAN' parameters, and which default to 'upper= 4.0, lower= 1.5, sigmaveto= 2.0', is instead modified to contain the implemented Cosmic Ray Rejection (CRR) parameters.[4]

Other minor differences may arise, such as the date-times stored in the 'SAL-TLM' and 'SMOSAIC' keywords, as they contain the date-times relating to the completion of the POLSALT pre-reductions. This accounts for the differences in the 'Cards' between the POLSALT and STOPS file header entries in Table 4.2.

Figure 4.1 shows the differences in the data between the POLSALT and STOPS wavelength calibrated files. It can be seen that the 'VAR' extensions (Figure 4.1b) are identical. The difference in the 'SCI' extensions (Figure 4.1a) is due to the CRR applied by STOPS

[2] A custom wavelength solution may also be used.

[3] The 'Dimensions' differ due to the aforementioned cropping of the top- and bottom-most rows of the pre-reduced FITS files data.

[4] The POLSALT pipeline performs CRR using a 10σ spike to cull cosmic rays. See the source code of POLSALT for more information.

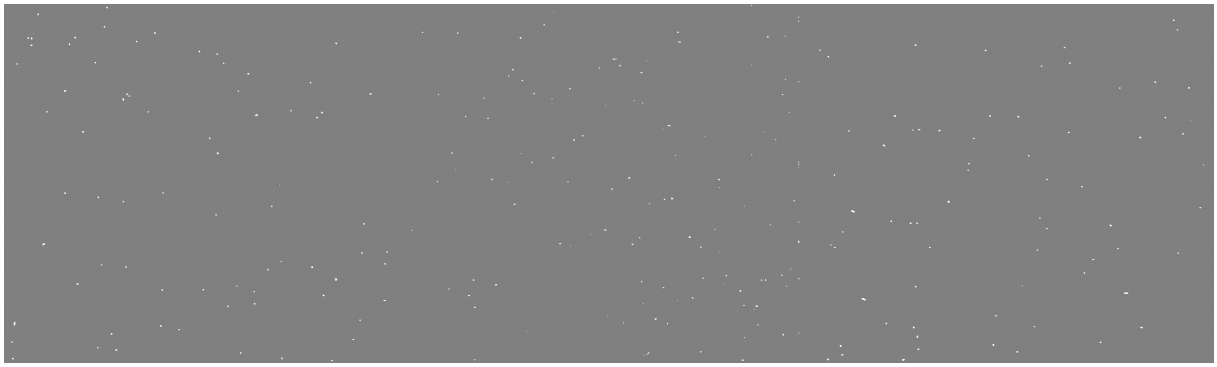

(a) The difference in the 'SCI' extensions.

(b) The difference in the 'VAR' extensions.

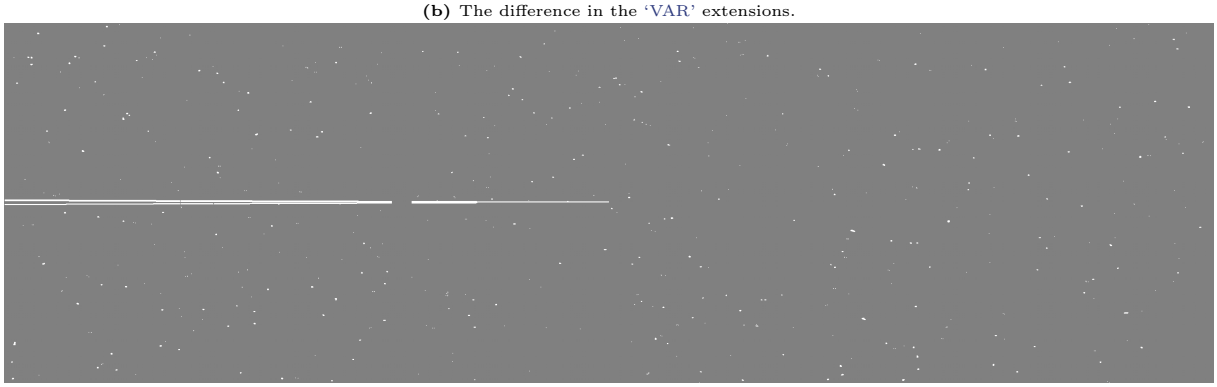

(c) The difference in the 'BPM' extensions.

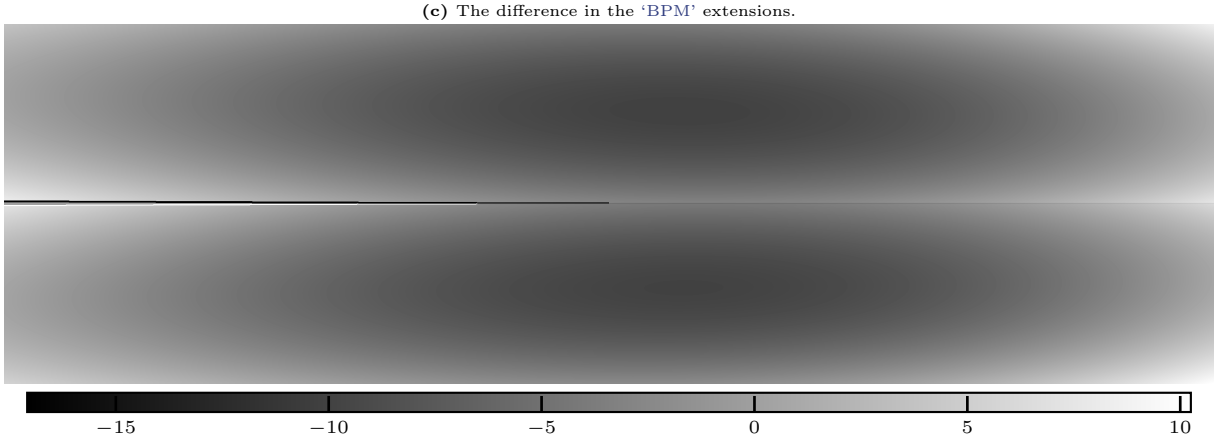

(d) The difference in the 'WAV' extensions.

Figure 4.1: The difference of the FITS file extensions between the POLSALT and STOPS ('wmxgbp'- prefixed) wavelength calibrated files. Figures created using both the POLSALT and STOPSversions of the POLSALT `spectral extraction` input.

which rejects cosmic rays from the 'SCI' extension instead of masking the 'BPM' extension (Figure 4.1c) which is the method implemented by POLSALT. The valid wavelength calibrated region is used as a mask and applied to the 'BPM' and 'WAV' extensions (Figure 4.1d). Slight differences arise near the centre of the frames, specifically Figure 4.1c and 4.1d, since the correction for the wollaston tilt, as implemented by POLSALT, is re-implemented in Python 3 by STOPS and as such may be affected by rounding differences. The differences are fortunately minor and are at the edges of the two polarimetric spectral regions The 'WAV' extensions contain the differing wavelength solutions and as such naturally differ. This accounts for the differences in the data between the POLSALT and STOPS files.

Finally, the STOPS `join` method was tested to ensure compatibility and correctness of the output data in comparison to POLSALT. This involved testing the `join` method with various data sets, with differing observation configurations, to ensure that the output files were accurate and consistent.

4.1.3 Cross Correlation Checks

The `correlate` method returns plots validating the wavelength solutions and so only has to accept the files output from the POLSALT `spectra extraction` method ('ecwmxgbp'-prefixed files).

The STOPS `correlate` method was tested by cross correlating synthetic *O*- and *E*-beam spectra with known offsets, with the aim of reacquiring said offsets, as shown in Figure 4.2. The spectra were generated with a feature in each CCD region, randomly offset in both the wavelength and intensity axes, Figure 4.2a. The features were purposefully chosen to be of low S/N's and FWHM to test the robustness of the `correlate` method. Non-synthetic spectra will include more features, with higher S/N's and FWHM, and as such will be more robust to the `correlate` method.

Through cross correlation, Figure 4.2b, the introduced offsets, or 'max lag', were reacquired. For spectral regions with few features or features with a low S/N (such as the left most CCD region of Figure 4.2b), correlation may fail to determine the correct offset. When a returned 'max lag' peak is not significant when compared to the noise in the correlation plots, the S/N of the features may be too low for an accurate calculation of the offset.

4.1.4 Sky Line Checks

The `skylines` method returns plots validating the wavelength solutions and so has to accept as input the files output from the STOPS `join` method.

In order to validate the STOPS `skylines` method, a synthetic two-dimension spectrum was created that contained sky lines. This is shown in Figure 4.3a, and consists of an average continuum (10 'counts') with added noise (normal-sampled, $\sigma = 4.5$), skyline emission features (provided by *SALT*, see § 3.3.3), and the characteristic RSS chip gaps. Figure 4.3b shows the result, which successfully retrieves the skyline emission features for the synthetic spectrum. Note that the closest peaks ($\Delta\lambda$) are nearly never 0, since

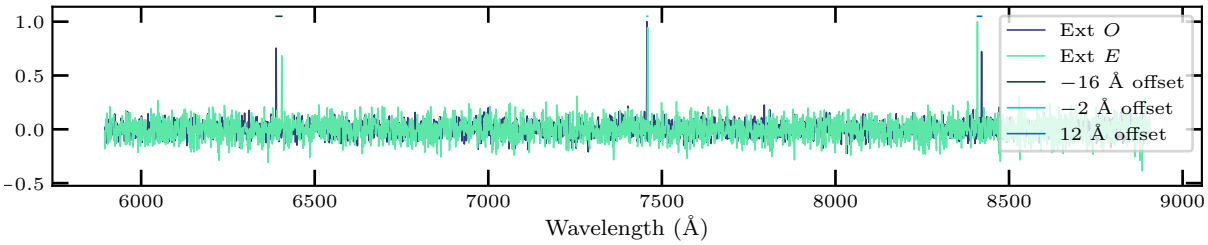

(a) Synthetic O- and E-beam spectra.

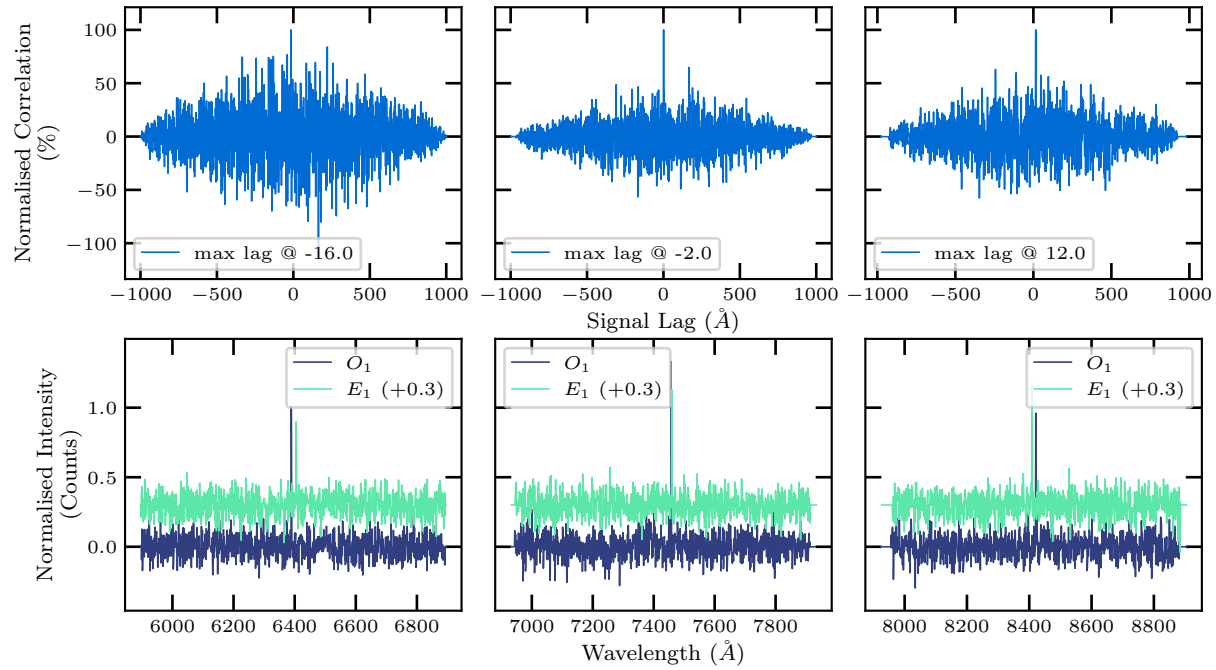

(b) The STOPS `correlate` result for the spectra displayed in a.

Figure 4.2: Reacquisition of offsets introduced to the O- and E-beam spectral features (a) by cross-correlation (b, bottom row).

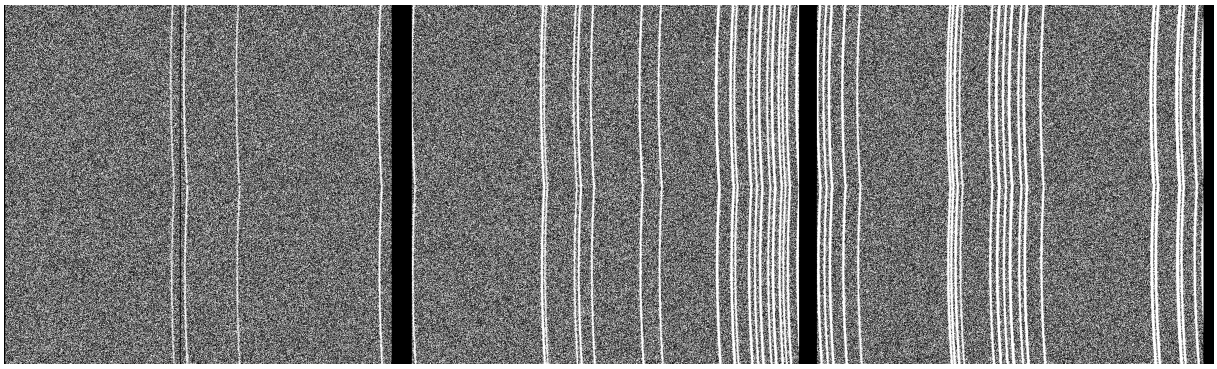

(a) A generated two-dimensional spectrum consisting of noise, skyline emission features, and the characteristic RSS chip gaps.

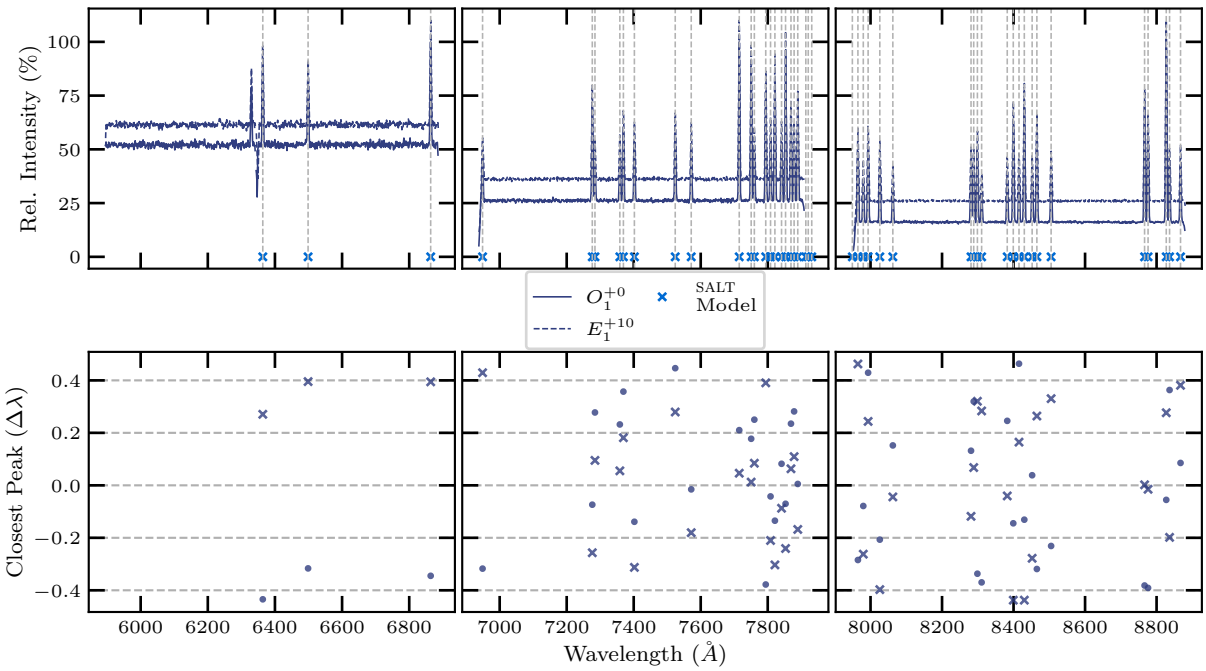

(b) The STOPS `skylines` output for the synthetic spectrum displayed in a.

Figure 4.3: The STOPS `skylines` method output b for a synthetic two-dimensional spectrum a. Figures generated using Python a and the STOPS `skylines` method b.

the skylines are only as accurate as the spectral pixel resolution ($\sim$ 1 Å in our synthetic spectrum) while those as provided by *SALT* are not similarly limited. Additionally, the noise in the spectrum may shift a skylines' peak position, further contributing to, albeit small, discrepancies.

Figure 4.4 shows the result of the STOPS `skylines` method when a constant offset of 4 Å is applied to all skyline emission features in Figure 4.3a. In general, the offset is recovered, with the minor variation in the closest peaks once again noticed. The closest peaks near $\Delta\lambda \sim -4$ Å are the most notable outliers, and are due to misidentifications of skyline features with neighbors closer than 8 Å.

4.2 Application of STOPS

The STOPS pipeline has been utilized for the reduction of a number of sources: this includes calibration tests using spectropolarimetric standards; and for scientific observations of transient sources, specifically Gamma-ray Burst's (GRB) and blazars. The following

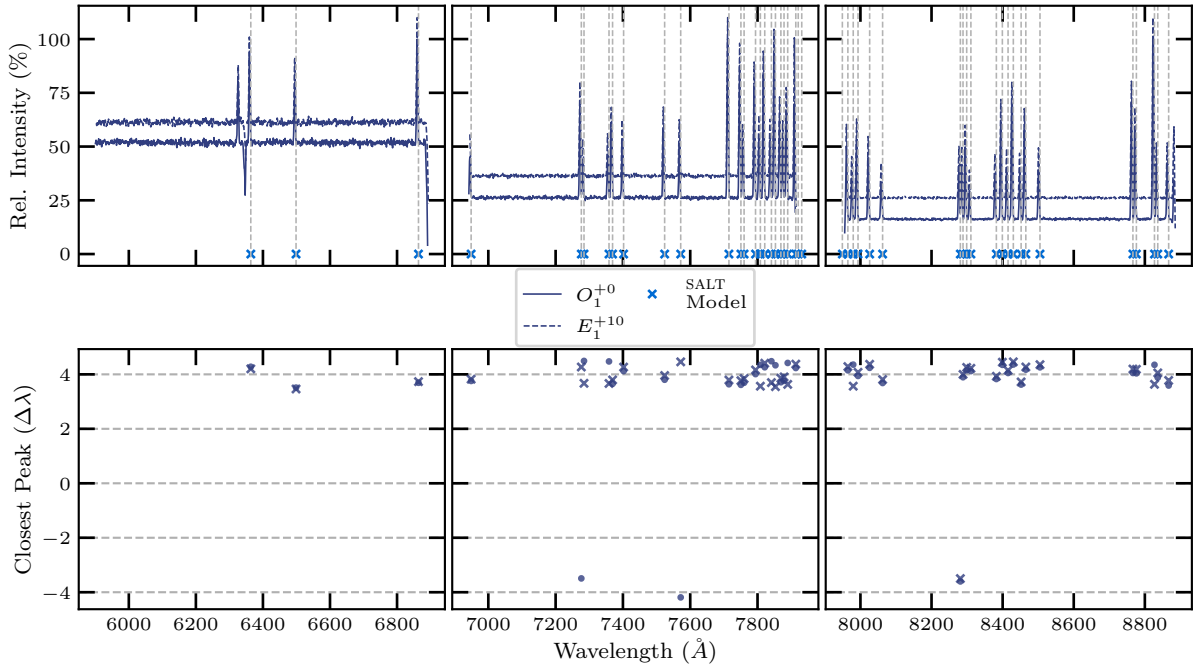

Figure 4.4: The STOPS `skylines` output for a two-dimensional spectrum, as described in Figure 4.3b, with a constant offset of 4 Åapplied to all skyline emission features. Figure created using the STOPS `skylines` method.

sections summarize works in which observations were analysed using, in part, the STOPS pipeline with IRAF wavelength calibrations, or from which the STOPS pipeline was developed. The list of sources observed are summarized in Table 4.3. In addition to the results discussed here, the STOPS pipeline has also been extensively used for the analysis of the blazers presented in Barnard et al. (2022, 2024).

4.2.1 Spectropolarimetry and Photometry of the Early Afterglow of the Gamma-ray Burst GRB 191221B (Buckley et al., 2021)

Buckley et al. (2021) discusses the spectropolarimetric and photometric results of the early afterglow of GRB 191221B, a γ-ray burst initially detected by the Neil Gerhels Swift Observatory (*Swift*) Burst Alert Telescope (BAT) (Barthelmy et al., 2005) on 2019 December 21 (Laha et al., 2019). The afterglow was observed using the *SALT* RSS in spectropolarimetric mode $\sim$ 3 h after the initial burst, with observations carried out during the re-brightening phase. Follow-up spectropolarimetric observations were also taken $\sim$ 10 h after the burst using the Very Large Telescope (*VLT*) Focal Reducer and Low Dispersion Spectrograph (FORS).

The *SALT* spectropolarimetric observations were reduced using a modified version of the POLSALT pipeline, allowing for relative flux calibrations of the spectra using the white dwarf, EGGR 21. GRB 191221B was observed at an average polarization level of $1.5 \pm 0.5\%$, and a polarization angle of $60 \pm 10^\circ$ across the $3900 - 8000$ Å. The FORS2 observations showed a similar polarization level (1.2%) and polarization angle (60°) across the $3200 - 9200$ Å wavelength region. These low polarization percentages are expected for afterglows this late, when the emission is understood to be dominated by the forward shock which exhibits no systematic orientation of the magnetic field configuration.

Table 4.3: Sources discussed from proceedings and publications within this section. Table adapted from observations presented in Buckley et al. (2021); Cooper and van Soelen (2023); Cooper et al. (2022); Schutte et al. (2022).

Source	Observation Date	Grating	Grating Angle (°)	Articulation Angle (°)	Exposure Time (sec)
4C +01.02	2016-07-09	PG0300	5.375	10.66	2400.82
	2017-07-25	PG0300	5.375	10.66	2400.83
Hiltner 600	2017-02-24	PG0900	12.500	24.91	135.60
			19.625	39.16	135.60
3C 279	2017-03-28	PG0900	12.498	24.91	480.81
			19.625	39.16	480.80
	2017-04-01	PG0900	12.500	24.92	480.78
			19.625	39.17	480.85
	2017-05-17	PG0300	5.375	10.68	720.84
		PG0900	12.500	24.92	720.83
			19.625	39.17	901.05
	2017-05-21	PG0300	5.375	10.66	1200.81
	2018-06-05	PG0300	5.375	10.72	1200.81
GRB 191221B	2019-12-21	PG0300	5.375	10.71	2400.84
EGGR 21	2020-01-10	PG0300	5.375	10.71	120.20
Hiltner 652	2022-06-10	PG0900	12.878	25.71	48.50

Figure 4.5 shows the normalized spectra of the *SALT* RSS and *VLT* FORS2 observations, offset by ±0.05, respectively. The spectra show a good agreement across the measured position of the proposed absorption features, with the FORS2 spectrum being able to resolve three close pairs of lines, namely, FeII 5096/5114 Å, MgII 5481/5494 Å, and MgII 6002/6018 Å, which were unresolved in the RSS spectrum.

Table 4.4 shows the measured absorption line properties, specifically for the FORS2 spectrum due to its higher S/N and better line resolution than the RSS spectrum. Two distinct redshifts were acquired from the absorption line measurements, namely $z = 0.960 \pm 0.0017$ and $z = 1.142 \pm 0.0078$. Initial analysis of the spectrum by the *Swift*/Ultraviolet Optical Telescope (*UVOT*) team (Kuin and Swift/UVOT Team, 2019) placed the redshift at $z = 1.19$, which was later further refined by Vielfaure et al. (2019) who reported a redshift for the host galaxy of $z = 1.148$, as well as a fainter intervening system at $z = 0.961$, firmly agreeing with the measured redshifts found with RSS and FORS2.

4.2.2 Development of Tools for the *SALT*/RSS Spectropolarimetry Reductions: Application to the Blazar 3C 279 (Proceedings of Science, HEASA 2021)

As discussed in Cooper et al. (2022, see also Appendix C), it was shown that alternative wavelength solutions, such as those created using IRAF, are capable of being applied to *SALT* spectropolarimetric data. The 'additional tools' mentioned therein, which were the precursor to the STOPS pipeline, were used during the reduction of the blazar 3C 279.

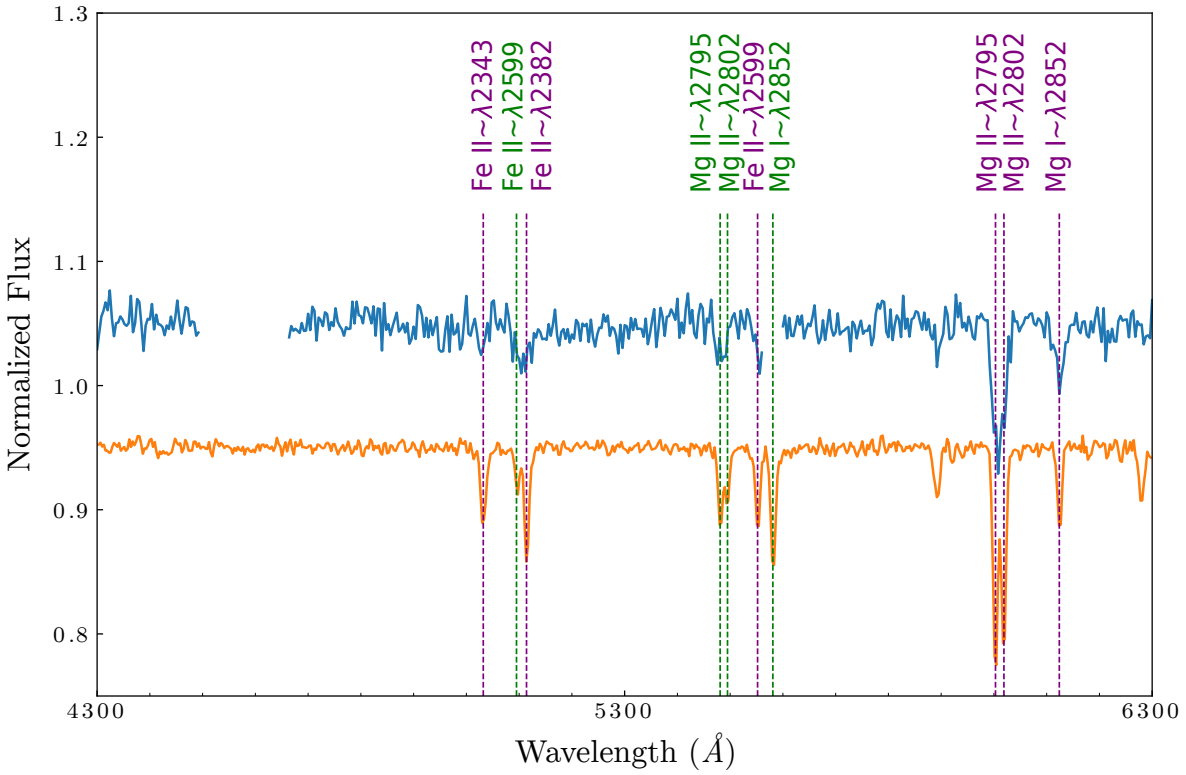

Figure 4.5: Comparison of the normalized (and offset by ±0.05) spectra as obtained with the *SALT* RSS (blue) and the *VLT* FORS2 orange. Note the chip gap and region of sky subtraction from the RSS spectrum. Figure adapted from (Buckley et al., 2021).

The blazar 3C 279 was observed in linear spectropolarimetry mode, on 2017 May 17, using the PG0900 grating with two different grating angles (12.5° and 19.5°). The grating and articulation angles used for the observations (see Table 4.3) matched those of observations of the spectrophotometric standard star, Hiltner 600, observed on 2017 February 24, allowing the intensity to be relatively flux calibrated.

Figure 4.6 shows the spectra and cross correlation of the *O*- and *E*-beams of the ThAr and Ne arc lamps, also with grating angles of 12.5° and 19.5°, respectively. The cross correlation of the arc lamps perpendicular polarization beams show clear peaks at 0 lag, indicating that the wavelength solutions are consistent across the two polarization beams.

Figure 4.7 shows the relative flux calibrated intensity, percentage of linear polarization, and polarization angle of the blazar 3C 279, across the visible spectrum. The spectra display a good overlap between the two grating angles, especially when considering the variable nature of blazars as well as the fact that the spectra are only relatively flux calibrated. Both the percentage of linear polarization and the polarization angle agree well across the grating angle overlap.

4.2.3 *SALT* Spectropolarimetric Pipeline Comparisons (Proceedings of Science, HEASA 2022)

As discussed in Cooper and van Soelen (2023, see also Appendix C), as well as expanding on the work presented in Cooper et al. (2022), it was shown that the STOPS pipeline has

Table 4.4: Properties of the identified absorption lines within the spectra. The measured redshifts of the identified features correspond neatly to two distinct redshifts. Table adapted from Buckley et al. (2021).

Line ID	Rest Wavelength (Å)	Observed Wavelength (Å)	FWHM (Å)	EW (Å)	z
Fe II	2343	5032.35 ± 1.44	5.44 ± 1.43	0.83 ± 0.26	1.148
Fe II	2599	5096.67 ± 2.19	4.70 ± 2.26	0.45 ± 0.23	0.961
Fe II	2382	5114.49 ± 0.90	4.67 ± 0.96	1.10 ± 0.23	1.147
Mg II	2795	5481.56 ± 1.57	4.10 ± 1.67	0.67 ± 0.21	0.961
Mg II	2802	5494.59 ± 2.19	3.93 ± 2.29	0.45 ± 0.19	0.961
Fe II	2599	5552.48 ± 1.25	4.01 ± 1.25	0.62 ± 0.19	1.136
Mg I	2852	5581.78 ± 0.91	4.44 ± 0.91	1.05 ± 0.22	0.957
Mg II	2795	6002.98 ± 0.37	4.56 ± 0.40	2.08 ± 0.25	1.148
Mg II	2802	6018.71 ± 0.14	4.38 ± 0.43	1.83 ± 0.24	1.148
Mg I	2852	6124.64 ± 1.28	4.10 ± 1.30	0.69 ± 0.22	1.128

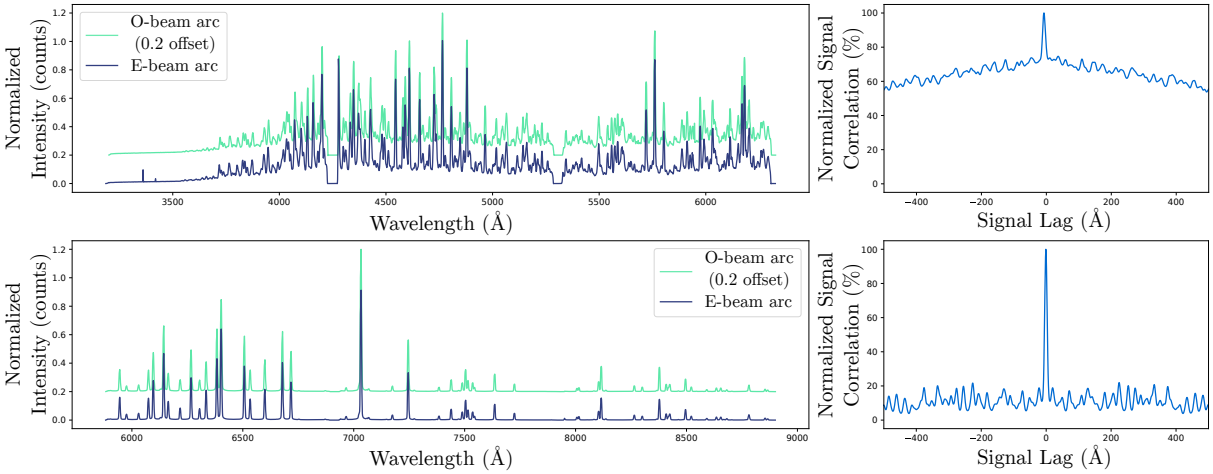

Figure 4.6: The spectra and cross correlation of the *O*- and *E*-beams of the ThAr (top) and Ne (bottom) arc lamps. Figure adapted from (Cooper et al., 2022).

no noticeable effect on the polarization properties of spectropolarimetric data and that the measure of the goodness of fit for the wavelength solutions could be measured, both through correlation and measuring the position of skyline features for both the *O*- and *E*-beams. The blazar 3C 279, the spectrophotometric standard star Hiltner 600, and the spectropolarimetric standard star Hiltner 652, were observed on the dates tabulated in Table 4.3. Observations of 3C 279 were taken during periods of enhanced and flaring γ-ray activity.

Figure 4.8 shows the γ-ray photon flux from 3C 279 for energies between $0.1-100$ GeV, observed using the Fermi Large Area Telescope (Fermi-*LAT*), as provided by the Fermi Light Curve Repository (Fermi LCR) (Abdollahi et al., 2023). This shows that on the dates of the optical observations, 3C 279 was between ~ 4 to ~ 8 times brighter compared to its quiescent state.

[5] https://fermi.gsfc.nasa.gov/ssc/data/access/lat/LightCurveRepository/source.html?source_name=4FGL_J1256.1-0547

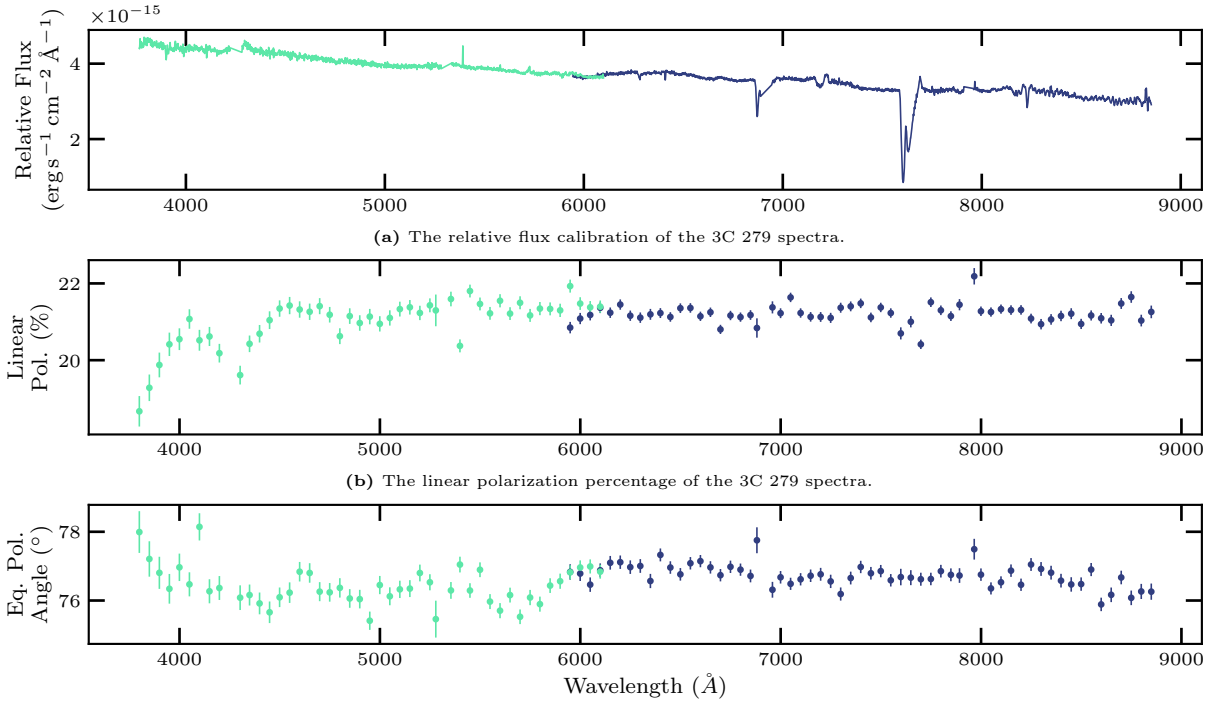

(a) The relative flux calibration of the 3C 279 spectra.

(b) The linear polarization percentage of the 3C 279 spectra.

(c) The polarization angle of the 3C 279 spectra, polarization relative to the instrument.

Figure 4.7: The relative flux calibrated spectra (a), linear polarization percentage (b), and polarization angle (c) of the blazar 3C 279 observed on 2017 May 17. Figure adapted from Cooper et al. (2022).

Figure 4.9 shows the spectropolarimetric results for 3C 279 during the periods of enhanced and flaring γ-ray activity as mentioned above. The figure shows, from top to bottom, the normalized, relative flux calibrated, spectra for both grating angles (12.5° and 19.625°, observed in that order), the percentage of linear polarization, and the polarization angle.

Although the spectral shape does not vary greatly across the wavelength region, the level of γ-ray activity during observation has a clear effect on the spectra. This is most notable for the 2017 March 31 observation which displays heightened spectral intensities in the blue. The linear polarization percentages and polarization angles also show variation over the course of the observations, varying between $\sim$ 12.23% and $\sim$ 24.22°. There is also good agreement between the polarization properties across the differing grating angles for the same observation dates. The difference of the polarization percentage and polarization angle between the two grating angles is $\sim$ 0.25% and $\sim$ 1.25°, respectively. The most notable disagreement of the polarization properties is seen, once again, during the 2017 March 31 observation, but may be explained due to the flaring state of the blazar, the asynchronous times for the two observations, and a lower S/N near the edges of the RSS.

Figure 4.10 shows the comparison between the reduced Q and U Stokes parameters for Hiltner 652 as observed with the FORS1 and FORS2 (as reported by Cikota et al., 2017; Fossati et al., 2007), and the *SALT* observations. This shows that the Stokes parameters of Hiltner 652 are consistent across the different instruments, mostly falling within a standard deviation of historical results. Minor discrepancies are present, but can be due to multiple compounding effects, such as differing instrumental setups, varying atmospheric conditions, as well as Hiltner 652 being classed as a spectrophotometric, and

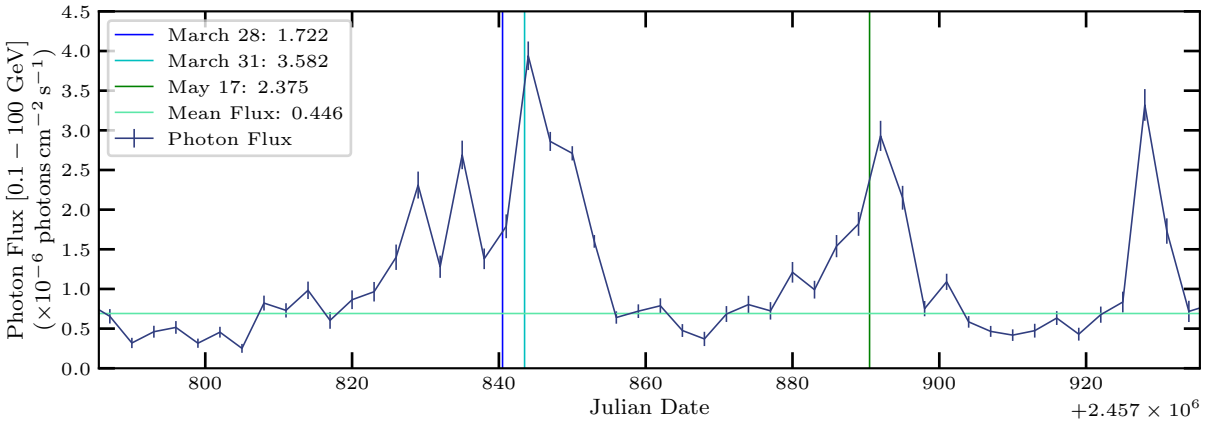

Figure 4.8: The Fermi-*LAT* photon flux [0.1 − 100 GeV] for 3C 279 as measured around the dates of the *SALT*/RSS spectropolarimetric observations (indicated by the vertical lines). Also included are the 'mean' γ-ray fluxes ($\times 10^{-6}$) for the observation dates, calculated using linear interpolation of the Fermi-*LAT* data points. The horizontal turquoise line shows the mean quiescent flux for this source. Figure created using data sourced from the Fermi LCR.[5]

not spectropolarimetric, standard.

4.2.4 Modeling the Spectral Energy Distributions and Spectropolarimetry of Blazars - Application to 4C +01.02 in 2016 − 2017 (Schutte et al., 2022)

Schutte et al. (2022) presented the results from spectropolarimetric observations and modeling of the Spectral Energy Distribution (SED) for the blazar 4C +01.02 during a flaring and a quiescent state. The optical spectropolarimetric observations of the blazar were completed using the *SALT* RSS in spectropolarimetric mode, with observations taken on 2016 July 09 and 2017 July 25, also noted in Table 4.3.

Figure 4.11 shows the photon flux of 4C +01.02 for energies of 0.1 − 100 GeV as provided by the Fermi LCR. The figure shows that during the optical observations of 4C +01.02, the source was at γ-ray fluxes of $\approx 1.9 \times 10^{-6}$ and $\approx 0.1 \times 10^{-6}$ ph. cm^{-2} s^{-1}, as compared to a quiescent 'median' flux of 0.21×10^{-6} ph. cm^{-2} s^{-1}.

The normalized, continuum-subtracted, intensity spectra as well as the polarization percentage for the 2016 and 2017 epochs are show in Figure 4.12. The spectral features were identified using the known redshift of 4C 01.02 of $z = 2.1$. The quiescent state spectrum exhibits more prominent features than during the flaring state, with the C IV line being the most prominent feature present in both spectra. The increase in the spectral line intensity during the quiescent γ-ray state is due to the non-thermal continuum emission being fainter, as compared to the flaring state.

The linear polarization percentages averaged $10.04 \pm 1.03\%$ and $1.72 \pm 0.93\%$ during flaring and quiescence, respectively.

[6] https://fermi.gsfc.nasa.gov/ssc/data/access/lat/LightCurveRepository/source.html?source_name=4FGL_J0108.6+0134

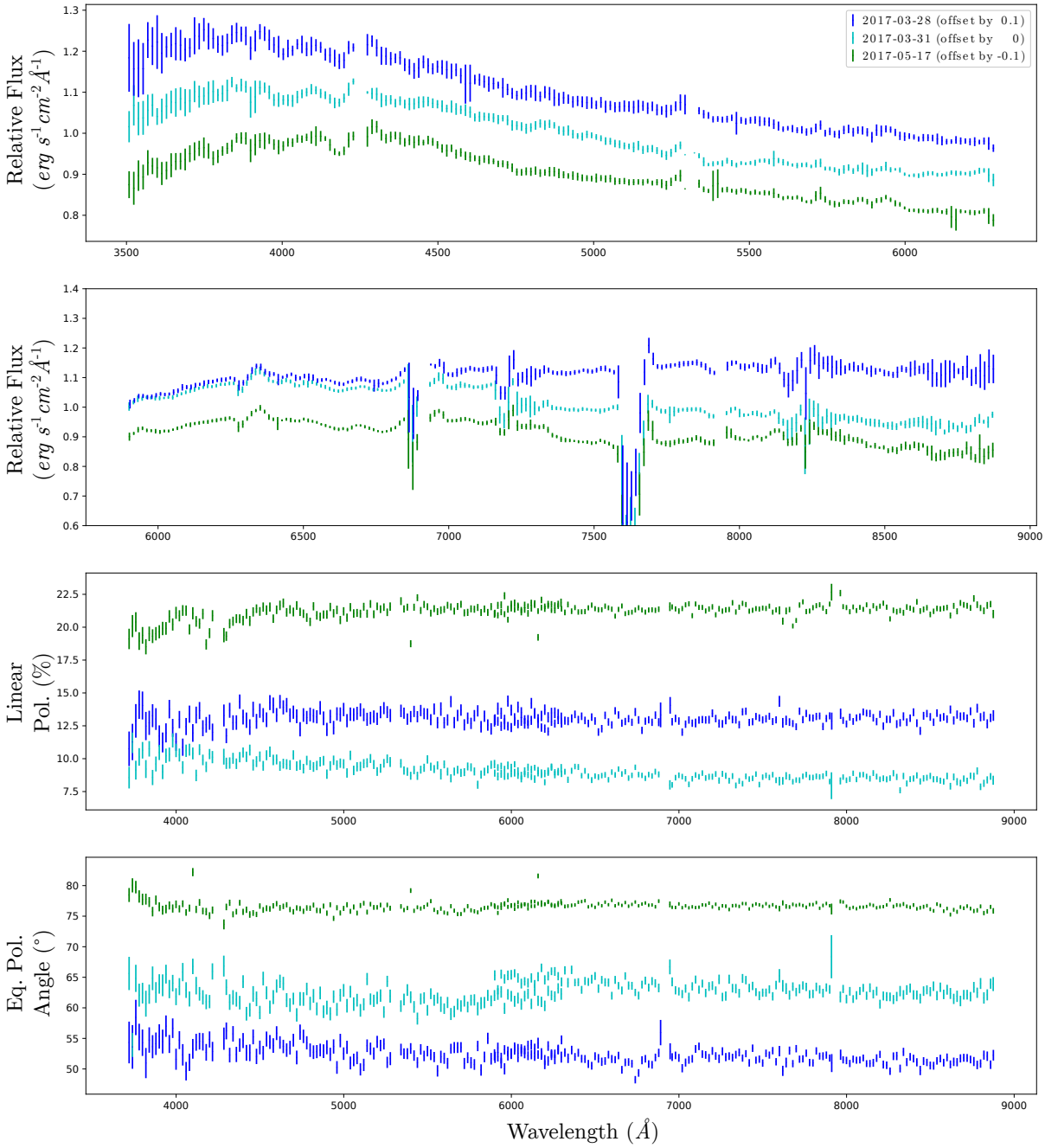

Figure 4.9: Spectropolarimetric results for 3C 279 during two distinct periods of flaring. The normalized relative flux is presented for both grating angles, 12.5°(top) and 19.625°(second from top). Figure sourced from (Cooper and van Soelen, 2023).

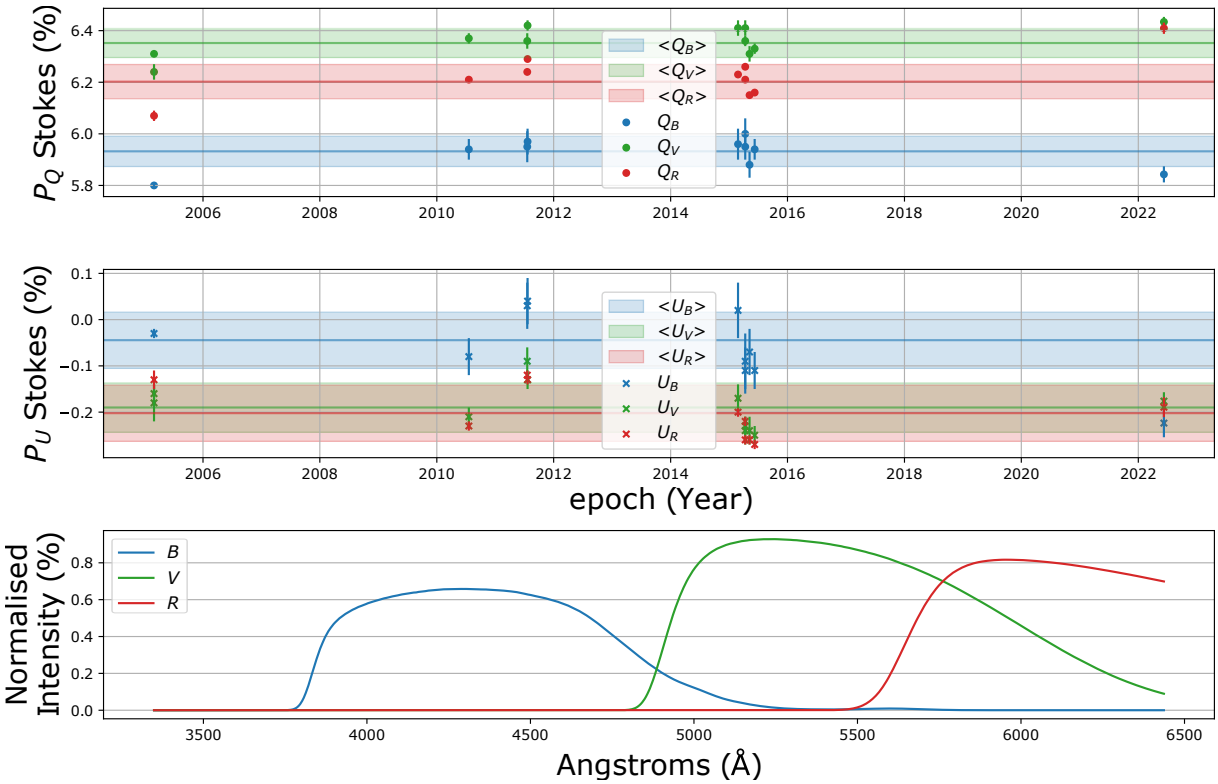

Figure 4.10: The reduced Q and U Stokes parameters for Hiltner 652, pre−2006 for published FORS1 data, 2010 − 2016 for published FORS2 data, and post−2022 for Stokes parameters observed with *SALT* and convolved with the Johnson-Cousins filter pass-bands. The horizontal lines and shaded regions refer to the FORS mean and 1σ regions, respectively. Finally, the bottom plot shows the Johnson-Cousins filter pass-band's used by POLSALT to calculate the Stokes parameters in the different filters. Figure sourced from (Cooper and van Soelen, 2023).

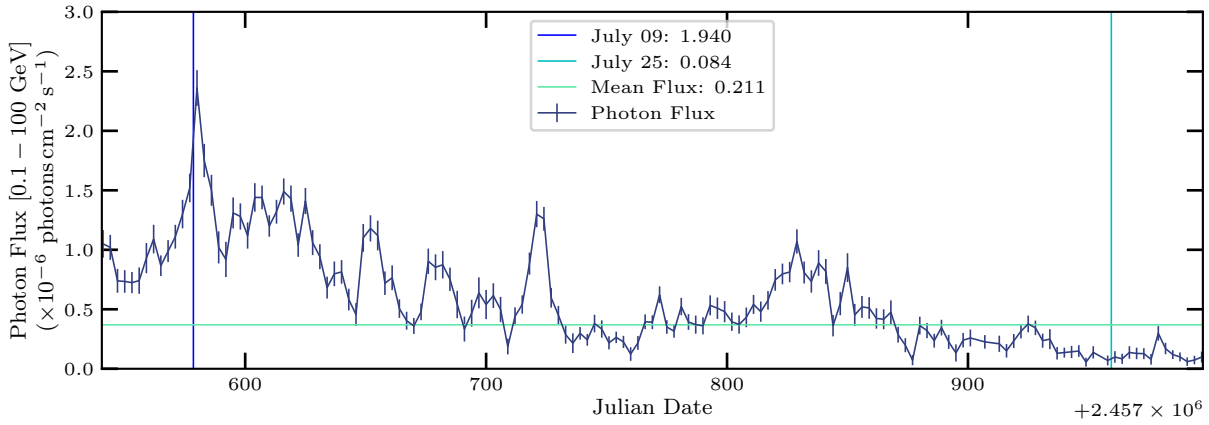

Figure 4.11: The Fermi-*LAT* photon flux [0.1 − 100 GeV] for 4C +01.02 as measured around the dates of the *SALT*/RSS spectropolarimetric observations (indicated by the vertical lines). Also included are the 'mean' γ-ray fluxes ($\times 10^{-6}$) for the observation dates, calculated using linear interpolation of the Fermi-*LAT* data points. The horizontal turquoise line shows the mean quiescent flux for this source. Figure created using data sourced from the Fermi Light Curve Repository (Fermi LCR).[6]

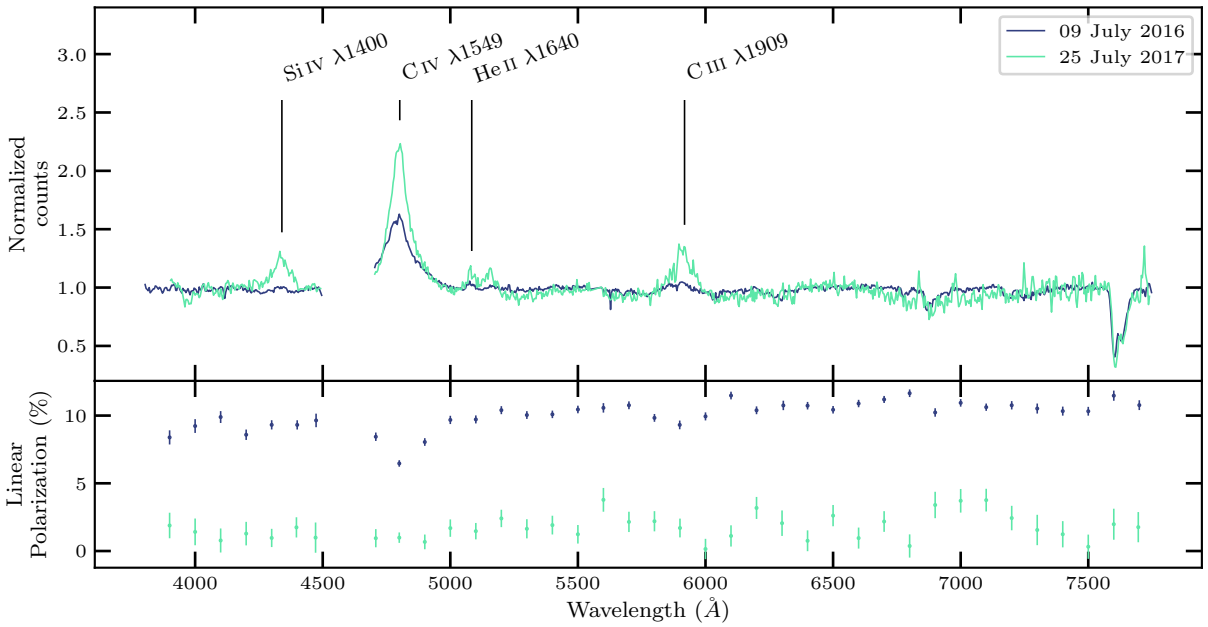

Figure 4.12: Spectropolarimetric results for 4C +01.02 during periods of flaring and quiescence. The spectra presented have been continuum subtracted and normalized. Figure adapted from (Schutte et al., 2022).

Chapter 5

Conclusions

TODO: A summary of the dissertation, main focus on the results and that the supplementary pipeline is a success since it allows an alternate method using IRAF to wavelength calibrate the polsalt data.

5.1 Future Work

It is possible to complete the data reductions of *SALT*/RSS spectropolarimetric data using only the POLSALT pipeline. This does not negate the fact that better tools and software better allow us to focus on the results of observations rather than the data reduction process. Due to the limitations inherent in software designed for use strictly as a pipeline, there is a lack of flexibility in data reduction processes, an over-reliance on the software to provide accurate results, and a lack of urgency when keeping 'completed' software up-to-date.

Newer software, such as Python 3, is trending for data reductions due to the compatibility and maintenance with modern systems, the rich packages available for use, and an active development environment. In this regard, the development of the STOPS software is a step in the right direction, providing a channel for alternate wavelength calibrations to be integrated with POLSALT, while still maintaining the integrity of the data reduction process. That said, the software is not without its limitations.

Future work would involve the continued development and maintenance of the STOPS software, further integration of the software with POLSALT, and possibly the development of a user-friendly interface or modification of the POLSALT GUI to include the STOPS functionality.

Wavelength calibrations completed in Python 3, with the help of Python Package Index (PyPI) packages, are already supported, but further integration of non-standard wavelength solutions would also be beneficial, as the current wavelength solutions are limited to Chebyshev and Legendre polynomials.

Bibliography

S. Abdollahi, M. Ajello, L. Baldini, J. Ballet, D. Bastieri, J. Becerra Gonzalez, R. Bellazzini, A. Berretta, E. Bissaldi, R. Bonino, A. Brill, P. Bruel, E. Burns, S. Buson, R. A. Cameron, R. Caputo, P. A. Caraveo, N. Cibrario, S. Ciprini, P. Cristarella Orestano, M. Crnogorcevic, S. Cutini, F. D'Ammando, S. De Gaetano, S. W. Digel, N. Di Lalla, L. Di Venere, A. Domínguez, V. Fallah Ramazani, S. J. Fegan, E. C. Ferrara, A. Fiori, H. Fleischhack, A. Franckowiak, Y. Fukazawa, P. Fusco, V. Gammaldi, F. Gargano, S. Garrappa, C. Gasbarra, D. Gasparrini, N. Giglietto, F. Giordano, M. Giroletti, D. Green, I. A. Grenier, S. Guiriec, M. Gustafsson, E. Hays, D. Horan, X. Hou, G. Jóhannesson, M. Kerr, D. Kocevski, M. Kuss, L. Latronico, J. Li, I. Liodakis, F. Longo, F. Loparco, L. Lorusso, B. Lott, M. N. Lovellette, P. Lubrano, S. Maldera, A. Manfreda, G. Martí-Devesa, M. N. Mazziotta, I. Mereu, M. Meyer, P. F. Michelson, T. Mizuno, M. E. Monzani, A. Morselli, I. V. Moskalenko, M. Negro, N. Omodei, E. Orlando, J. F. Ormes, D. Paneque, G. Panzarini, J. S. Perkins, M. Persic, M. Pesce-Rollins, R. Pillera, T. A. Porter, G. Principe, J. L. Racusin, S. Rainò, R. Rando, B. Rani, M. Razzano, S. Razzaque, A. Reimer, O. Reimer, M. Sánchez-Conde, P. M. Saz Parkinson, Jeff Scargle, L. Scotton, D. Serini, C. Sgrò, E. J. Siskind, G. Spandre, P. Spinelli, D. J. Suson, H. Tajima, D. J. Thompson, D. F. Torres, J. Valverde, T. Venters, Z. Wadiasingh, S. Wagner, and K. Wood. The fermi-lat lightcurve repository*. *The Astrophysical Journal Supplement Series*, 265(2):31, March 2023. ISSN 1538-4365. doi: 10.3847/1538-4365/acbb6a. URL http://dx.doi.org/10.3847/1538-4365/acbb6a.

Anaconda. Anaconda software distribution, 2020. URL https://docs.anaconda.com/.

R. R. J. Antonucci and J. S. Miller. Spectropolarimetry and the nature of NGC 1068. ApJ, 297:621–632, October 1985. doi: 10.1086/163559.

George B. Arfken and Hans J. Weber. Mathematical methods for physicists, 1999.

Astropy Collaboration, T. P. Robitaille, E. J. Tollerud, P. Greenfield, M. Droettboom, E. Bray, T. Aldcroft, M. Davis, A. Ginsburg, A. M. Price-Whelan, W. E. Kerzendorf, A. Conley, N. Crighton, K. Barbary, D. Muna, H. Ferguson, F. Grollier, M. M. Parikh, P. H. Nair, H. M. Unther, C. Deil, J. Woillez, S. Conseil, R. Kramer, J. E. H. Turner, L. Singer, R. Fox, B. A. Weaver, V. Zabalza, Z. I. Edwards, K. Azalee Bostroem, D. J. Burke, A. R. Casey, S. M. Crawford, N. Dencheva, J. Ely, T. Jenness, K. Labrie, P. L. Lim, F. Pierfederici, A. Pontzen, A. Ptak, B. Refsdal, M. Servillat, and O. Streicher. Astropy: A community Python package for astronomy. A&A, 558:A33, October 2013. doi: 10.1051/0004-6361/201322068.

Astropy Collaboration, A. M. Price-Whelan, B. M. Sipőcz, H. M. Günther, P. L. Lim, S. M. Crawford, S. Conseil, D. L. Shupe, M. W. Craig, N. Dencheva, A. Ginsburg, J. T. VanderPlas, L. D. Bradley, D. Pérez-Suárez, M. de Val-Borro, T. L. Aldcroft, K. L. Cruz, T. P. Robitaille, E. J. Tollerud, C. Ardelean, T. Babej, Y. P. Bach, M. Bachetti, A. V. Bakanov, S. P. Bamford, G. Barentsen, P. Barmby, A. Baumbach, K. L. Berry, F. Biscani, M. Boquien, K. A. Bostroem, L. G. Bouma, G. B. Brammer, E. M. Bray, H. Breytenbach, H. Buddelmeijer, D. J. Burke, G. Calderone, J. L. Cano Rodríguez, M. Cara, J. V. M. Cardoso, S. Cheedella, Y. Copin, L. Corrales, D. Crichton, D. D'Avella, C. Deil, É. Depagne, J. P. Dietrich, A. Donath, M. Droettboom, N. Earl, T. Erben, S. Fabbro, L. A. Ferreira, T. Finethy, R. T. Fox, L. H. Garrison, S. L. J. Gibbons, D. A. Goldstein, R. Gommers, J. P. Greco, P. Greenfield, A. M. Groener, F. Grollier, A. Hagen, P. Hirst, D. Homeier, A. J. Horton, G. Hosseinzadeh, L. Hu, J. S. Hunkeler, Ž. Ivezić, A. Jain, T. Jenness, G. Kanarek, S. Kendrew, N. S. Kern, W. E. Kerzendorf, A. Khvalko, J. King, D. Kirkby, A. M. Kulkarni, A. Kumar, A. Lee, D. Lenz, S. P. Littlefair, Z. Ma, D. M. Macleod, M. Mastropietro, C. McCully, S. Montagnac, B. M. Morris, M. Mueller, S. J. Mumford, D. Muna, N. A. Murphy, S. Nelson, G. H. Nguyen, J. P. Ninan, M. Nöthe, S. Ogaz, S. Oh, J. K. Parejko, N. Parley, S. Pascual, R. Patil, A. A. Patil, A. L. Plunkett, J. X. Prochaska, T. Rastogi, V. Reddy Janga, J. Sabater, P. Sakurikar, M. Seifert, L. E. Sherbert, H. Sherwood-Taylor, A. Y. Shih, J. Sick, M. T. Silbiger, S. Singanamalla, L. P. Singer, P. H. Sladen, K. A. Sooley, S. Sornarajah, O. Streicher, P. Teuben, S. W. Thomas, G. R. Tremblay, J. E. H. Turner, V. Terrón, M. H. van Kerkwijk, A. de la Vega, L. L. Watkins, B. A. Weaver, J. B. Whitmore, J. Woillez, V. Zabalza, and Astropy Contributors. The Astropy Project: Building an Open-science Project and Status of the v2.0 Core Package. AJ, 156(3):123, September 2018. doi: 10.3847/1538-3881/aabc4f.

Astropy Collaboration, A. M. Price-Whelan, P. L. Lim, N. Earl, N. Starkman, L. Bradley, D L. Shupe, A. A. Patil, L. Corrales, C. E. Brasseur, M. Nöthe, A. Donath, E. Tollerud, B. M. Morris, A. Ginsburg, E. Vaher, B. A. Weaver, J. Tocknell, W. Jamieson, M. H. van Kerkwijk, T. P. Robitaille, B. Merry, M. Bachetti, H. M. Günther, T. L. Aldcroft, J. A. Alvarado-Montes, A. M. Archibald, A. Bódi, S. Bapat, J. Barentsen, G.and Bazán, M. Biswas, M. Boquien, D. J. Burke, D. Cara, M. Cara, K. E. Conroy, S. Conseil, M. W. Craig, R. M. Cross, K. L. Cruz, F. D'Eugenio, N. Dencheva, H. A. R. Devillepoix, J. P. Dietrich, A. D. Eigenbrot, T. Erben, L. Ferreira, D. Foreman-Mackey, R. Fox, N. Freij, S. Garg, R. Geda, L. Glattly, Y. Gondhalekar, K. D. Gordon, D. Grant, P. Greenfield, A. M. Groener, S. Guest, S. Gurovich, R. Handberg, A. Hart, Z. Hatfield-Dodds, D. Homeier, G. Hosseinzadeh, T. Jenness, C. K. Jones, P. Joseph, J. B. Kalmbach, E. Karamehmetoglu, M. Kałuszyński, M. S. P. Kelley, N. Kern, W. E. Kerzendorf, E. W. Koch, S. Kulumani, A. Lee, C. Ly, Z. Ma, C. MacBride, J. M. Maljaars, D. Muna, N. A. Murphy, H. Norman, R. O'Steen, K. A. Oman, C. Pacifici, S. Pascual, J. Pascual-Granado, R. R. Patil, G. I. Perren, T. E. Pickering, T. Rastogi, B. R. Roulston, D. F. Ryan, E. S. Rykoff, J. Sabater, P. Sakurikar, J. Salgado, A. Sanghi, N. Saunders, V. Savchenko, L. Schwardt, M. Seifert-Eckert, A. Y. Shih, A. S. Jain, G. Shukla, J. Sick, C. Simpson, S. Singanamalla, L. P. Singer, J. Singhal, M. Sinha, B. M. Sipőcz, L. R. Spitler, D. Stansby, O. Streicher, J. Šumak, J. D. Swinbank, D. S. Taranu, N. Tewary, G. R. Tremblay, M. de Val-Borro, S. J. Van Kooten, Z. Vasović, S. Verma, J. V. de Miranda Cardoso, P. K. G. Williams, T. J. Wilson, B. Winkel, W. M. Wood-Vasey, R. Xue, P. Yoachim, C. Zhang, A. Zonca, and Astropy Project

Contributors. The Astropy Project: Sustaining and Growing a Community-oriented Open-source Project and the Latest Major Release (v5.0) of the Core Package. ApJ, 935(2):167, August 2022. doi: 10.3847/1538-4357/ac7c74.

S. Bagnulo, M. Landolfi, J. D. Landstreet, E. Landi Degl'Innocenti, L. Fossati, and M. Sterzik. Stellar spectropolarimetry with retarder waveplate and beam splitter devices. *Publications of the Astronomical Society of the Pacific*, 121(883):993, aug 2009. doi: 10.1086/605654. URL https://dx.doi.org/10.1086/605654.

J. Barnard, B. van Soelen, J. Cooper, R. Britto, J. P. Marais, I. van der Westhuizen, D. Buckley, H. Schutte, M. Böttcher, B. Vaidya, S. Achariya, and A. Martin-Carrillo. Optical Spectropolarimetry Observations of the BL Lac-type object PKS 0537-441 after a period of quiescence. In *High Energy Astrophysics in Southern Africa 2021*, page 9, May 2022. doi: 10.22323/1.401.0009.

Joleen Barnard, B. van Soelen, S. Acharya, M. Böttcher, R. J. Britto, J. Cooper, D. A. H. Buckley, A. Martin-Carrillo, B. Vaidya, I. P. van der Westhuizen, and M. Zacharias. The optical spectropolarimetric behaviour of a selection of high-energy blazars. MNRAS, 532(2):1991–2005, August 2024. doi: 10.1093/mnras/stae1576.

Scott D Barthelmy, Louis M Barbier, Jay R Cummings, Ed E Fenimore, Neil Gehrels, Derek Hullinger, Hans A Krimm, Craig B Markwardt, David M Palmer, Ann Parsons, et al. The burst alert telescope (bat) on the swift midex mission. *Space Science Reviews*, 120:143–164, 2005.

Erasmus Bartholinus. Experimenta crystalli islandici dis-diaclastici, quibus mira et insolita refractio detegitur (copenhagen, 1670). *Edinburgh Philosophical Journal*, 1:271, 1670.

D. Scott Birney, Guillermo Gonzalez, and David Oesper. *Observational Astronomy - 2nd Edition*. Cambridge University Press, 2006. doi: 10.2277/0521853702.

Janus D. Brink, Moses K. Mogotsi, Melanie Saayman, Nicolaas M. Van der Merwe, Jonathan Love, and Alrin Christians. Preparing the SALT for near-infrared observations. In Heather K. Marshall, Jason Spyromilio, and Tomonori Usuda, editors, *Ground-based and Airborne Telescopes IX*, volume 12182 of *Society of Photo-Optical Instrumentation Engineers (SPIE) Conference Series*, page 121822E, August 2022. doi: 10.1117/12.2627328.

D. A. H. Buckley, J. Brink, N. S. Loaring, A. Swat, and H. L. Worters. The Southern African Large Telescope (SALT) calibration system. In Ian S. McLean and Mark M. Casali, editors, *Ground-based and Airborne Instrumentation for Astronomy II*, volume 7014, page 70146H. International Society for Optics and Photonics, SPIE, 2008. doi: 10.1117/12.790385. URL https://doi.org/10.1117/12.790385.

D. A. H. Buckley, S. Bagnulo, R. J. Britto, J. Mao, D. A. Kann, J. Cooper, V. Lipunov, D. M. Hewitt, S. Razzaque, N. P. M. Kuin, I. M. Monageng, S. Covino, P. Jakobsson, A. J. van der Horst, K. Wiersema, M. Böttcher, S. Campana, V. D'Elia, E. S.

Gorbovskoy, I. Gorbunov, D. N. Groenewald, D. H. Hartmann, V. G. Kornilov, C. G. Mundell, R. Podesta, J. K. Thomas, N. Tyurina, D. Vlasenko, B. van Soelen, and D. Xu. Spectropolarimetry and photometry of the early afterglow of the gamma-ray burst GRB 191221B. MNRAS, 506(3):4621–4631, September 2021. doi: 10.1093/mnras/stab1791.

David A. H. Buckley, Gerhard P. Swart, and Jacobus G. Meiring. Completion and commissioning of the Southern African Large Telescope. In Larry M. Stepp, editor, *Society of Photo-Optical Instrumentation Engineers (SPIE) Conference Series*, volume 6267 of *Society of Photo-Optical Instrumentation Engineers (SPIE) Conference Series*, page 62670Z, June 2006. doi: 10.1117/12.673750.

Christian Buil. *CCD astronomy : construction and use of an astronomical CCD camera / Christian Buil ; translated and adapted from the French by Emmanuel and Barbara Davoust.* Willmann-Bell, Richmond, Va, 1st english ed. edition, 1991. ISBN 0943396298.

Eric B. Burgh, Kenneth H. Nordsieck, Henry A. Kobulnicky, Ted B. Williams, Darragh O'Donoghue, Michael P. Smith, and Jeffrey W. Percival. Prime Focus Imaging Spectrograph for the Southern African Large Telescope: optical design. In Masanori Iye and Alan F. M. Moorwood, editors, *Instrument Design and Performance for Optical/Infrared Ground-based Telescopes*, volume 4841 of *Society of Photo-Optical Instrumentation Engineers (SPIE) Conference Series*, pages 1463–1471, March 2003. doi: 10.1117/12.460312.

Subrahmanyan Chandrasekhar. Radiative transfer, 1950.

Aleksandar Cikota, Ferdinando Patat, Stefan Cikota, and Tamar Faran. Linear spectropolarimetry of polarimetric standard stars with VLT/FORS2. MNRAS, 464(4):4146–4159, February 2017. doi: 10.1093/mnras/stw2545.

Marshall H. Cohen. Genesis of the 1000-foot Arecibo dish. *Journal of Astronomical History and Heritage*, 12(2):141–152, July 2009.

E. Collett. *Field Guide to Polarization.* Field Guides. SPIE Press, 2005. ISBN 9780819458681. URL https://books.google.co.za/books?id=5lJwcCsLbLsC.

J. Cooper and B. van Soelen. SALT Spectropolarimetric Pipeline Comparisons. In *High Energy Astrophysics in Southern Africa 2022*, page 56, December 2023.

J. Cooper, B. van Soelen, and R. Britto. Development of tools for SALT/RSS spectropolarimetry reductions: application to the blazar 3C279. In *High Energy Astrophysics in Southern Africa 2021*, page 56, May 2022. doi: 10.22323/1.401.0056.

M. Craig, S. Crawford, M. Seifert, T. Robitaille, B. Sipőcz, J. Walawender, Z. Vinícius, J. P. Ninan, M. Droettboom, J. Youn, E. Tollerud, E. Bray, N. Walker, Janga V. R., C. Stotts, H. M. Günther, E. Rol, Yoonsoo P. Bach, L. Bradley, C. Deil, A. Price-Whelan, K. Barbary, A. Horton, W. Schoenell, N. Heidt, F. Gasdia, S. Nelson, and

O. Streicher. astropy/ccdproc: v1.3.0.post1, December 2017. URL https://doi.org/10.5281/zenodo.1069648.

G. Dahlquist and Å. Björck. *Numerical Methods*. Dover Books on Mathematics. Dover Publications, 2003. ISBN 9780486428079. URL https://books.google.co.ls/books?id=armfeHpJIwAC.

E. Landi Degl'Innocenti, S. Bagnulo, and L. Fossati. Polarimetric standardization, 2006.

Egidio Landi Degl'Innocenti. The physics of polarization. *Proceedings of the International Astronomical Union*, 10(S305):1–1, 2014.

Egidio Landi Degl'Innocenti and M. Landolfi. *Polarization in Spectral Lines*, volume 307. Springer Dordrecht, 2004. doi: 10.1007/978-1-4020-2415-3.

Königlich Bayerische Akademie der Wissenschaften. *Denkschriften der Königlichen Akademie der Wissenschaften zu München für das Jahre 1820 und 1821*, volume 8. Die Akademie, 1824. URL https://books.google.co.za/books?id=k-EAAAAAYAAJ.

J. F. Donati, M. Semel, B. D. Carter, D. E. Rees, and A. Collier Cameron. Spectropolarimetric observations of active stars. MNRAS, 291(4):658–682, November 1997. doi: 10.1093/mnras/291.4.658.

I. V. Florinsky and A. N. Pankratov. Digital terrain modeling with the chebyshev polynomials. *Machine Learning and Data Analysis*, 1(12):1647 – 1659, 2015. doi: 10.48550/ARXIV.1507.03960. URL https://arxiv.org/abs/1507.03960.

L. Fossati, S. Bagnulo, E. Mason, and E. Landi Degl'Innocenti. Standard Stars for Linear Polarization Observed with FORS1. In C. Sterken, editor, *The Future of Photometric, Spectrophotometric and Polarimetric Standardization*, volume 364 of *Astronomical Society of the Pacific Conference Series*, page 503, April 2007.

Augustin Fresnel. *Oeuvres completes d'Augustin Fresnel: 3*. Imprimerie impériale, 1870.

L. M. Freyhammer, M. I. Andersen, T. Arentoft, C. Sterken, and P. Nørregaard. On Cross-talk Correction of Images from Multiple-port CCDs. *Experimental Astronomy*, 12(3):147–162, January 2001. doi: 10.1023/A:1021820418263.

David J Griffiths. Introduction to electrodynamics, 2005.

George E. Hale. The Zeeman Effect in the Sun. PASP, 20(123):287, December 1908. doi: 10.1086/121847.

George E. Hale. *16. On the Probable Existence of a Magnetic Field in Sun-Spots*, pages 96–105. Harvard University Press, Cambridge, MA and London, England, 1979. ISBN 9780674366688. doi: doi:10.4159/harvard.9780674366688.c19. URL https://doi.org/10.4159/harvard.9780674366688.c19.

P. D. Hale and G. W. Day. Stability of birefringent linear retarders(waveplates). *Appl. Opt.*, 27(24):5146–5153, Dec 1988. doi: 10.1364/AO.27.005146. URL https://opg.optica.org/ao/abstract.cfm?URI=ao-27-24-5146.

C. R. Harris, K. J. Millman, S. J. van der Walt, R. Gommers, P. Virtanen, D. Cournapeau, E. Wieser, J. Taylor, S. Berg, N. J. Smith, R. Kern, M. Picus, S. Hoyer, M. H. van Kerkwijk, M. Brett, A. Haldane, J. F. del Río, M. Wiebe, P. Peterson, P. Gérard-Marchant, K. Sheppard, T. Reddy, W. Weckesser, H. Abbasi, C. Gohlke, and T. E. Oliphant. Array programming with NumPy. *Nature*, 585(7825):357–362, September 2020. doi: 10.1038/s41586-020-2649-2. URL https://doi.org/10.1038/s41586-020-2649-2.

E. Hecht. *Optics*. Pearson Education, Incorporated, 2017. ISBN 9780133977226. URL https://books.google.co.za/books?id=ZarLoQEACAAJ.

Steve B. Howell. *Handbook of CCD Astronomy*, volume 5. Cambridge University Press, 2006.

J. D. Hunter. Matplotlib: A 2d graphics environment. *Computing in Science & Engineering*, 9(3):90–95, 2007. doi: 10.1109/MCSE.2007.55.

Christian Huygens. Treatise on light, 1690. translated by Thompson, s. p., 1690. URL https://www.gutenberg.org/files/14725/14725-h/14725-h.htm.

Mourad E. H. Ismail. *Classical and Quantum Orthogonal Polynomials in One Variable*. Encyclopedia of Mathematics and its Applications. Cambridge University Press, 2005. doi: 10.1017/CBO9781107325982.

James Janesick, James T. Andrews, and Tom Elliott. Fundamental performance differences between CMOS and CCD imagers: Part 1. In David A. Dorn and Andrew D. Holland, editors, *Society of Photo-Optical Instrumentation Engineers (SPIE) Conference Series*, volume 6276 of *Society of Photo-Optical Instrumentation Engineers (SPIE) Conference Series*, page 62760M, June 2006. doi: 10.1117/12.678867.

F.A. Jenkins and H.E. White. *Fundamentals of Optics*. International student edition. McGraw-Hill, 1976. ISBN 9780070323308. URL https://books.google.co.za/books?id=dCdRAAAAMAAJ.

Christoph U. Keller. Instrumentation for astrophysical spectropolarimetry. *Astrophysical Spectropolarimetry*, 1:303–354, 2002.

G. Kirchhoff and R. Bunsen. Chemische Analyse durch Spectralbeobachtungen. *Annalen der Physik*, 189(7):337–381, January 1861. doi: 10.1002/andp.18611890702.

Henry A. Kobulnicky, Kenneth H. Nordsieck, Eric B. Burgh, Michael P. Smith, Jeffrey W. Percival, Ted B. Williams, and Darragh O'Donoghue. Prime focus imaging spectrograph for the Southern African large telescope: operational modes. In Masanori Iye and Alan F. M. Moorwood, editors, *Instrument Design and Performance for Optical/Infrared Ground-based Telescopes*, volume 4841 of *Society of Photo-Optical Instru-*

mentation Engineers (SPIE) Conference Series, pages 1634–1644, March 2003. doi: 10.1117/12.460315.

N. P. M. Kuin and Swift/UVOT Team. GRB 191221B: Swift/UVOT redshift. *GRB Coordinates Network*, 26538:1, December 2019.

S Laha, KK Simpson, et al. Grb 191221b: Swift detection of a burst and a very bright optical candidate. *GRB Coordinates Network*, 26534:1, 2019.

Gerard Leng. Compression of aircraft aerodynamic database using multivariable chebyshev polynomials. *Advances in Engineering Software*, 28(2):133–141, 1997. ISSN 0965-9978. doi: https://doi.org/10.1016/S0965-9978(96)00043-9. URL https://www.sciencedirect.com/science/article/pii/S0965997896000439.

Dave Litwiller. Ccd vs. cmos. *Photonics spectra*, 35(1):154–158, 2001.

Dongyue Liu and Bryan M. Hennelly. Improved wavelength calibration by modeling the spectrometer. *Applied Spectroscopy*, 76(11):1283–1299, 2022. doi: 10.1177/00037028221111796. URL https://doi.org/10.1177/00037028221111796. PMID: 35726593.

Etienne L. Malus. Sur une propriété de la lumière réfléchie. *Mém. Phys. Chim. Soc. d'Arcueil*, 2:143–158, 1809.

Curtis McCully, Steve Crawford, Gabor Kovacs, Erik Tollerud, Edward Betts, Larry Bradley, Matt Craig, James Turner, Ole Streicher, Brigitta Sipocz, Thomas Robitaille, and Christoph Deil. astropy/astroscrappy: v1.0.5 zenodo release, November 2018. URL https://doi.org/10.5281/zenodo.1482019.

I. Newton and W. Innys. *Opticks:: Or, A Treatise of the Reflections, Refractions, Inflections and Colours of Light*. Opticks:: Or, A Treatise of the Reflections, Refractions, Inflections and Colours of Light. William Innys at the West-End of St. Paul's., 1730. URL https://books.google.co.za/books?id=GnAFAAAAQAAJ.

Kenneth H. Nordsieck, Kurt P. Jaehnig, Eric B. Burgh, Henry A. Kobulnicky, Jeffrey W. Percival, and Michael P. Smith. Instrumentation for high-resolution spectropolarimetry in the visible and far-ultraviolet. In Silvano Fineschi, editor, *Polarimetry in Astronomy*, volume 4843 of *Society of Photo-Optical Instrumentation Engineers (SPIE) Conference Series*, pages 170–179, February 2003. doi: 10.1117/12.459288.

D. O'Donoghue, D. A. H. Buckley, L. A. Balona, D. Bester, L. Botha, J. Brink, D. B. Carter, P. A. Charles, A. Christians, F. Ebrahim, R. Emmerich, W. Esterhuyse, G. P. Evans, C. Fourie, P. Fourie, H. Gajjar, M. Gordon, C. Gumede, M. de Kock, A. Koeslag, W. P. Koorts, H. Kriel, F. Marang, J. G. Meiring, J. W. Menzies, P. Menzies, D. Metcalfe, B. Meyer, L. Nel, J. O'Connor, F. Osman, C. Du Plessis, H. Rall, A. Riddick, E. Romero-Colmenero, S. B. Potter, C. Sass, H. Schalekamp, N. Sessions, S. Siyengo, V. Sopela, H. Steyn, J. Stoffels, J. Scholtz, G. Swart, A. Swat, J. Swiegers, T. Tiheli, P. Vaisanen, W. Whittaker, and F. van Wyk. First science with

the Southern African Large Telescope: peering at the accreting polar caps of the eclipsing polar SDSS J015543.40+002807.2. MNRAS, 372(1):151–162, October 2006. doi: 10.1111/j.1365-2966.2006.10834.x.

Darragh O'Donoghue. Correction of spherical aberration in the Southern African Large Telescope (SALT). In Philippe Dierickx, editor, *Optical Design, Materials, Fabrication, and Maintenance*, volume 4003 of *Society of Photo-Optical Instrumentation Engineers (SPIE) Conference Series*, pages 363–372, July 2000. doi: 10.1117/12.391526.

Darragh O'Donoghue. Atmospheric dispersion corrector for the Southern African Large Telescope (SALT). In Richard G. Bingham and David D. Walker, editors, *Large Lenses and Prisms*, volume 4411 of *Society of Photo-Optical Instrumentation Engineers (SPIE) Conference Series*, pages 79–84, February 2002. doi: 10.1117/12.454874.

Ferdinando Patat and Martino Romaniello. Error Analysis for Dual-Beam Optical Linear Polarimetry. PASP, 118(839):146–161, January 2006. doi: 10.1086/497581.

Alba Peinado, Angel Lizana, Josep Vidal, Claudio Iemmi, and Juan Campos. Optimization and performance criteria of a stokes polarimeter based on two variable retarders. *Opt. Express*, 18(10):9815–9830, May 2010. doi: 10.1364/OE.18.009815. URL https://opg.optica.org/oe/abstract.cfm?URI=oe-18-10-9815.

W. H. Press, S. A. Teukolsky, W. T. Vetterling, and B. P. Flannery. *Numerical Recipes 3rd Edition: The Art of Scientific Computing*. Cambridge University Press, 2007. ISBN 9780521880688. URL https://books.google.co.za/books?id=1aAOdzK3FegC.

J. R. Priebe. Operational form of the mueller matrices. *J. Opt. Soc. Am.*, 59(2):176–180, Feb 1969. doi: 10.1364/JOSA.59.000176. URL https://opg.optica.org/abstract.cfm?URI=josa-59-2-176.

Lawrence W. Ramsey, M. T. Adams, Thomas G. Barnes, John A. Booth, Mark E. Cornell, James R. Fowler, Niall I. Gaffney, John W. Glaspey, John M. Good, Gary J. Hill, Philip W. Kelton, Victor L. Krabbendam, L. Long, Phillip J. MacQueen, Frank B. Ray, Randall L. Ricklefs, J. Sage, Thomas A. Sebring, W. J. Spiesman, and M. Steiner. Early performance and present status of the Hobby-Eberly Telescope. In Larry M. Stepp, editor, *Advanced Technology Optical/IR Telescopes VI*, volume 3352 of *Society of Photo-Optical Instrumentation Engineers (SPIE) Conference Series*, pages 34–42, August 1998. doi: 10.1117/12.319287.

Hester M. Schutte, Richard J. Britto, Markus Böttcher, Brian van Soelen, Johannes P. Marais, Amanpreet Kaur, Abraham D. Falcone, David A. H. Buckley, Andry F. Rajoelimanana, and Justin Cooper. Modeling the Spectral Energy Distributions and Spectropolarimetry of Blazars - Application to 4C+01.02 in 2016-2017. ApJ, 925(2):139, February 2022. doi: 10.3847/1538-4357/ac3cb5.

Maria C. Simon. Wollaston prism with large split angle. *Appl. Opt.*, 25(3):369–376, Feb 1986. doi: 10.1364/AO.25.000369. URL https://opg.optica.org/ao/abstract.cfm?URI=ao-25-3-369.

G. G. Stokes. On the Composition and Resolution of Streams of Polarized Light from different Sources. *Transactions of the Cambridge Philosophical Society*, 9:399, January 1852.

Doug Tody. The IRAF Data Reduction and Analysis System. In David L. Crawford, editor, *Instrumentation in astronomy VI*, volume 627 of *Society of Photo-Optical Instrumentation Engineers (SPIE) Conference Series*, page 733, January 1986. doi: 10.1117/12.968154.

Doug Tody. IRAF in the Nineties. In R. J. Hanisch, R. J. V. Brissenden, and J. Barnes, editors, *Astronomical Data Analysis Software and Systems II*, volume 52 of *Astronomical Society of the Pacific Conference Series*, page 173, January 1993.

Stephen F. Tonkin. *Practical Amateur Spectroscopy*. The Patrick Moore Practical Astronomy Series. Springer London, 2013. ISBN 9781447101277. URL https://books.google.fr/books?id=b2fgBwAAQBAJ.

Pieter G. van Dokkum. Cosmic-Ray Rejection by Laplacian Edge Detection. PASP, 113 (789):1420–1427, November 2001. doi: 10.1086/323894.

J. B. Vielfaure, M. Arabsalmani, K. E. Heintz, N. R. Tanvir, A. de Ugarte Postigo, D. B. Malesani, J. P. U. Fynbo, K. Wiersema, S. D. Vergani, D. Xu, G. Pugliese, S. Schulze, D. Burgarella, and Stargate Collaboration. GRB 191221B: VLT/X-shooter redshift. *GRB Coordinates Network*, 26553:1, December 2019.

Pauli Virtanen, Ralf Gommers, Travis E. Oliphant, Matt Haberland, Tyler Reddy, David Cournapeau, Evgeni Burovski, Pearu Peterson, Warren Weckesser, Jonathan Bright, Stéfan J. van der Walt, Matthew Brett, Joshua Wilson, K. Jarrod Millman, Nikolay Mayorov, Andrew R. J. Nelson, Eric Jones, Robert Kern, Eric Larson, C J Carey, İlhan Polat, Yu Feng, Eric W. Moore, Jake VanderPlas, Denis Laxalde, Josef Perktold, Robert Cimrman, Ian Henriksen, E. A. Quintero, Charles R. Harris, Anne M. Archibald, Antônio H. Ribeiro, Fabian Pedregosa, Paul van Mulbregt, and SciPy 1.0 Contributors. SciPy 1.0: Fundamental Algorithms for Scientific Computing in Python. *Nature Methods*, 17:261–272, 2020. doi: 10.1038/s41592-019-0686-2.

L. Wang and J. C. Wheeler. Spectropolarimetry of supernovae. ARA&A, 46:433–474, September 2008. doi: 10.1146/annurev.astro.46.060407.145139.

Marsha J. Wolf, Matthew A. Bershady, Michael P. Smith, Kurt P. Jaehnig, Jeffrey W. Percival, Joshua E. Oppor, Mark P. Mulligan, and Ron J. Koch. Laboratory performance and commissioning status of the SALT NIR integral field spectrograph. In Christopher J. Evans, Julia J. Bryant, and Kentaro Motohara, editors, *Ground-based and Airborne Instrumentation for Astronomy IX*, volume 12184 of *Society of Photo-Optical Instrumentation Engineers (SPIE) Conference Series*, page 1218407, August 2022. doi: 10.1117/12.2630242.

William H. Wollaston. XII. A Method of Examining Refractive and Dispersive Powers, by

Prismatic Reflection. *Philosophical Transactions of the Royal Society of London Series I*, 92:365–380, January 1802. doi: 10.1098/rstl.1802.0013.

Appendix A

The Modified Reduction Process

This section of the Appendix aims to provide a minimum working example of the commands necessary to reduce POLSALT data using STOPS and IRAF. It contains the commands necessary to activate all software and run through the reduction process but makes no attempt at discussion.

Both POLSALT and IRAF are launched from the default CLI but use independent interfaces during the reduction process. To distinguish which window is in focus, the '`$`' token is used for default CLI commands while the '`cl>`' and '`>>>`' tokens are used for IRAF's 'xgterm' single- and multi-line commands, respectively. CLI commands may also require a specific Python environment. The environment being used is denoted using the '`(salt)$`' or '`(base)$`' tokens for the 'salt' or default 'base' environments.[1]

General instructions for the reduction process (I.E. not CLI line-fed commands) may either be discussed outside a 'Listing' environment or included as part of a 'Listing' environment preceded with a comment '`#`' token. Finally, POLSALT implements a GUI and thus takes no line-fed commands. As such, instructions referring to the POLSALT GUI also follow those of the general instructions.

As a final note, some parameters are distinguished using '<angle brackets>'. They signify necessary parameters that may vary from reduction to reduction. Notable uses of this notation include the date of observation, <*OBSDATE*> (formatted 'YYYYMMDD'), the split science FITS files, <*O-beam FILES*> or <*E-beam FILES*>, the split arc FITS files, <*O-beam ARC*> or <*E-beam ARC*>, and a wildcard symbol, <*>.

<*OBSDATE*>
- raw
  - P<*OBSDATE*><*>.fits
- sci
  - mxgbpP<*OBSDATE*><*>.fits

Figure A.1: The typical minimal file structure of data provided by *SALT*.

[1] It is assumed a Python environment manager, such as 'conda', is installed.

Ensure the data is formatted in a file structure similar to that in Figure A.1. Data located in the 'sci' folder is often provided by *SALT* but is not strictly necessary to begin the reduction process. If 'mxgbp' prefixed data is available, the reductions may be begun starting at Listing A.2. The POLSALT GUI is launched from the default CLI running the commands in Listing A.1.

Listing A.1: Launching the POLSALT GUI

```
$ cd ~/polsalt-beta
$ conda activate salt
(salt)$ python -W ignore reducepoldataGUI.py &
```

Refer to Figure 3.1 for a depiction of the POLSALT GUI. To complete the POLSALT pre-calibrations, and with the GUI in focus:

- Ensure that the 'POLSALT code directory' is correct. I.E. '~/polsalt-beta'.
- Set the 'Top level data directory' to <*OBSDATE*>.
- Ensure 'Raw data directory' is correct.
- Ensure 'Science data directory' is correct.
- Select 'Raw image reduction' from the 'Data reduction step' drop down menu.
- Check the tick boxes of all raw images to be processed (include the arc) in the display box covering the lower half of the GUI.
- Proceed with the reductions by clicking the 'OK' button.

The pre-calibrated 'mxgbp' FITS files are now available in the 'sci' folder. The files may be split using STOPS by running the commands in Listing A.2.

Listing A.2: Splitting data using STOPS

```
$ cd <OBSDATE>/sci
$ conda activate
(base)$ python -m STOPS . split
```

The split *O*- and *E*-beam FITS files are now available. The IRAF wavelength calibrations are now run. The IRAF xgterm CLI is launched using Listing A.3.

Listing A.3: Launching IRAF in xgterm

```
$ cd ~/iraf
$ xgterm -sb &
cl> conda activate salt
cl> cl
cl> cd <OBSDATE>/sci
cl> noao
cl> twodspec
cl> longslit
cl> unlearn longslit
cl> longslit.dispaxis=1
```

The IRAF `identify` task requires an average feature width, 'fwidth', as a parameter. The width of a feature may be found in IRAF using the `implot` task[2] along with cursor commands, but may also be found using FITS viewing software, such as `ds9`.[3] The `identify` task may be run using the commands in Listing A.4.

Listing A.4: Running the IRAF `identify` task

```
cl> mkscript 01_identify.cl
cl> # Add identify to 01_identify.cl twice, for both beams
cl> # Edit the parameters of 01_identify.cl in a text editor
cl> # Paste an identify script into the CLI, resulting in:
cl>
cl> identify ("<O-beam ARC>",
>>> "", "", section="middle line", database="database",
>>> coordlist="linelists$idhenear.dat", units="", nsum="10", match=-3.,
>>> maxfeatures=50, zwidth=100., ftype="emission", fwidth=8.,
>>> cradius=5., threshold=0., minsep=2., function="spline3", order=2,
>>> sample="*", niterate=0, low_reject=3., high_reject=3., grow=0.,
>>> autowrite=no, graphics="stdgraph", cursor="", aidpars="")
```

The `identify` task will launch an interactive window. Cursor commands refer to keys that provide unique functionality to the interactive IRAF tasks. The cursor commands for `identify` allow the arc lines to be identified using 'm' (and typing the relevant wavelength), while 'd' and 'i' will delete a single and all identified arc lines, respectively. The 'f' cursor command will perform a preliminary fit which can be quit using the 'q' cursor command. The 'l' cursor command will attempt to identify any unidentified arc lines. Once complete, a figure of the identified lines may be saved using ':labels coord' and ':.snap eps', and the task safely quit with the 'q' cursor command.[4] The `identify` procedure is repeated, replacing $<$*O-beam ARC*$>$ with $<$*E-beam ARC*$>$.

The `reidentify` task may be run using the commands in Listing A.5.

Listing A.5: Running the IRAF `reidentify` task

```
cl> mkscript 02_reidentify.cl
cl> # Add reidentify to 02_reidentify.cl twice, for both beams
cl> # Edit the parameters of 02_reidentify.cl in a text editor
cl> # Paste a reidentify script into the CLI, resulting in:
cl>
cl> reidentify ("<O-beam ARC>",
>>> "<O-beam ARC>", "yes", "", "", interactive="no", section="middle
>>> line", newaps=yes, override=no, refit=yes, trace=yes, step="10",
>>> nsum="10", shift="0.", search=0., nlost=0, cradius=5.,
>>> threshold=0., addfeatures=no, coordlist="linelists$idhenear.dat",
>>> match=-3., maxfeatures=50, minsep=2., database="database",
>>> logfiles="logfile", plotfile="", verbose=yes, graphics="stdgraph",
>>> cursor="", aidpars="")
```

[2] See https://astro.uni-bonn.de/~sysstw/lfa_html/iraf/plot.implot.html for documentation on the `implot` task.

[3] See https://sites.google.com/cfa.harvard.edu/saoimageds9 for documentation on the `ds9` software.

[4] See https://astro.uni-bonn.de/~sysstw/lfa_html/iraf/noao.onedspec.identify.html for documentation on the `identify` task.

The `reidentify` task will run autonomously so long as the `interactive` parameter is set to "no".[5] Repeat the `reidentify` procedure, replacing <*O-beam ARC*> with <*E-beam ARC*> at both the 'reference' and 'image' parameter locations.

The `fitcoords` task may be run using the commands in Listing A.6.

Listing A.6: Running the IRAF `fitcoords` task

```
cl> mkscript 03_fitcoords.cl
cl> # Add fitcoords to 03_fitcoords.cl twice, for both beams
cl> # Edit the parameters of 03_fitcoords.cl in a text editor
cl> # Paste a fitcoords script into the CLI, resulting in:
cl>
cl> fitcoords ("<O-beam ARC> (exclude the file extension)",
>>> fitname="", interactive=yes, combine=no, database="database",
>>> deletions="deletions.db", function="chebyshev", xorder=6, yorder=6,
>>> logfiles="STDOUT,logfile", plotfile="plotfile",
>>> graphics="stdgraph", cursor="")
```

The `fitcoords` task will launch an interactive window. The x- and y-axis being plotted may be changed using the 'x' or 'y' cursor commands followed by the desired data axis ('x' for the x-axis, 'y' for the y-axis, or 'r' for the residuals).[6] Repeat the `fitcoords` procedure, replacing <*O-beam ARC*> with <*E-beam ARC*>.

The `transform` task may be run using the commands in Listing A.7.

Listing A.7: Running the IRAF `transform` task

```
cl> mkscript 04_transform.cl
cl> # Add transform to 04_transform.cl twice, for both beams
cl> # Edit the parameters of 04_transform.cl in a text editor
cl> # Paste a transform script into the CLI, resulting in:
cl>
cl> transform ("@<O-beam FILES>",
>>> "t//@<O-beam FILES>", "<O-beam ARC> (exclude the file extension)",
>>> minput="", moutput="", database="database", interptype="linear",
>>> x1="INDEF", x2="INDEF", dx="INDEF", nx="INDEF", xlog="no",
>>> y1="INDEF", y2="INDEF", dy="INDEF", ny="INDEF", ylog="no",
>>> flux="yes", blank="INDEF", logfiles="STDOUT,logfile")
```

The `transform` task will run autonomously.[7] Repeat the `transform` procedure, replacing the <*O-beam FILES*> and <*O-beam ARC*> with <*E-beam FILES*> and <*E-beam ARC*> at both parameter locations. Inspect the transformed images, most notably the arc images, using any FITS viewer as a cursory check that the wavelength calibrations were completed without error.

The 'gain' and 'read noise' are now needed as the cosmic-ray rejection of the STOPS `join` method accepts them as parameters. These parameters may be found using the '*GAINSET*' and '*ROSPEED*' keywords in the FITS headers. The cosmic ray rejection

[5] See https://astro.uni-bonn.de/~sysstw/lfa_html/iraf/noao.onedspec.reidentify.html for documentation on the `reidentify` task.

[6] See https://astro.uni-bonn.de/~sysstw/lfa_html/iraf/noao.twodspec.longslit.fitcoords.html for documentation on the `fitcoords` task.

[7] See https://astro.uni-bonn.de/~sysstw/lfa_html/iraf/noao.twodspec.longslit.transform.html for documentation on the `transform` task.

defaults to *GAINSET*='FAINT', and *ROSPEED*='SLOW'. If the gain and read noise values differ from the defaults, the parameters should be updated when running `join`.[8]

The STOPS `join` method may be run using the commands in Listing A.8.

Listing A.8: Joining the data using STOPS

```
$ cd <OBSDATE>/sci
$ conda activate
(base)$ python -m STOPS . join
```

The STOPS `skylines` method may be run on any 'joined' or transformed FITS files, <*FILE(S)*>, using the commands in Listing A.9.

Listing A.9: Running the STOPS `skylines` method

```
$ cd <OBSDATE>/sci
$ conda activate
(base)$ python -m STOPS . skylines <FILE(S)>
```

The '`sci/`' directory may now be optionally organized by running the commands in Listing A.10, moving all the files relevant to the wavelength calibrations into either the '`database`' or '`split_files`' directories.

Listing A.10: Directory cleanup for POLSALT

```
$ cd <OBSDATE>/sci
$ mkdir split_files
$ mv *beam0* *beamE* *arc0* *arcE* split_files/
$ mv *.eps *.cl *.db database/
```

The POLSALT `spectra extraction` is now run. If the POLSALT GUI was closed it should now be reopened using Listing A.1. With the GUI in focus:

- Ensure all directories are still correct.
- Select 'Spectra extraction' from the 'Data reduction step' drop down menu.
- Check the tick boxes of all wavelength calibrated images to be processed (exclude the arc) in the display box covering the lower half of the GUI.
- Proceed with the reductions by clicking 'OK'.

The POLSALT `spectra extraction` is interactive and will launch a separate GUI for the background subtraction and spectral extraction (see Figure 3.2). The background and spectral regions to be extracted may be adjusted, noting that adjustments affect both *O*- and *E*-beams. Once both background regions contain no trace and the spectral region fully contains only the science trace, the reduction may be completed by clicking 'OK'.

[8]The read noise and gain may be determined from http://pysalt.salt.ac.za/proposal_calls/current/ProposalCall.html, specifically Table 6.1 and Table 6.2.

The STOPS `correlate` method may now be run on any 'joined' FITS files by running the commands in Listing A.11.

Listing A.11: Running the STOPS `correlate` method

```
$ cd <OBSDATE>/sci
$ conda activate
(base)$ python -m STOPS . correlate <FILE(S)>
```

The POLSALT `raw Stokes calculation`, `final Stokes calculation`, and `results visualisation` may now be completed. For the last time, if the POLSALT GUI was closed it should now be reopened using Listing A.1. With the GUI in focus:

- Ensure all directories are still correct.
- Select 'Raw Stokes calculation' from the 'Data reduction step' drop down menu.
- Check the tick boxes of all the extracted spectra images to be processed in the display box covering the lower half of the GUI.
- Proceed with the `raw Stokes calculation` by clicking 'OK'.
- Select 'Final Stokes calculation' from the 'Data reduction step' drop down menu.
- Check the tick boxes of all the "raw Stokes" images to be processed in the display box covering the lower half of the GUI.
- Proceed with the `Final Stokes calculation` by clicking 'OK'.
- Select 'Results visualisation - interactive' from the 'Data reduction step' drop down menu.
- Check the tick boxes of the "final Stokes" image to be visualized in the display box covering the lower half of the GUI.
- Proceed with the `visualisation` by clicking 'OK'.

The POLSALT `visualisation` is interactive and will launch a separate GUI (See Figure 3.3). The GUI may be used to change the binning and parameters of the plot before saving the plot to a PDF file.

This concludes the minimum working example of the POLSALT reduction process when substituting the POLSALT `wavelength calibrations` with those done in IRAF. Aside from the final results, the file structure after reductions should resemble something akin to that provided in Figure A.2.

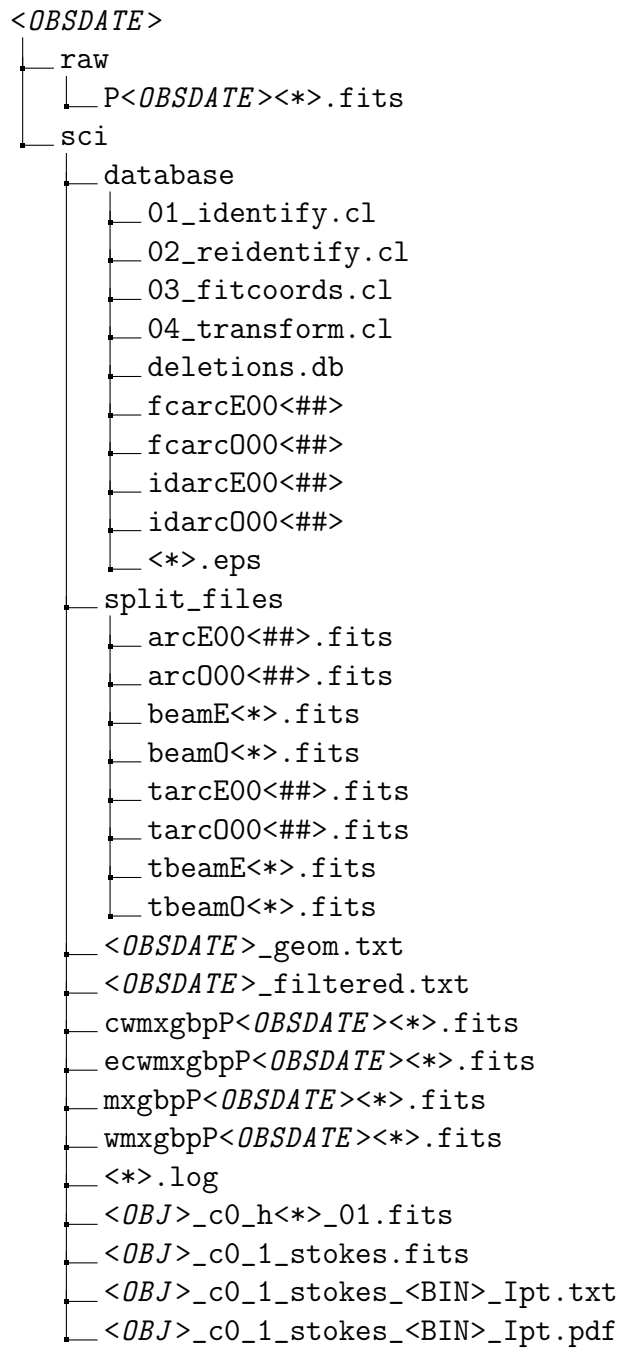

Figure A.2: The typical file structure after completing the reduction process.

Appendix B

STOPS Source Code

This section of Appendix includes all the major STOPS source code files related to the reduction process. Files such as those related to python initialization, testing directories, and other non-essential modules have been excluded for brevity and clarity.

Listing B.1: The source code for **__main__.py**

```
#!/usr/bin/env python3
# -*- coding: utf-8 -*-

"""
The Command Line Interface (CLI) for STOPS, handling argument parsing,
class instantiation, processing, and logging.

Usage
-----
`python -m STOPS`

Suffix the above command with `-h` for help on usage.

Description
-----------
This module is the entry point for the STOPS package. It provides
the CLI argument parser for the supplementary tools provided by STOPS.
The parser is built using the `argparse` module and is designed to be
user-friendly.

See Also
--------
IRAF:
    For more information on the IRAF package, see the IRAF website:
    https://iraf-community.github.io/

POLSALT:
    For more information on the POLSALT pipeline, see the POLSALT website:
    https://github.com/saltastro/polsalt

PYSALT:
    For more information on the PYSALT package, see the PYSALT website:
    https://astronomers.salt.ac.za/software/pysalt-documentation/

PYRAF:
    For more information on the PYRAF package, see the PYRAF website:
    https://pyraf.readthedocs.io/en/latest/

"""

# MARK: Imports
```

```
42 import sys
43 import argparse
44 import logging
45 from pathlib import Path
46
47 from STOPS import __version__
48 from STOPS import Split, Join, CrossCorrelate, Skylines
49 from STOPS.utils import ParserUtils as Parser
50 from STOPS.utils.Constants import SPLIT_ROW, PREFIX, PARSE, SAVE_CORR, SAVE_SKY
51
52
53 # MARK: Constants
54 PROG = "STOPS"
55 DESCRIPTION = """
56 Supplementary TOols for Polsalt Spectropolarimetry (STOPS) is a
57 collection of supplementary tools created for SALT's POLSALT pipeline,
58 allowing for wavelength calibrations with IRAF. The tools provide
59 support for splitting and joining polsalt formatted data as well as
60 cross correlating complementary polarimetric beams.
61
62 Pre-release Reference:
63     DOI: 10.22323/1.401.0056
64 """
65
66
67 # MARK: Universal Parser
68 parser = argparse.ArgumentParser(
69     prog=PROG,
70     description=DESCRIPTION,
71     formatter_class=argparse.RawDescriptionHelpFormatter,
72 )
73 parser.add_argument(
74     "-V",
75     "--version",
76     action="version",
77     version=f"%(prog)s as of {__version__}",
78 )
79 parser.add_argument(
80     "-v",
81     "--verbose",
82     action="count",
83     default=PARSE['VERBOSE'],
84     help=(
85         "Counter flag which enables and increases verbosity. "
86         "Use -v or -vv for greater verbosity levels."
87     ),
88 )
89 parser.add_argument(
90     "-l",
91     "--log",
92     action="store",
93     type=Parser.parse_logfile,
94     help=(
95         "Filename of the logging file. "
96         "File is created if it does not exist. Defaults to None."
97     ),
98 )
99 parser.add_argument(
100     "data_dir",
101     action="store",
102     nargs="?",
103     default=PARSE['DATA_DIR'],
104     type=Parser.parse_path,
105     help=(
106         "Path of the directory which contains the working data. "
107         f"Defaults to the cwd -> `{PARSE['DATA_DIR']}` (I.E. '.')."
108     ),
109 )
110
111
112 # MARK: Split\Join Parent
113 split_join_args = argparse.ArgumentParser(add_help=False)
114 split_join_args.add_argument(
```

```
    "-n",
    "--no_arc",
    action="store_true",
    help="Flag to exclude arc files from processing.",
)
split_join_args.add_argument(
    "-s",
    "--split_row",
    default=SPLIT_ROW,
    type=int,
    help=(
        "Row along which the O and E beams are split. "
        f"Defaults to polsalt's default -> {SPLIT_ROW}."
    ),
)
split_join_args.add_argument(
    "-p",
    "--save_prefix",
    nargs=2,
    default=PREFIX,
    help=(
        "Prefix appended to the filenames, "
        "with which the O and E beams are saved. "
        f"Defaults to {PREFIX}."
    ),
)


# MARK: Corr.\Sky. Parent
corr_sky_args = argparse.ArgumentParser(add_help=False)
corr_sky_args.add_argument(
    "filenames",
    action="store",
    nargs="+",
    type=Parser.parse_file,
    help=(
        "File name(s) of FITS file(s) to be processed."
        "A minimum of one filename is required."
    ),
)
corr_sky_args.add_argument(
    "-b",
    "--beams",
    choices=["O", "E", "OE"],
    type=str.upper,
    default=PARSE['BEAMS'],
    help=(
        "Beams to process. "
        f"Defaults to {PARSE['BEAMS']}, but "
        "may be given 'O', 'E', or 'OE' to "
        "determine which beams are processed."
    ),
)
corr_sky_args.add_argument(
    "-ccd",
    "--split_ccd",
    action="store_false",
    help=(
        "Flag to NOT split CCD's. "
        "Recommended to leave off unless the chip gaps "
        "have been removed from the data."
    ),
)
corr_sky_args.add_argument(
    "-c",
    "--continuum_order",
    type=int,
    default=PARSE['CONT_ORD'],
    dest="cont_ord",
    help=(
        "Order of continuum to remove from spectra. "
        "Higher orders recommended to remove most variation, "
        "leaving only significant features."
```

```
    ),
)
corr_sky_args.add_argument(
    "-p",
    "--plot",
    action="store_true",
    help="Flag for additional plot outputs.",
)


# MARK: Create subparser modes
subparsers = parser.add_subparsers(
    dest="mode",
    help="Operational mode of supplementary tools",
)


# MARK: Split Subparser
split_parser = subparsers.add_parser(
    "split",
    aliases=["s"],
    help="Split mode",
    parents=[split_join_args],
)
# 'children' split args here
# Change `split` defaults here
split_parser.set_defaults(
    mode="split",
    func=Split,
)


# MARK: Join Subparser
join_parser = subparsers.add_parser(
    "join",
    aliases=["j"],
    help="Join mode",
    parents=[split_join_args],
)
# 'children' join args here
join_parser.add_argument(
    "-c",
    "--coefficients",
    dest="solutions_list",
    nargs='*',
    type=Parser.parse_file,
    help=(
        "Custom coefficients to use instead of the `IRAF` fitcoords "
        "database. Use as either '-c <o_solution> <e_solution>' or "
        "a regex descriptor '-c <*solution*extention>'."
    ),
)
# Change `join` defaults here
join_parser.set_defaults(
    mode="join",
    func=Join,
)


# MARK: Correlate Subparser
corr_parser = subparsers.add_parser(
    "correlate",
    aliases=["x"],
    help="Cross correlation mode",
    parents=[corr_sky_args],
)
# 'children' correlate args here
corr_parser.add_argument(
    "-o",
    "--offset",
    type=int,
    default=PARSE['OFFSET'],
    help=(
```

```
        "Introduces an offset when correcting for "
        "known offset in spectra or for testing purposes. "
        f"Defaults to {PARSE['OFFSET']}. "
        "(For testing, not used during regular operation.)"
    ),
)
corr_parser.add_argument(
    "-s",
    "--save_prefix",
    action="store",
    nargs="?",
    type=lambda path: Path(path).expanduser().resolve(),
    const=SAVE_CORR,
    help=(
        "Prefix used when saving plot. "
        "Excluding flag does not save output plot, "
        f"flag usage of option uses default prefix {SAVE_CORR}, "
        "and a provided prefix overwrites default prefix."
    ),
)
# Change `correlate` defaults here
corr_parser.set_defaults(
    mode="correlate",
    func=CrossCorrelate,
)


# MARK: Skyline Subparser
sky_parser = subparsers.add_parser(
    "skylines",
    aliases=["sky"],
    help="Sky line check mode",
    parents=[corr_sky_args],
)
# 'children' skyline args here
sky_parser.add_argument(
    "-t",
    "--transform",
    action="store_false",
    help=(
        "Flag to force transform images. "
        "Recommended to use only when input image(s) "
        "are prefixed 't' but are not yet transformed."
    ),
)
sky_parser.add_argument(
    "-s",
    "--save_prefix",
    action="store",
    nargs="?",
    type=lambda path: Path(path).expanduser().resolve(),
    const=SAVE_SKY,
    help=(
        "Prefix used when saving plot. "
        "Excluding flag does not save output plot, "
        f"flag usage of option uses default prefix {SAVE_SKY}, "
        "and a provided prefix overwrites default prefix."
    ),
)
# Change `skylines` defaults here
sky_parser.set_defaults(
    mode="skyline",
    func=Skylines,
)


# MARK: Keyword Clean Up
args = parser.parse_args()

if len(sys.argv) == 1:
    parser.print_help(sys.stderr)
    sys.exit(2)

```

```
334 args.verbose = Parser.parse_loglevel(args.verbose)
335
336 if 'log' in args and args.log not in ["", None]:
337     args.log = args.data_dir / args.log
338
339 if "filenames" in args:
340     args.filenames = Parser.flatten(args.filenames)
341
342 if "solutions_list" in args and isinstance(args.solutions_list, list):
343     args.solutions_list = Parser.flatten(args.solutions_list)
344
345 # MARK: Begin logging
346 logging.basicConfig(
347     filename=args.log,
348     format="%(asctime)s - %(module)s - %(levelname)s - %(message)s",
349     datefmt="%Y-%m-%d %H:%M:%S",
350     level=args.verbose,
351 )
352
353 # MARK: Call Relevant Class(Args)
354 logging.debug(f"Argparse namespace: {args}")
355 logging.info(f"Mode:{args.mode}")
356 args.func(**vars(args)).process()
357
358
359 # Confirm all processes completed and exit without error
360 logging.info("All done! Come again!\n")
```

Listing B.2: The source code for **split.py**

```
#!/usr/bin/env python3
# -*- coding: utf-8 -*-

"""Module for splitting ``polsalt`` FITS files."""

# MARK: Imports
import os
import sys
import logging
from copy import deepcopy
from pathlib import Path

import numpy as np
from astropy.io import fits as pyfits

from STOPS.utils.SharedUtils import find_files, find_arc
from STOPS.utils.Constants import SAVE_PREFIX, CROP_DEFAULT, SPLIT_ROW


# MARK: Split Class
class Split:
    """
    The `Split` class allows for the splitting of `polsalt` FITS files
    based on the polarization beam. The FITS files must have basic
    `polsalt` pre-reductions already applied (`mxgbp...` FITS files).

    Parameters
    ----------
    data_dir : str | Path
        The path to the data to be split
    fits_list : list[str], optional
        A list of pre-reduced `polsalt` FITS files to be split
        within `data_dir`.
        (The default is None, `Split` will search for `mxgbp*.fits` files)
    split_row : int, optional
        The row along which to split the data of each extension in
        the FITS file.
        (The default is SPLIT_ROW (See Notes), the SALT RSS CCD's middle row)
    no_arc : bool, optional
        Decides whether the arc frames should be recombined.
        (The default is False, `polsalt` has no use for the arc after
        wavelength calibrations)
    save_prefix : dict[str, list[str]], optional
        The prefix with which to save the  O & E beams.
        Setting `save_prefix` = ``None`` does not save the split O & E beams.
        (The default is SAVE_PREFIX (See Notes))

    Attributes
    ----------
    arc : str
        Name of arc FITS file within `data_dir`.
        `arc` = `""` if `no_arc` or not detected in `data_dir`.
    o_files, e_files : list[str]
        A list of the `O`- and `E`-beam FITS file names.
        The first entry is the arc file if `arc` defined.
    data_dir
    fits_list
    split_row
    save_prefix

    Methods
    -------
    split_file(file: os.PathLike)
        -> tuple[astropy.io.fits.HDUList]
        Handles creation and saving the separated FITS files
    split_ext(hdulist: astropy.io.fits.HDUList, ext: str = 'SCI')
        -> astropy.io.fits.HDUList
        Splits the data in the `ext` extension along the `split_row`
    crop_file(hdulist: astropy.io.fits.HDUList, crop: int = CROP_DEFAULT)
        -> tuple[numpy.ndarray]
        Crops the data along the edge of the frame, that is,
```

```
        `O`-beam cropped as [crop:], and
        `E`-beam cropped as [:-crop].
    update_beam_lists(o_name: str, e_name: str)
        -> None
        Updates `o_files` and `e_files`.
    save_beam_lists(file_suffix: str = 'frames')
        -> None
        Creates (Overwrites if exists) and writes the `o_files` and `e_files`
        to files named `o_{file_suffix}` and `e_{file_suffix}`, respectively.
    process()
        -> None
        Calls `split_file` and `save_beam_lists` on each file in `fits_list`
        for automation.

    Other Parameters
    ----------------
    **kwargs : dict
        keyword arguments. Allows for passing unpacked dictionary to
        the class constructor.

    Notes
    -----
    Constants Imported (See utils.Constants):
        SAVE_PREFIX
        CROP_DEFAULT
        SPLIT_ROW
    """

    # MARK: Split init
    def __init__(
            self,
            data_dir: Path,
            fits_list: list[str] = None,
            split_row: int = SPLIT_ROW,
            no_arc: bool = False,
            save_prefix: Path | None = None,
            **kwargs,
    ) -> None:
        self.data_dir = data_dir
        self.fits_list = find_files(
            data_dir=data_dir,
            filenames=fits_list,
            prefix="mxgbp",
            ext="fits"
        )
        self.split_row = split_row
        self.save_prefix = SAVE_PREFIX
        if isinstance(save_prefix, dict):
            self.save_prefix = save_prefix

        self.arc = "" if no_arc else find_arc(self.fits_list)
        self.o_files = []
        self.e_files = []

        logging.debug(f"__init__\n{repr(self)}")

        return

    def __repr__(self) -> str:
        template = (
            "Split(\n"
            f"\tdata_dir={self.data_dir},\n"
            f"\tfits_list=[\n\t\t{"\n\t\t".join(
                map(str, self.fits_list)
            )}\n\t],\n"
            f"\tsplit_row={self.split_row},\n"
            f"\tno_arc={self.arc == ''},\n"
            f"\tsave_prefix={self.save_prefix}\n"
            ")\n"
        )

        return template

```

```
    # MARK: Split Files
    def split_file(
            self,
            file: os.PathLike
    ) -> tuple[pyfits.HDUList, pyfits.HDUList]:
        """
        Split the single FITS file into separated `O`- and `E`- FITS files.

        Parameters
        ----------
        file : os.PathLike
            The name of the FITS file to be split.

        Returns
        -------
        tuple[astropy.io.fits.HDUList, astropy.io.fits.HDUList]
            Tuple containing the split O and E beam HDULists.
        """
        # Create empty HDUList
        o_beam = pyfits.HDUList()
        e_beam = pyfits.HDUList()

        # Open file and split O & E beams
        with pyfits.open(file) as hdul:
            o_beam.append(hdul["PRIMARY"].copy())
            e_beam.append(hdul["PRIMARY"].copy())

            # Split specific extention
            raw_split = self.split_ext(hdul, "SCI")

            # o_beam[0].data = raw_split['SCI'].data[1]
            # e_beam[0].data = raw_split['SCI'].data[0]
            o_beam[0].data, e_beam[0].data = self.crop_file(raw_split)

            # Handle prefix and names
            pref = "arc" if file == self.arc else "beam"
            o_name = self.save_prefix[pref][0] + file.name[-9:]
            e_name = self.save_prefix[pref][1] + file.name[-9:]

            # Add split data to O & E beam lists
            self.update_beam_lists(o_name, e_name, pref == "arc")

            # Handle don't save case
            if self.save_prefix is None:
                return o_beam, e_beam

            # Handle save case
            o_beam.writeto(o_name, overwrite=True)
            e_beam.writeto(e_name, overwrite=True)

            return o_beam, e_beam

    # MARK: Split extensions
    def split_ext(
            self,
            hdulist: pyfits.HDUList,
            ext: str = "SCI"
    ) -> pyfits.HDUList:
        """
        Split the data of the specified extension of `hdulist` into
        its `O`- and `E`- beams.

        Parameters
        ----------
        hdulist : astropy.io.fits.HDUList
            The FITS HDUList to be split.
        ext : str, optional
            The name of the extension to be split.
            (Defaults to 'SCI')

        Returns
        -------
        astropy.io.fits.HDUList
```

```
218             The HDUList with the split applied.
219         """
220         hdu = deepcopy(hdulist)
221         rows, cols = hdu[ext].data.shape
222 
223         # if odd number of rows, strip off the last one
224         rows = int(rows / 2) * 2
225 
226         # how far split is from center of detector
227         offset = int(self.split_row - rows / 2)
228 
229         # split arc into o/e images
230         ind_rc = np.indices((rows, cols))[0]
231         padbins = (ind_rc < offset) | (ind_rc > rows + offset)
232 
233         # Roll split_row to be centre row
234         image_rc = np.roll(hdu[ext].data[:rows, :], -offset, axis=0)
235         image_rc[padbins] = 0.0
236 
237         # Split columns equally
238         hdu[ext].data = image_rc.reshape((2, int(rows / 2), cols))
239 
240         return hdu
241 
242     # MARK: Crop files
243     @staticmethod
244     def crop_file(
245             hdulist: pyfits.HDUList,
246             crop: int = CROP_DEFAULT
247     ) -> tuple[np.ndarray, np.ndarray]:
248         """
249         Crop the data with respect to the `O`/`E` beam.
250 
251         Parameters
252         ----------
253         hdulist : astropy.io.fits.HDUList
254             The HDUList containing the data to be cropped.
255         crop : int, optional
256             The number of rows to be cropped from the bottom and top
257             of the `O` and `E` beam, respectively.
258             (Defaults to 40)
259 
260         Returns
261         -------
262         tuple[numpy.ndarray, np.ndarray]
263             Tuple containing the cropped O and E beam data arrays.
264         """
265         o_data = hdulist["SCI"].data[1, 0:-crop]
266         e_data = hdulist["SCI"].data[0, crop:]
267 
268         return o_data, e_data
269 
270     # MARK: Update beam lists
271     def update_beam_lists(
272             self,
273             o_name,
274             e_name,
275             arc: bool = True
276     ) -> None:
277         """
278         Update the `o_files` and `e_files` attributes.
279 
280         Parameters
281         ----------
282         o_name : str
283             The filename of the O beam.
284         e_name : str
285             The filename of the E beam.
286         arc : bool, optional
287             Indicates whether the first entry should be the arc frame.
288             (Defaults to True)
289 
290         Returns
```

```
        -------
        None

        """
        if arc:
            self.o_files.insert(0, o_name)
            self.e_files.insert(0, e_name)
        else:
            self.o_files.append(o_name)
            self.e_files.append(e_name)

        return

    # MARK: Save beam lists
    def save_beam_lists(self, file_suffix: str = 'frames') -> None:
        with open(f"o_{file_suffix}", "w+") as f_o, \
                open(f"e_{file_suffix}", "w+") as f_e:
            for i, j in zip(self.o_files, self.e_files):
                f_o.write(i + "\n")
                f_e.write(j + "\n")

        return

    # MARK: Process all Listed Images
    def process(self) -> None:
        """
        Process all FITS images stored in the `fits_list` attribute

        Returns
        -------
        None
        """
        for target in self.fits_list:
            logging.debug(f"Processing {target}")
            self.split_file(target)

        self.save_beam_lists()

        return


# MARK: Main function
def main(argv) -> None:
    """Main function."""

    return


if __name__ == "__main__":
    main(sys.argv[1:])
```

Listing B.3: The source code for **join.py**

```
#!/usr/bin/env python3
# -*- coding: utf-8 -*-

"""
Module for joining the split FITS files with an external wavelength solution.
"""

# MARK: Imports
import os
import sys
import logging
import re
from pathlib import Path

import numpy as np
from numpy.polynomial.chebyshev import chebgrid2d as chebgrid2d
from numpy.polynomial.legendre import leggrid2d as leggrid2d
from astropy.io import fits as pyfits

# from lacosmic import lacosmic # Deprecated: ccdproc is ~6x faster
from ccdproc import cosmicray_lacosmic as lacosmic

from STOPS.utils.specpolpy3 import read_wollaston, split_sci
from STOPS.utils.SharedUtils import find_files, find_arc
from STOPS.utils.Constants import DATADIR, SAVE_PREFIX, SPLIT_ROW, CR_PARAMS


# MARK: Join Class
class Join:
    """
    The `Join` class allows for the joining of previously split files
    and the appending of an external wavelength solution in the
    `polsalt` FITS file format.

    Parameters
    ----------
    data_dir : str | Path
        The path to the data to be joined
    database : str, optional
        The name of the `IRAF` database folder.
        (The default is "database")
    fits_list : list[str], optional
        A list of pre-reduced `polsalt` FITS files to be joined
        within `data_dir`.
        (The default is ``None``, `Join` will search for `mxgbp*.fits` files)
    solutions_list: list[str], optional
        A list of solution filenames from which the wavelength solution
        is created.
        (The default is ``None``, `Join` will search for `fc*` files within
        the `database` directory)
    split_row : int, optional
        The row along which the data of each extension in the FITS file
        was split.
        Necessary when Joining cropped files.
        (The default is 517, the SALT RSS CCD's middle row)
    save_prefix : dict[str, list[str]], optional
        The prefix with which the previously split `O`- & `E`-beams were saved.
        Used for detecting if cropping was applied during
        the splitting procedure.
        (The default is SAVE_PREFIX (See Notes))
    verbose : int, optional
        The level of verbosity to use for the Cosmic ray rejection
        (The default is 30, I.E. logging.INFO)

    Attributes
    ----------
    fc_files : list[str]
        Valid solutions found from `solutions_list`.
    custom : bool
        Internal flag for whether `solutions_list` uses the `IRAF`
        or a custom format.
```

```
72          See Notes for custom solution formatting.
73          (Default (inherited from `solutions_list`) is False)
74      arc : str
75          Deprecated. Name of arc FITS file within `data_dir`.
76      data_dir
77      database
78      fits_list
79      split_row
80      save_prefix
81
82      Methods
83      -------
84      get_solutions(wavlist: list | None, prefix: str = "fc") ->
85          (fc_files, custom): tuple[list[str], bool]
86          Parse `solutions_list` and return valid solution files and if they are
87          non-`IRAF` solutions.
88      parse_solution(fc_file: str, x_shape: int, y_shape: int) ->
89          tuple[dict[str, int], np.ndarray]
90          Loads the wavelength solution file and parses keywords necessary for
91          creating the wavelength extension.
92      join_file(file: os.PathLike) -> None
93          Joins the files,
94          attaches the wavelength solutions,
95          performs cosmic ray cleaning,
96          masks the extension,
97          and checks cropping performed in `Split`.
98          Writes the FITS file in a `polsalt` valid format.
99      check_crop(hdu: pyfits.HDUList, o_file: str, e_file: str) -> int
100         Opens the split `O`- and `E`-beam FITS files and returns the amount of
101         cropping that was performed.
102     process() -> None
103         Calls `join_file` on each file in `fits_list` for automation.
104
105     Other Parameters
106     ----------------
107     no_arc : bool, optional
108         Deprecated. Decides whether the arc frames should be processed.
109         (The default is False, `polsalt` has no use for the arc after
110         wavelength calibrations)
111     **kwargs : dict
112         keyword arguments. Allows for passing unpacked dictionary to the
113         class constructor.
114
115     Notes
116     -----
117     Constants Imported (See utils.Constants):
118         DATADIR, SAVE_PREFIX, SPLIT_ROW, CR_PARAMS
119
120     Custom wavelength solutions must be formatted containing:
121         `x`, `y`, *coefficients...
122     where a solution are of order (`x` by `y`) and
123     must contain x*y coefficients, all separated by newlines.
124     The name of the custom wavelength solution file must contain
125     either "cheb" or "leg" for Chebyshev or Legendre wavelength solutions,
126     respectively.
127
128     Cosmic ray rejection is performed using lacosmic [1]_
129     implemented in ccdproc via astroscrappy [2]_.
130
131     References
132     ----------
133     .. [1] van Dokkum 2001, PASP, 113, 789, 1420
134            (article : https://adsabs.harvard.edu/abs/2001PASP..113.1420V)
135     .. [2] https://zenodo.org/records/1482019
136
137     """
138
139     # MARK: Join init
140     def __init__(
141             self,
142             data_dir: Path,
143             database: str = "database",
144             fits_list: list[str] = None,
```

```
            solutions_list: list[Path] = None,
            split_row: int = SPLIT_ROW,
            no_arc: bool = True,
            save_prefix: Path | None = None,
            verbose: int = 30,
            **kwargs,
    ) -> None:
        self.data_dir = data_dir
        self.database = Path(data_dir) / database
        self.fits_list = find_files(
            data_dir=self.data_dir,
            filenames=fits_list,
            prefix="mxgbp",
            ext="fits",
        )
        self.fc_files, self.custom = self.get_solutions(solutions_list)
        self.split_row = split_row
        self.save_prefix = SAVE_PREFIX
        if isinstance(save_prefix, dict):
            self.save_prefix = save_prefix

        self.no_arc = no_arc
        self.arc = find_arc(self.fits_list)

        self.verbose = verbose < 30

        logging.debug(f"__init__\n{repr(self)}")

        return

    # MARK: Join repr
    def __repr__(self) -> str:
        template = (
            "Join(\n"
            f"\tdata_dir={self.data_dir},\n"
            f"\tdatabase={self.database},\n"
            f"\tfits_list=[\n\t\t{"\n\t\t".join(
                map(str, self.fits_list)
            )}\n\t],\n"
            f"\tsolutions_list={self.fc_files},\n"
            f"\tsplit_row={self.split_row},\n"
            f"\tno_arc={self.no_arc},\n"
            f"\tsave_prefix={self.save_prefix},\n"
            f"\tverbose={self.verbose}\n"
            ")\n"
        )

        return template

    # MARK: Find 2D WAV Functions
    def get_solutions(
            self,
            wavlist: list[str] | None,
            prefix: str = "fc",
            reverse: bool = False,
    ) -> tuple[list[str], bool]:
        """
        Get the list of wavelength solution files.

        Parameters
        ----------
        wavlist : list[str] | None
            A list of custom wavelength solutions files.
            If ``None``, `Join` will search for wavelength solutions
            in the `database` directory.
        prefix : str, optional
            The prefix of the wavelength solution files.
            (Defaults to "fc")
        reverse : bool, optional
            Whether to reverse the wavelength solution files.
            Necessary when `wavlist` ordered ['O', 'E']
            (Defaults to False)

```

```
        Returns
        -------
        tuple[list[str], bool]
            A tuple containing the list of wavelength solutions files and
            a boolean indicating whether custom solutions were provided.

        """
        # No custom solutions
        if not wavlist:
            # Handle finding solutions
            ws = []
            for fl in os.listdir(self.database):
                if os.path.isfile(
                    self.database / fl
                ) and (prefix == fl[0:len(prefix)]):
                    ws.append(fl)

            if len(ws) != 2:
                # Handle incorrect number of solutions found
                msg = (
                    f"Incorrect amount of wavelength solutions "
                    f"({len(ws)} fc... files) found in the solution "
                    f"dir.: {self.database}"
                )
                logging.error(msg)
                raise FileNotFoundError(msg)

            sols = {
                i: j for i, j in zip(['O', 'E'], sorted(ws, reverse=reverse))
            }
            logging.debug(f"get_solutions - Found {sols} in {self.database}")

            return sorted(ws, reverse=reverse), False

        # Custom solution
        if len(wavlist) >= 2:
            if len(wavlist) > 2:
                logging.warning(
                    f" Too many solutions, only {wavlist[:2]} are considered"
                )
                wavlist = wavlist[:2]

            for fl in wavlist:
                if not os.path.isfile(os.path.join(self.data_dir, fl)):
                    msg = (
                        f"{fl} not found in the "
                        f"data directory {self.data_dir}"
                    )
                    logging.error(msg)
                    raise FileNotFoundError(msg)

            sols = {
                i: j for i, j in zip(
                    ['O', 'E'],
                    sorted(wavlist, reverse=reverse)
                )
            }
            logging.debug(f"get_solutions - Found {sols} in {self.database}")

            return sorted(wavlist, reverse=reverse), True

    # MARK: Parse 2D WAV Function
    def parse_solution(
            self,
            fc_file: str,
            x_shape: int,
            y_shape: int
    ) -> tuple[dict[str, int], np.ndarray]:
        """
        Parse the 2D wavelength solution function from `fc_file`.

        Parameters
        ----------
```

```
        fc_file : str
            The filename of the wavelength solutions file.
        x_shape : int
            The x-order of the 2D solution.
        y_shape : int
            The y-order of the 2D solution.

        Returns
        -------
        tuple[dict[str, int], np.ndarray]
            A tuple containing a dictionary of
            the parameters of the solution function
            and the function coefficients.

        """
        fit_params = {}

        if self.custom:
            # Load coefficients
            coeff = np.loadtxt(fc_file)

            fit_params["xorder"] = int(coeff[0].astype(int))
            fit_params["yorder"] = int(coeff[1].astype(int))
            coeff = coeff[2:]

            f_type = 3
            if "cheb" in str(fc_file):
                f_type = 1
            elif "leg" in str(fc_file):
                f_type = 2
            fit_params["function"] = f_type

            fit_params["xmin"], fit_params["xmax"] = 1, x_shape
            fit_params["ymin"], fit_params["ymax"] = 1, y_shape

        else:
            # Parse IRAF fc database files
            file_contents = []
            with open(self.database / fc_file) as fcfile:
                for i in fcfile:
                    file_contents.append(re.sub(r"[\n\t\s]*", "", i))

            if file_contents[9] != "1.":  # xterms - Cross-term type
                msg = (
                    "Cross-term not recognised (always 1 for "
                    "FITCOORDS), redo FITCOORDS or change manually."
                )
                raise Exception(msg)

            fit_params["function"] = int(file_contents[6][:-1])

            fit_params["xorder"] = round(float(file_contents[7][:-1]), None)
            fit_params["yorder"] = round(float(file_contents[8][:-1]), None)

            fit_params["xmin"] = int(file_contents[10][:-1])
            fit_params["xmax"] = x_shape
            # int(file_contents[11][:-1])# stretch fit over x
            fit_params["ymin"] = int(file_contents[12][:-1])
            fit_params["ymax"] = y_shape
            # int(file_contents[13][:-1])# stretch fit over y

            coeff = np.array(file_contents[14:], dtype=float)

        coeff = np.reshape(
            coeff,
            (fit_params["xorder"], fit_params["yorder"])
        )

        return fit_params, coeff

    # MARK: Join Files
    def join_file(self, file: os.PathLike) -> None:
        """
```

```
364         Join the `O`- and `E`-beams, attach the wavelength solutions,
365         perform cosmic ray cleaning, mask the extensions,
366         and checks cropping performed by `Split`.
367         Write the FITS file in a `polsalt` valid format.
368
369         Parameters
370         ----------
371         file : os.PathLike
372             The path of the FITS file to be joined.
373
374         See Also
375         --------
376         IRAF - `fitcoords` task
377             https://iraf.net/irafdocs/formats/fitcoords.php,
378         numpy 2D grid functions
379             https://numpy.org/doc/stable/reference/generated/numpy
380             Chebyshev: + '.polynomial.chebyshev.chebgrid2d.html'
381             Legendre: + '.polynomial.legendre.leggrid2d.html'
382
383         """
384         # Create empty wavelength appended hdu list
385         whdu = pyfits.HDUList()
386
387         # Handle prefix and names
388         pref = "arc" if file == self.arc else "beam"
389         o_file = self.save_prefix[pref][0] + file.name[-9:]
390         e_file = self.save_prefix[pref][1] + file.name[-9:]
391
392         # Open file
393         with pyfits.open(file) as hdu:
394             # Check if file has been cropped
395             cropsize = self.check_crop(hdu, o_file, e_file)
396
397             y_shape = int(hdu["SCI"].data.shape[0] / 2) - cropsize
398             x_shape = hdu["SCI"].data.shape[1]
399
400             # No differences in "PRIMARY" extention header
401             primary_ext = hdu["PRIMARY"]
402             primary_ext.header["HISTORY"] = f"CRCLEAN: {CR_PARAMS}"
403             whdu.append(primary_ext)
404
405             for ext in ["SCI", "VAR", "BPM"]:
406                 whdu.append(pyfits.ImageHDU(name=ext))
407                 whdu[ext].header = hdu[ext].header.copy()
408                 whdu[ext].header["CTYPE3"] = "O,E"
409
410                 # Create empty extentions with correct order and format
411                 if ext == "BPM":
412                     whdu[ext].data = np.zeros(
413                         (2, y_shape, x_shape),
414                         dtype="uint8"
415                     )
416                     whdu[ext].header["BITPIX"] = "-uint8"
417                 else:
418                     whdu[ext].data = np.zeros(
419                         (2, y_shape, x_shape),
420                         dtype=">f4"
421                     )
422                     whdu[ext].header["BITPIX"] = "-32"
423
424                 # Fill in empty extentions
425                 if cropsize:
426                     temp_split = split_sci(
427                         hdu,
428                         self.split_row,
429                         ext=ext
430                     )[ext].data
431                     whdu[ext].data[0] = temp_split[0, cropsize:]
432                     whdu[ext].data[1] = temp_split[1, 0:-cropsize]
433
434                 else:
435                     whdu[ext].data = split_sci(
436                         hdu,
```

```
                        self.split_row,
                        ext=ext
                    )[ext].data
        # End of hdu calls, close hdu

        # MARK: Join (Wav. Ext.)
        whdu.append(pyfits.ImageHDU(name="WAV"))
        wav_header = whdu["SCI"].header.copy()
        wav_header["EXTNAME"] = "WAV"
        wav_header["CTYPE3"] = "O,E"
        whdu["WAV"].header = wav_header

        whdu["WAV"].data = np.zeros(
            whdu["SCI"].data.shape,
            dtype=">f4"
        )

        for num, fname in enumerate(self.fc_files):
            params, coeffs = self.parse_solution(
                fname,
                x_shape,
                y_shape
            )

            if params["function"] == 1:  # Function type (1 = chebyshev)
                # Set wavelength extention values to function
                whdu["WAV"].data[num] = chebgrid2d(
                    x=np.linspace(-1, 1, params["ymax"]),
                    y=np.linspace(-1, 1, params["xmax"]),
                    c=coeffs,
                )

            elif params["function"] == 2:  # Function type (2 = legendre)
                # Set wavelength extention values to function
                whdu["WAV"].data[num] = leggrid2d(
                    x=np.linspace(-1, 1, params["ymax"]),
                    y=np.linspace(-1, 1, params["xmax"]),
                    c=coeffs,
                )

            else:
                msg = (
                    "Function type not recognised, please wavelength "
                    "calibrate using either Chebyshev or Legendre."
                )
                raise Exception(msg)

            # MARK: Cosmic Ray Cleaning
            # See utils.Constants for `CR_PARAMS` discussion
            whdu["SCI"].data[num] = lacosmic(
                whdu["SCI"].data[num],
                # contrast=CR_PARAMS['CR_CONTRAST'],
                # threshold=CR_PARAMS['CR_THRESHOLD'],
                # neighbor_threshold=CR_PARAMS['CR_NEIGH_THRESH'],
                # effective_gain=CR_PARAMS['GAIN'],
                # background=CR_PARAMS['BACKGROUND'],
                readnoise=CR_PARAMS['READ_NOISE'],
                gain=CR_PARAMS['GAIN'],
                gain_apply=CR_PARAMS['GAIN_APPLY'],
                objlim=CR_PARAMS['OBJ_LIM'],
                verbose=self.verbose,
            )[0]

        # MARK: WAV masking
        # Left & Right Crop
        whdu["WAV"].data[whdu["WAV"].data[:] < 3_000] = 0.0
        whdu["WAV"].data[whdu["WAV"].data[:] >= 10_000] = 0.0

        # Top & Bottom Crop (shift\tilt)
        rpix_oc, cols, rbin, lam_c = read_wollaston(
            whdu,
            DATADIR + "wollaston.txt"
        )
```

```
510
511         drow_oc = (rpix_oc - rpix_oc[:, int(cols / 2)][:, None]) / rbin
512
513         # Cropping as suggested
514         for c, col in enumerate(drow_oc[0]):
515             if np.isnan(col):
516                 continue
517
518             if int(col) < 0:
519                 whdu["WAV"].data[0, int(col):, c] = 0.0
520             elif int(col) > cropsize:
521                 whdu["WAV"].data[0, 0: int(col) - cropsize, c] = 0.0
522
523         for c, col in enumerate(drow_oc[1]):
524             if np.isnan(col):
525                 continue
526
527             if int(col) > 0:
528                 whdu["WAV"].data[1, 0: int(col), c] = 0.0
529             elif (int(col) < 0) & (abs(int(col)) > cropsize):
530                 whdu["WAV"].data[1, int(col) + cropsize:, c] = 0.0
531
532         # MARK: BPM masking
533         whdu["BPM"].data[0] = np.where(
534             whdu["WAV"].data[0] == 0,
535             1,
536             whdu["BPM"].data[0]
537         )
538         whdu["BPM"].data[1] = np.where(
539             whdu["WAV"].data[1] == 0,
540             1,
541             whdu["BPM"].data[1]
542         )
543
544         whdu.writeto(f"w{os.path.basename(file)}", overwrite="True")
545
546         return
547
548     # MARK: Check Crop
549     @staticmethod
550     def check_crop(
551             hdu: pyfits.HDUList,
552             o_file: str,
553             e_file: str
554     ) -> int:
555         """
556         Check if cropping is necessary when joining `O`- and `E`-beams.
557
558         Parameters
559         ----------
560         hdu : astropy.io.fits.HDUList
561             The HDUList to check for cropping.
562         o_file : str
563             The name of the previously split `O`-beam FITS file.
564         e_file : str
565             The name of the previously split `E`-beam FITS file.
566
567         Returns
568         -------
569         int
570             The number of rows which were cropped by `Split`.
571
572         """
573         cropsize = 0
574
575         with pyfits.open(o_file) as o, \
576                 pyfits.open(e_file) as e:
577             o_y = o[0].data.shape[0]
578             e_y = e[0].data.shape[0]
579
580         if hdu["SCI"].data.shape[0] != (o_y + e_y):
581             # Get crop size, assuming crop same on both sides
582             cropsize = int((hdu["SCI"].data.shape[0] - o_y - e_y) / 2)
```

```
583
584         return cropsize
585
586     # MARK: Process all Listed Images
587     def process(self) -> None:
588         """Process all FITS images stored in the `fits_list` attribute"""
589         for target in self.fits_list:
590             logging.debug(f"Processing {target}")
591             self.join_file(target)
592
593         return
594
595
596 def main(argv) -> None:
597     """Main function."""
598
599     return
600
601
602 if __name__ == "__main__":
603     main(sys.argv[1:])
```

Listing B.4: The source code for **cross_correlate.py**

```
#!/usr/bin/env python3
# -*- coding: utf-8 -*-

"""Module for cross correlating polarization beams."""

# MARK: Imports
import sys
import logging
import itertools as iters
from pathlib import Path
from importlib.resources import files
from typing import Callable

import numpy as np
from numpy.polynomial import chebyshev
import matplotlib.pyplot as plt
import matplotlib.axes
from astropy.io import fits as pyfits
from scipy import signal

from STOPS.utils.SharedUtils import find_files, continuum
from STOPS.utils.Constants import SAVE_CORR, OFFSET
import STOPS.utils

# MARK: Logging init.
mpl_logger = logging.getLogger('matplotlib')
mpl_logger.setLevel(logging.INFO)


# MARK: Correlate class
class CrossCorrelate:
    """
    Cross correlate allows for comparing the extensions of multiple
    FITS files, or comparing the $O$- and $E$-beams of a single FITS file.

    Parameters
    ----------
    data_dir : str | Path
        The path to the data to be cross correlated
    filenames : list[str]
        The ecwmxgbp*.fits files to be cross correlated.
        If only one filename is defined, correlation is done against the two
        polarization beams.
    split_ccd : bool, optional
        Decides whether the CCD regions should each be individually
        cross correlated.
        (The default is True, which splits the spectrum up into its separate
        CCD regions)
    cont_ord : int, optional
        The degree of a chebyshev to fit to the continuum.
        (The default is 11)
    plot : bool, optional
        Decides whether the continuum fitting should be plotted
        (The default is False, so no continua plots are displayed)
    save_prefix : str, optional
        The name or directory to save the figure produced to.
        "." saves a default name to the current working. A default name is
        also used when save_prefix is a directory.
        (The default is None, I.E. The figure is not saved, only displayed)

    Attributes
    ----------
    data_dir
    fits_list
    beams : str
        The mode of correlation.
        'OE' for same file, and 'O' or 'E' for different files but same
        extension.
    ccds : int
        The number of CCD's in the data.
        Used to split the CCD's if split_ccd is True.
```

```
    cont_ord : int
        The degree of the chebyshev to fit to the continuum.
    can_plot : bool
        Decides whether the continuum fitting should be plotted
    offset : int, DEPRECATED
        The amount the spectrum is shifted, mainly to test the effect of the
        cross correlation.
        (The default is 0, I.E. no offset introduced)
    save_prefix
    wav_unit : str
        The units of the wavelength axis.
        (The default is Angstroms)
    wav_cdelt : int
        The wavelength increment.
        (The default is 1)
    alt : Callable
        An alternate method of cross correlating the data.
        (The default is None)

    Methods
    -------
    load_file(filename: Path) -> tuple[np.ndarray, np.ndarray, np.ndarray]
        Loads the data from a FITS file.
    get_bounds(bpm: np.ndarray) -> np.ndarray
        Finds the bounds for the CCD regions.
    remove_cont(spec: list, wav: list, bpm: list, plot_cont: bool) -> None
        Removes the continuum from the data.
    correlate(filename1: Path, filename2: Path | None = None) -> None
        Cross correlates the data.
    ftcs(filename1: Path, filename2: Path | None = None) -> None
        Cross correlates the data using the Fourier Transform.
    plot(spec, wav, bpm, corrdb, lagsdb) -> None
        Plots the data.
    process() -> None
        Processes the data.

    Other Parameters
    ----------------
    offset : int, optional
        The amount the spectrum is shifted, mainly to test the effect of the
        cross correlation.
        (The default is 0, I.E. no offset introduced)
    **kwargs : dict
        keyword arguments.
        Allows for passing unpacked dictionary to the class constructor.
        ftcs : bool, optional
            Boolean whether to use Fourier Transform for cross correlation.

    See Also
    --------
    scipy:
        https://docs.scipy.org/doc/scipy/reference/generated/
        correlation:
            scipy.signal.correlate.html
    matplotlib custom style:
        https://matplotlib.org/stable/users/explain/customizing.html

    Notes
    -----
    Constants Imported (See utils.Constants):
        SAVE_CORR:
            The default save name for the correlation plot.
        OFFSET:
            The vertical offset of spectra in the output plot.
    """

    # MARK: Correlate init
    def __init__(
            self,
            data_dir: Path,
            filenames: list[str],
            beams: str = "OE",
            split_ccd: bool = True,
```

```
            cont_ord: int = 11,
            plot: bool = False,
            offset: int = 0,
            save_prefix: Path | None = None,
            **kwargs,
    ) -> None:
        self.data_dir = data_dir
        self.fits_list = find_files(
            data_dir=self.data_dir,
            filenames=filenames,
            prefix="ecwmxgbp",
            ext="fits",
        )
        self._beams = None
        self.beams = beams

        self.ccds = 1
        if split_ccd:
            # with pyfits.open(self.fits_list[0]) as hdu:
            #     BPM == 2 near center of CCD (extract version != *_sc)
            #     self.ccds = sum(hdu["BPM"].data.sum(axis=1)[0] == 2)
            self.ccds = 3

        self.cont_ord = cont_ord
        self.can_plot = plot

        self.offset = offset
        if offset != 0:
            # logging.warning("'offset' is only for testing.")
            # # Add an offset to the spectra to test cross correlation
            # self.spec1 = np.insert(
            #     self.spec1, [0] * offset, self.spec1[:, :offset], axis=-1
            # )[:, : self.spec1.shape[-1]]

            err_msg = "Offset deprecated after testing finalized."
            logging.error(err_msg)
            raise DeprecationWarning(err_msg)

        self.save_prefix = save_prefix
        # Handle directory save name
        if self.save_prefix and self.save_prefix.is_dir():
            self.save_prefix /= SAVE_CORR
            logging.warning((
                f"Correlation save name resolves to a directory. "
                f"Saving under {self.save_prefix}"
            ))

        self.wav_unit = "$\\AA$"
        self.wav_cdelt = 1

        self.alt = self.ftcs if kwargs.get("ftcs") else None

        logging.debug(f"__init__ - \n{repr(self)}")

        return

    # MARK: Correlate repr
    def __repr__(self) -> str:
        template = (
            "CrossCorrelate(\n"
            f"\tdata_dir={self.data_dir},\n"
            f"\tfits_list=[\n\t\t{"\n\t\t".join(
                map(str, self.fits_list)
            )}\n\t],\n"
            f"\tbeams={self._beams},\n"
            f"\tsplit_ccd={self.ccds},\n"
            f"\tcont_ord={self.cont_ord},\n"
            f"\tplot={self.can_plot},\n"
            f"\toffset={self.offset},\n"
            f"\tsave_prefix={self.save_prefix},\n"
            f"\twav_unit={self.wav_unit},\n"
            f"\twav_cdelt={self.wav_cdelt},\n"
            f"\talt={self.alt},\n"
```

```
            ")\n"
        )

        return template

    # MARK: Beams property
    @property
    def beams(self) -> str:
        return self._beams

    @beams.setter
    def beams(self, mode: str) -> None:
        if mode not in ['O', 'E', 'OE']:
            err_msg = f"Correlation mode '{mode}' not recognized."
            logging.error(err_msg)
            raise ValueError(err_msg)

        self._beams = mode

        return

    # MARK: Load file
    def load_file(
            self,
            filename: Path
    ) -> tuple[np.ndarray, np.ndarray, np.ndarray]:
        """
        Load the data from a FITS file.

        Parameters
        ----------
        filename : Path
            The name of the FITS file to load.

        Returns
        -------
        tuple[np.ndarray, np.ndarray, np.ndarray]
            The spectrum, wavelength, and bad pixel mask.

        """

        # Open HDU
        with pyfits.open(filename) as hdul:
            spec = hdul["SCI"].data.sum(axis=1)
            wav = (
                    np.arange(spec.shape[-1])
                    * hdul["SCI"].header["CDELT1"]
                    + hdul["SCI"].header["CRVAL1"]
            )
            wav = np.array((wav, wav))
            bpm = hdul["BPM"].data.sum(axis=1)

            self.wav_cdelt = float(hdul["SCI"].header["CDELT1"])

            if hdul["SCI"].header["CTYPE1"] != 'Angstroms':
                self.wav_unit = hdul["SCI"].header["CTYPE1"]

        return spec, wav, bpm

    # MARK: Get bounds
    def get_bounds(self, bpm: np.ndarray, gap_length: int = 30) -> np.ndarray:
        """
        Find the bounds for a file based on the CCD count.

        Parameters
        ----------
        bpm : np.ndarray
            The bad pixel mask.
        gap_length : int, optional
            The minimum length of a gap to be considered a CCD region.
            (Defaults to 30)

        Returns
```

```
        -------
        np.ndarray
            The bounds for the CCD regions.

        """
        if not 0 <= gap_length <= 60:
            msg = f"An invalid gap length of {gap_length} was encountered."
            logging.error(msg)
            raise ValueError(msg)

        # Check if get_bounds is needed
        if self.ccds == 1:
            return np.array(
                [[(0, bpm[0].shape[-1])], [(0, bpm[1].shape[-1])]]
            ).astype(int)

        # bounds.shape -> (0|E, CCD's, low./up. bound)
        bounds = np.zeros((2, self.ccds, 2))

        # Check if `BPM` contains any `2`'s
        if np.any(bpm == 2):
            for ext, ccd in iters.product(range(2), range(self.ccds)):
                mid = np.where(bpm[ext] == 2)[0][ccd]
                ccds = self.ccds * 2
                bounds[ext, ccd] = (
                    max(mid - bpm.shape[-1] // ccds, 0),
                    min(mid + bpm.shape[-1] // ccds, bpm.shape[-1])
                )

            return bounds.astype(int)

        for ext in range(len(self._beams)):

            # Find min and max vals
            min_val, max_val = 0, bpm[ext].shape[-1]

            while True:
                if bpm[ext][min_val] == 0:
                    break
                min_val += 1

            while True:
                if bpm[ext][max_val - 1] == 0:
                    break
                max_val -= 1

            # Find ranges of non zero values
            regions: list[np.ndarray] = np.split(
                np.where(bpm[ext, min_val: max_val] == 1)[0],
                np.where(
                    np.diff(np.where(bpm[ext, min_val: max_val] == 1)[0]) != 1
                )[0] + 1
            )

            # If less than 2 regions, raise error
            if len(regions) < 2:
                msg = "Less than 2 regions found in BPM. Returning bounds."
                logging.error(msg)
                raise ValueError(msg)

            # Find `regions` longer than `gap_length`
            regions = [
                region for region in regions
                if len(region) >= gap_length
            ]

            # Ensure 2 regions are found
            if len(regions) < 2:
                logging.debug(
                    "get_bounds - Less than 2 regions found in BPM." +
                    f"Calling get_bounds with gap_length = {gap_length - 10}"
                )
                return self.get_bounds(bpm, gap_length - 10)
```

```
364
365             elif len(regions) > 2:
366                 logging.debug(
367                     "get_bounds - More than 2 regions found in BPM. " +
368                     f"Calling get_bounds with gap_length = {gap_length + 5}"
369                 )
370                 return self.get_bounds(bpm, gap_length - 10)
371
372             # Ensure region order correct
373             if regions[0][0] > regions[1][0]:
374                 regions = regions[::-1]
375
376             # Assign bounds from regions
377             bounds[ext] = np.array([
378                 (min_val, regions[0][0]),
379                 (regions[0][-1], regions[1][0]),
380                 (regions[1][-1], max_val),
381             ])
382
383             # Get lower and upper bound for each ccd, save to bounds
384             # Lower -> min is zero, Upper -> max is bpm length
385
386             # for ext in range(2):
387             #     cedge = ccdcenter(bpm[ext])
388             #     bounds[ext] = np.array(cedge)
389
390         logging.debug(f"get_bounds - found bounds at \n{bounds.astype(int)}")
391
392         return bounds.astype(int)
393
394     # MARK: Remove Continua
395     def remove_cont(
396             self,
397             spec: np.ndarray,
398             wav: np.ndarray,
399             bpm: np.ndarray,
400             plot_cont: bool
401     ) -> np.ndarray:
402         """
403         Remove the continuum from the data.
404
405         Parameters
406         ----------
407         spec : np.ndarray
408             The spectrum to remove the continuum from.
409         wav : np.ndarray
410             The wavelength of the spectrum.
411         bpm : np.ndarray
412             The bad pixel mask.
413         plot_cont : bool
414             Decides whether the continuum fitting should be plotted
415
416         Returns
417         -------
418         spec : np.ndarray
419
420         """
421         # Mask out the bad pixels for fitting continua
422         okwav = np.where(bpm != 1)
423
424         # Define continua
425         ctm = continuum(
426             wav[okwav],
427             spec[okwav],
428             deg=self.cont_ord,
429             plot=plot_cont,
430         )
431
432         # Normalise spectra
433         spec /= chebyshev.chebval(wav, ctm)
434         spec -= 1
435
436         return spec
```

```
437
438     # MARK: Correlate
439     def correlate(
440             self,
441             filename1: Path,
442             filename2: Path | None = None,
443             alt: Callable = None
444     ) -> tuple[np.ndarray, np.ndarray, np.ndarray, list[list], list[list]]:
445         """
446         Cross correlates the data.
447
448         Parameters
449         ----------
450         filename1 : Path
451             The name of the first FITS file to cross correlate.
452         filename2 : Path, optional
453             The name of the second FITS file to cross correlate.
454             (Defaults to None)
455         alt : Callable, optional
456             An alternate method of cross correlating the data.
457             (Defaults to None)
458
459         Returns
460         -------
461         spec, wav, bpm, lagsdb, corrdb:
462             tuple[np.ndarray, np.ndarray, np.ndarray, list[list], list[list]]
463
464         """
465         #  mode: 0E -> '01' & 'E1', 0 -> '01' & '02', E -> 'E1' & 'E2'
466         # Load data
467         spec, wav, bpm = self.load_file(filename1)
468         if filename2 and self._beams != '0E':
469             def unpack(exts, *args):
470                 return [arr[exts] for arr in args]
471
472             if self._beams == '0':
473                 spec[-1], wav[-1], bpm[-1] = unpack(
474                     0, *self.load_file(filename2)
475                 )
476
477             else:
478                 spec[0], wav[0], bpm[0] = spec[-1], wav[-1], bpm[-1]
479                 spec[-1], wav[-1], bpm[-1] = unpack(
480                     -1, *self.load_file(filename2)
481                 )
482
483         bounds = self.get_bounds(bpm)
484
485         logging.debug(
486             f"correlate - data shape:\n\tspec/wav/bpm: {spec.shape}"
487         )
488
489         corrdb = [[] for _ in range(self.ccds)]
490         lagsdb = [[] for _ in range(self.ccds)]
491         for ccd in range(self.ccds):
492             sig = []
493             for ext in range(2):
494                 lb, ub = bounds[ext, ccd]
495
496                 if self.cont_ord > 0:
497                     spec[ext, lb:ub] = self.remove_cont(
498                         spec[ext, lb:ub],
499                         wav[ext, lb:ub],
500                         bpm[ext, lb:ub],
501                         self.can_plot
502                     )
503
504                 # Invert BPM (and account for 2); zero bad pixels
505                 sig.append((
506                     spec[ext, lb:ub]
507                     * abs(bpm[ext, lb:ub].astype(np.int8) * -1 + 1)
508                 ))
509
```

```
510             # Finally(!!!) cross correlate signals and scale max -> 1
511             corrdb[ccd] = signal.correlate(*sig) if not alt else alt(*sig)
512             corrdb[ccd] /= np.max(corrdb[ccd])
513             # noinspection PyTypeChecker
514             lagsdb[ccd] = signal.correlation_lags(
515                 sig[0].shape[-1],
516                 sig[1].shape[-1]
517             ) * self.wav_cdelt
518 
519         return spec, wav, bpm, corrdb, lagsdb
520 
521     # MARK: ftcs alternate
522     def ftcs(
523             self,
524             signal1: np.ndarray,
525             signal2: np.ndarray
526     ) -> np.ndarray:
527         """
528         Cross correlates the data using the Fourier Transform.
529 
530         Parameters
531         ----------
532         signal1 : np.ndarray
533             The first signal to cross correlate.
534         signal2 : np.ndarray
535             The second signal to cross correlate.
536 
537         Returns
538         -------
539         np.ndarray
540             The correlation data using the Fourier Transform.
541 
542         """
543         logging.debug(
544             f"ftcs - data shape:\n\tspec/wav/bpm: {signal1.shape}"
545         )
546 
547         # Invert BPM (and account for 2); zero bad pixels
548         ft_spec1 = np.fft.fft(signal1)
549         ft_spec2 = np.fft.fft(signal2)
550 
551         if self.can_plot:
552             plt.plot(ft_spec1)
553             plt.plot(ft_spec2)
554             plt.show()
555 
556         # Cross correlate signals
557         # ft_spectrum1 * np.conj(ft_spectrum2)
558         corr_entry = signal.correlate(ft_spec1, ft_spec2)
559 
560         return np.fft.ifft(corr_entry)
561 
562     # MARK: Plot
563     def plot(self, spec, wav, bpm, corrdb, lagsdb) -> None:
564         """
565         Plot the data.
566 
567         Parameters
568         ----------
569         spec : np.ndarray
570             The spectrum.
571         wav : np.ndarray
572             The wavelength.
573         bpm : np.ndarray
574             The bad pixel mask.
575         corrdb : np.ndarray
576             The cross correlation data.
577         lagsdb : np.ndarray
578             The `lags` data.
579 
580         Returns
581         -------
582         None
```

```
583
584         """
585         plt.style.use([
586             files(STOPS.utils).joinpath('STOPS.mplstyle'),
587             files(STOPS.utils).joinpath('STOPS_correlate.mplstyle'),
588         ])
589         bounds = self.get_bounds(bpm)
590
591         fig, axs = plt.subplots(2, self.ccds, sharey="row")
592
593         if self.ccds == 1:
594             # Convert axs to a 2D array
595             # noinspection PyTypeChecker
596             axs: np.ndarray[matplotlib.axes.Axes] = np.swapaxes(
597                 np.atleast_2d(axs), 0, 1
598             )
599
600         # for ext, ccd in iters.product(range(2), range(self.ccds)):
601
602         for ccd in range(self.ccds):
603             axs[0, ccd].plot(
604                 lagsdb[ccd],
605                 corrdb[ccd] * 100,
606                 color='C4',
607                 label=f"max lag @ {lagsdb[ccd][corrdb[ccd].argmax()] - (bounds[1, ccd,
                    ↪ 0] - bounds[0, ccd, 0])}",
608             )
609
610             for ext in range(2):
611                 lb, ub = bounds[ext, ccd]
612                 logging.debug(f"fl-{ext}: {wav[ext, lb]}:{wav[ext, ub - 1]}")
613
614                 axs[1, ccd].plot(
615                     wav[ext, lb:ub],
616                     spec[ext, lb:ub]
617                     * abs(bpm[ext, lb:ub].astype(np.int8) * -1 + 1)
618                     + OFFSET * ext,
619                     label=(
620                         f"${self._beams if self._beams != 'OE' else self._beams[ext]}"
621                         f"_{ext + 1 if self._beams != 'OE' else 1}$"
622                         f"{(' (+' + str(OFFSET * ext) + ')') if ext > 0 else ''}"
623                     ),
624                 )
625
626         axs[0, 0].set_ylabel("Normalised Correlation\n($\\%$)")
627         for ax in axs[1:, 0]:
628             ax.set_ylabel("Normalised Intensity\n(Counts)")
629         xcol = int(self.ccds != 1)
630         axs[0, xcol].set_xlabel(f"Signal Lag ({self.wav_unit})")
631         axs[-1, xcol].set_xlabel(f"Wavelength ({self.wav_unit})")
632         for ax in axs.flatten():
633             leg = ax.legend()
634             leg.set_draggable(True)
635
636         plt.show()
637
638         # Handle do not save
639         if not self.save_prefix:
640             return
641
642         # Handle save
643         fig.savefig(fname=self.save_prefix)
644
645         return
646
647     # MARK: Process all listed images
648     def process(self) -> None:
649         """
650         Process the data.
651
652         Returns
653         -------
654         None
```

```
655
656         """
657         if self._beams != 'OE' and len(self.fits_list) == 1:
658             # change mode to OE with warning
659             logging.warning((
660                 f"`{self._beams}` correlation not possible for "
661                 "a single file. correlation `mode` changed to 'OE'."
662             ))
663             self._beams = 'OE'
664
665         # OE `mode` (same file, diff. ext.)
666         if self._beams == 'OE':
667             for fl in self.fits_list:
668                 logging.info(f"'OE' correlation of {fl}.")
669                 spec, wav, bpm, corr, lags = self.correlate(fl, alt=self.alt)
670                 self.plot(spec, wav, bpm, corr, lags)
671
672             return
673
674         # O|E `mode` (diff. files, same ext.)
675         for fl1, fl2 in iters.combinations(self.fits_list, 2):
676             logging.info(f"{self._beams} correlation of {fl1} vs {fl2}.")
677             spec, wav, bpm, corr, lags = self.correlate(fl1, fl2, alt=self.alt)
678             self.plot(spec, wav, bpm, corr, lags)
679
680         return
681
682
683 # MARK: Main function
684 def main(argv) -> None:
685     return
686
687
688 if __name__ == "__main__":
689     main(sys.argv[1:])
```

Listing B.5: The source code for **skylines.py**

```python
#!/usr/bin/env python3
# -*- coding: utf-8 -*-

"""
Module for analyzing the sky lines of a wavelength calibrated image.
"""

# MARK: Imports
import sys
import logging
from pathlib import Path
from importlib.resources import files

import numpy as np
import matplotlib.pyplot as plt
import matplotlib.axes
from astropy.io import fits as pyfits
from scipy import signal

from STOPS.utils.SharedUtils import find_files, get_arc_lamp
from STOPS.utils.Constants import SAVE_SKY, FIND_PEAK_PARAMS
import STOPS.data
import STOPS.utils
import STOPS.data.RSS_arc


# print(
#  [logging.getLogger(name) for name in logging.root.manager.loggerDict]
# )
mpl_logger = logging.getLogger('matplotlib')
mpl_logger.setLevel(logging.INFO)
pil_logger = logging.getLogger('PIL')
pil_logger.setLevel(logging.INFO)


# MARK: Skylines Class
class Skylines:
    """
    Class representing the Skylines object.

    Parameters
    ----------
    data_dir : Path
        The directory containing the data files.
    filenames : list[str]
        The list of filenames to be processed.
    beam : str, optional
        The beam mode, by default "OE".
    plot : bool, optional
        Flag indicating whether to plot the continuum, by default False.
    save_prefix : Path | None, optional
        The prefix for saving the data, by default None.
    **kwargs
        Additional keyword arguments.

    Attributes
    ----------
    data_dir : Path
        The directory containing the data files.
    fits_list : list[str]
        The list of fits file paths.
    beams : str
        The beam mode.
    can_plot : bool
        Flag indicating whether to plot the continuum.
    save_prefix : Path | None
        The prefix for saving the data.
    wav_unit : str
        The unit of wavelength.

    Methods
```

```
    -------
    checkLoad(self, path1: str) -> np.ndarray:
        Checks and loads the data from the given path.
    transform(self, wav_sol: np.ndarray, spec: np.ndarray) -> np.ndarray:
        Transforms the input wavelength and spectral data based on
        the given wavelength solution.
    rmvCont(self) -> np.ndarray:
        Removes the continuum from the spectrum.
    process(self) -> None:
        Placeholder method for processing the data.

    See Also
    --------
    matplotlib custom style:
        https://matplotlib.org/stable/users/explain/customizing.html

    Notes
    -----
    Constants imported (see utils.Constants):
        SAVE_SKY:
            The default save name for the skylines plot.
        FIND_PEAK_PARAMS:
            The default parameters for finding peaks in the spectrum.
    """

    # MARK: Skylines init
    def __init__(
            self,
            data_dir: Path,
            filenames: list[str],
            beams: str = "OE",
            split_ccd: bool = False,
            cont_ord: int = 11,
            plot: bool = False,
            transform: bool = True,
            save_prefix: Path | None = None,
            **kwargs,
    ) -> None:
        self.data_dir = data_dir
        self.fits_list, self.arc_list = find_files(
            data_dir=self.data_dir,
            filenames=filenames,
            prefix="wmxgbp",  # t[o|e]beam
            ext="fits",
            sep_arc=True,
        )
        if self.arc_list:
            self.arc_lamp = get_arc_lamp(self.arc_list[0])

        self._beams = None
        self.beams = beams
        self.ccds = 1
        if split_ccd:
            # See cross_correlate for initial implementation
            self.ccds = 3

        self.cont_ord = cont_ord
        self.can_plot = plot
        self.must_transform = transform

        self.save_prefix = save_prefix
        # Handle directory save name
        if self.save_prefix and self.save_prefix.is_dir():
            self.save_prefix /= SAVE_SKY
            logging.warning((
                f"Skylines save name resolves to a directory. "
                f"Saving under {self.save_prefix}"
            ))

        self.max_difference = 5

        self.wav_unit = "$\\AA$"

```

```
145         logging.debug(f"__init__\n{repr(self)}")
146 
147         return
148 
149     # MARK: Skylines repr
150     def __repr__(self) -> str:
151         template = (
152             "Skylines(\n"
153             f"\tdata_dir={self.data_dir},\n"
154             f"\tfits_list=[\n\t\t{"\n\t\t".join(
155                 map(str, self.fits_list)
156             )}\n\t],\n"
157             f"\tbeams={self.beams},\n"
158             f"\tplot={self.can_plot},\n"
159             f"\tsave_prefix={self.save_prefix},\n"
160             f"\twav_unit={self.wav_unit}\n"
161             ")\n"
162         )
163 
164         return template
165 
166     # MARK: Beams property
167     @property
168     def beams(self) -> str:
169         return self._beams
170 
171     @beams.setter
172     def beams(self, mode: str) -> None:
173         if mode not in ['O', 'E', 'OE']:
174             err_msg = f"Correlation mode '{mode}' not recognized."
175             logging.error(err_msg)
176             raise ValueError(err_msg)
177 
178         self._beams = mode
179 
180         return
181 
182     # MARK: Find Peaks
183     def find_peaks(
184             self,
185             spec: np.ndarray,
186             axis: int | None = None,
187             min_height: float = 0.5,
188             **kwargs,
189     ) -> tuple[list[np.ndarray], list[dict]]:
190         """
191         Finds the peaks in the given spectral data.
192 
193         Parameters
194         ----------
195         spec : np.ndarray
196             The spectral data.
197         axis: int | None, optional
198             The axis along which the peaks are found.
199         min_height : float, optional
200             The minimum height of the peaks, by default 0.5.
201 
202         Returns
203         -------
204         peaks, properties : tuple[list[np.ndarray], list[dict]]
205             The peaks and their properties.
206         """
207         peaks = []
208         props = []
209         row_means = []
210 
211         for ext in range(len(self.beams)):
212             row_mean = spec[ext] if axis is None else np.mean(
213                 spec[ext], axis=axis
214             )
215 
216             peak, prop = signal.find_peaks(
217                 row_mean,
```

```
                prominence=min_height * np.max(row_mean),
                width=0,
                **kwargs,
            )
            peaks.append(peak)
            props.append(prop)
            row_means.append(row_mean)

        if self.can_plot:
            fig, axs = plt.subplots(2, 1)
            for ext in range(len(self.beams)):
                axs[ext].plot(
                    row_means[ext],
                    label=f"{'E' if ext else 'O'}"
                )
                axs[ext].plot(
                    peaks[ext],
                    row_means[ext][peaks[ext]],
                    "x",
                    label=f"{'E' if ext else 'O'} peaks"
                )
                axs[ext].legend()
            plt.show()

        logging.debug(f"find_peaks - peaks: {[len(i) for i in peaks]}")
        # logging.debug(
        #     f"find_peaks - props: {[key for key in props[0].keys()]}"
        # )

        return peaks, props

    # MARK: Min. of Diff. Matrix
    @staticmethod
    def min_diff_matrix(
            a: np.ndarray,
            b: np.ndarray,
            max_diff: int = 100
    ) -> tuple[np.ndarray, np.ndarray, np.ndarray]:
        """
        Find the minimum difference between the elements of two arrays.

        Parameters
        ----------
        a : np.ndarray
            The first 1d array.
        b : np.ndarray
            The second 1d array.
        max_diff : int, optional
            The maximum difference allowed, by default 100.

        Returns
        -------
        a : np.ndarray (len(a))
            The elements of the first array.
        min_vals : np.ndarray (len(a))
            The minimum difference between the elements of the two arrays.
        min_idxs : np.ndarray (len(a))
            The indices of the minimum difference between
            the elements of the two arrays.
        """
        # Compute the difference matrix using transpose
        diff = a - b[:, np.newaxis]

        # Find the minimum value in each row (A) of `diff`
        min_idxs = np.abs(diff).argmin(axis=0)

        min_vals = np.array([diff[j, i] for i, j in enumerate(min_idxs)])
        # TODO: Recalculate min_val after selecting best min_val and
        # TODO: removing the corresponding row/column

        logging.debug(
            f"min_diff_matrix - min_vals=\n{np.round(min_vals, 2).astype(int)}"
        )
```

```
291         logging.debug(f"min_diff_matrix - min_idxs=\n{min_idxs}")
292
293         max_mask = (min_vals <= max_diff) & (min_vals >= -1 * max_diff)
294
295         return a[max_mask], min_vals[max_mask], min_idxs[max_mask]
296
297     # MARK: Load File Data
298     def load_file_data(
299             self,
300             filename: Path
301     ) -> tuple[np.ndarray, np.ndarray, np.ndarray]:
302         """
303         Loads the data from the given file.
304
305         Parameters
306         ----------
307         filename : Path
308             The path to the file to be loaded.
309
310         Returns
311         -------
312         spec, wav, bpm : tuple[np.ndarray, np.ndarray, np.ndarray]
313             The wavelength, spectral, and bad pixel mask data.
314         """
315         # Load data from self.beams extension
316         with pyfits.open(filename) as hdul:
317             exts = [0, 1]
318             if len(self.beams) != 2:
319                 exts = 0 + int(self.beams == 'E')
320
321             spec2d = np.atleast_3d(hdul["SCI"].data[exts])
322             wav2d = np.atleast_3d(hdul["WAV"].data[exts])
323             bpm2d = np.atleast_3d(hdul["BPM"].data[exts].astype(bool))
324
325             logging.info(
326                 f"load_file_data - {filename.name} - shape: {spec2d.shape}"
327             )
328
329             return spec2d, wav2d, bpm2d
330
331     # MARK: Load Sky or Arc Lines
332     @staticmethod
333     def load_lines(
334             filename: str | Path | None = None,
335             dtype: list[tuple] = [('wav', float), ('flux', float)],
336             skip_header: int = 3,
337             skip_footer: int = 1
338     ) -> np.ndarray:
339         """
340         Loads the sky or arc lines from the given file.
341
342         Parameters
343         ----------
344         filename : str | Path | None, optional
345             The path to the file to be loaded.
346             Defaults to loading the skylines from `data/sky.salt`
347         dtype : list[tuple], optional
348             The data type of the sky lines.
349             (Default is [('wav', float), ('flux', float)])
350         skip_header : int, optional
351             The amount of lines to skip of the `filenames` header.
352             (Default is 3)
353         skip_footer : int, optional
354             The amount of lines to skip of the `filename`s footer.
355             (Default is 1)
356
357         Returns
358         -------
359         sky_lines : np.ndarray['wav', 'flux']
360             The sky lines from the file.
361         """
362         lines: np.ndarray = None
363
```

```
364         usecols = None
365         if filename:
366             filename = files(STOPS.data.RSS_arc).joinpath(filename)
367             usecols = (0, 1)
368         else:
369             filename = files(STOPS.data).joinpath('sky.salt')
370 
371         lines = np.genfromtxt(
372             filename,
373             dtype=dtype,
374             skip_header=skip_header,
375             skip_footer=skip_footer,
376             usecols=usecols
377         )
378 
379         logging.debug(
380             f"load_lines - {filename.name} - shape: {lines.shape}"
381         )
382 
383         return lines
384 
385     # MARK: Mask Traces
386     def mask_traces(
387             self,
388             spec: np.ndarray,
389             bpm: np.ndarray,
390             max_traces: int = 1,
391             tr_pad: int = 5,
392             bg_margin: int = 10,
393             lr_margins: list[int] = [10, 10],
394             h_min: float = 0.5,
395             h_rel: float = 1 - 0.05,
396     ) -> np.ndarray:
397         """
398         Masks the traces in the bad pixel mask.
399 
400         Parameters
401         ----------
402         spec : np.ndarray
403             The spectral data.
404         bpm : np.ndarray
405             The bad pixel mask.
406         max_traces : int, optional
407             The maximum number of traces to be masked.
408             (Default is 1)
409         tr_pad : int, optional
410             The amount to pad traces by.
411             (Default is 5)
412         bg_margin : int, optional
413             The margin size for the background.
414             (Default is 10)
415         lr_margins : list[int, int], optional
416             The left and right background margins at the spectrum edge.
417             (Default is [10, 10])
418         h_min: float, optional
419             The minimum height of a detected peak.
420             (Default is 0.5)
421         h_rel: float, optional
422             The relative height for the properties of a detected peak.
423             (Default is 1)
424 
425         Returns
426         -------
427         bpm : np.ndarray
428             The updated bad pixel mask.
429         """
430         # Base mask
431         bpm[:, :bg_margin] = True
432         bpm[:, -bg_margin:] = True
433         bpm[:, :, :lr_margins[0]] = True
434         bpm[:, :, -lr_margins[1]:] = True
435 
436         # Get the traces
```

```
        traces, tr_props = self.find_peaks(
            spec,
            axis=1,
            min_height=h_min,
            rel_height=h_rel
        )

        for ext in range(len(self.beams)):
            # Mask the traces
            for i in range(len(traces[ext][:max_traces])):
                lb = max(
                    0,
                    int(tr_props[ext]['left_ips'][i]) - tr_pad
                )
                ub = min(
                    spec.shape[-1],
                    int(tr_props[ext]['right_ips'][i]) + tr_pad
                )
                bpm[ext, lb: ub] = True
                # TODO: Relocate targets after initial masking

        logging.info(
            f"mask_traces - {min(max_traces, len(traces))} " +
            f"of {len(traces)} traces masked."
        )

        return bpm

    # MARK: Transform Spectra
    def transform(
            self,
            spec: np.ndarray,
            wav_sol: np.ndarray,
            row_max: int | None = None,
            res_plot: bool = False,
    ) -> tuple[np.ndarray, np.ndarray]:
        """
        Transforms the input wavelength and spectral data
        based on the given wavelength solution.

        Parameters
        ----------
        spec : np.ndarray
            The spectral data.
        wav_sol : np.ndarray
            The wavelength solution.
        row_max : int, optional
            The row along which the spectral data is to be transformed.
            (Default is None)
        res_plot : bool, optional
            Flag indicating whether to plot the results.
            (Default is False)

        Returns
        -------
        spec, wav : np.ndarray
            The transformed wavelength and spectral data.

        """
        # Create arrays to return
        cs = np.zeros_like(spec)
        cw = np.zeros_like(wav_sol.mean(axis=1))

        for ext in range(len(self.beams)):

            if row_max:
                avg_max = row_max
            else:
                # Get middle row (to interpolate the rest of the rows to)
                avg_max = np.mean(spec[ext], axis=1).argmax()

            # Correct extensions based on wavelength
            # Get wavelength values at row with most trace
```

```
            cw[ext] = wav_sol[ext, avg_max]

            # Spec ext
            for row in range(cs.shape[1]):
                cs[ext, row] = np.interp(
                    cw[ext],
                    wav_sol[ext, row],
                    spec[ext, row]
                )
                # f_2d = interpolate.interp2d(
                #     wav_sol[ext, row],
                #     np.arange(rows),
                #     spec[ext],
                # )
                # cs[ext] = f_2d(cw[ext, row], np.arange(rows))

        # Plot results
        if res_plot:
            fig, axs = plt.subplots(2, 1, figsize=[20, 4])
            for ext in range(len(self.beams)):
                axs[ext].imshow(
                    cs[ext],
                    vmax=cs[ext].mean() + 2 * cs[ext].std(),
                    vmin=cs[ext].mean() - 2 * cs[ext].std()
                )

                logging.debug(
                    f"{'E' if ext else 'O'} Average continuum = " +
                    f"{np.median(np.median(cs[ext], axis=0)):4.3f}"
                )

                axx = axs[ext].twinx()
                axx.hlines(
                    np.median(np.median(cs[ext], axis=0)),
                    0,
                    cs[ext].shape[-1],
                    colors='black'
                )
                axx.plot(
                    cs[ext].mean(axis=0),
                    "k",
                    label=f"mean {'E' if ext else 'O'}"
                )
                axx.plot(
                    np.median(cs[ext], axis=0),
                    "r",
                    label=f"median {'E' if ext else 'O'}"
                )
                axx.legend()
            plt.show()

        logging.info(f"transform - {cs.shape} transformed.")

        return cs, cw

    # MARK: Plot
    def plot(
            self,
            spectra,
            wavelengths,
            peaks,
            properties,
            arc: bool = False,
    ) -> None:
        plt.style.use([
            files(STOPS.utils).joinpath('STOPS.mplstyle'),
            files(STOPS.utils).joinpath('STOPS_skylines.mplstyle'),
        ])
        plt.rcParams['figure.subplot.hspace'] *= len(self.beams)

        def norm(vals):
            return (vals - np.min(vals)) / (np.max(vals) - np.min(vals))

```

```
583         # Load known lines
584         if arc:
585             lines = self.load_lines(filename=self.arc_lamp)
586         else:
587             lines = self.load_lines()
588 
589         # noinspection PyTypeChecker
590         lines = lines[
591             (lines['wav'] > wavelengths[1][0][0].min()) &
592             (lines['wav'] < wavelengths[1][0][0].max())
593             ]
594 
595         # Create plot for results
596         fig, axs = plt.subplots(2, self.ccds, sharex='col', sharey='row')
597 
598         # Convert axs to a 2D array if ccd count is 1
599         if self.ccds == 1:
600             # noinspection PyTypeChecker
601             axs: np.ndarray[matplotlib.axes.Axes] = np.swapaxes(
602                 np.atleast_2d(axs),
603                 0,
604                 1
605             )
606 
607         for fl in range(len(self.arc_list if arc else self.fits_list)):
608 
609             # set color cycle
610             # private deprecated
611             # color = next(axs[0, 0]._get_lines.prop_cycler)['color']
612             color = axs[0, 0]._get_lines.get_next_color()
613 
614             for ext in range(len(self.beams)):
615 
616                 ccdrange = spectra[1][fl][ext].shape[-1] // self.ccds
617                 for ccd in range(self.ccds):
618                     # MARK: plot spectrum
619                     # (transformed)
620                     axs[0, ccd].plot(
621                         wavelengths[1][fl][ext][
622                             ccdrange * ccd:ccdrange * (ccd + 1)
623                         ],
624                         norm(spectra[1][fl][ext][
625                             ccdrange * ccd:ccdrange * (ccd + 1)
626                         ]) * 100 + 10 * ext + 30 * fl,
627                         color=color,
628                         linestyle='dashed' if ext else 'solid',
629                         label=f"${{{{{self.beams[ext]}}}}_{{{fl + 1}}}^{{+ {10 * ext + 30 *
                            ↪ fl}}}$" if ccd == 0 else None,
630                     )
631 
632                     # MARK: plot dev
633                     # noinspection PyTypeChecker
634                     sky_wavs, dev, peak_idx = self.min_diff_matrix(
635                         lines['wav'],
636                         wavelengths[1][fl][ext][peaks[1][fl][ext]],
637                         max_diff=self.max_difference,
638                     )
639 
640                     # # MARK: width/width_init
641                     # width = properties[1][fl][ext]['widths'][peak_idx]
642                     # width_i = np.zeros_like(width)
643 
644                     # sky_i, i_dev, i_idx = self.min_diff_matrix(
645                     #     lines['wav'],
646                     #     wavelengths[0][fl][ext][peaks[0][fl][ext]],
647                     #     max_diff=self.max_difference,
648                     # )
649 
650                     # width_i = np.array([
651                     #     properties[0][fl][ext]['widths'][
652                     #         np.where(wav == sky_i)[0][0]
653                     #     ]
654                     #     if wav in sky_i else 1000
```

```
655                     #     for wav in sky_wavs
656                     # ])
657                     # width_ratio = (width / width_i) - 1
658                     # width_ratio[width_ratio < 0] = 0
659
660                     # ylolims = width_ratio > self.max_difference
661                     # width_ratio[
662                     #     width_ratio > self.max_difference
663                     # ] = self.max_difference // 2
664
665                     ok = np.where(
666                         (sky_wavs >= wavelengths[1][fl][ext].data[
667                             ccdrange * ccd
668                         ]) &
669                         (sky_wavs <= wavelengths[1][fl][ext].data[
670                             ccdrange * (ccd + 1)
671                         ])
672                     )
673                     axs[1, ccd].plot(
674                         sky_wavs[ok],
675                         dev[ok],
676                         # yerr=(width_ratio[ok] * 0, width_ratio[ok]),
677                         # lolims=ylolims[ok],
678                         "." if ext else "x",
679                         # fmt="." if ext else "x",
680                         alpha=0.8,
681                         color=color,
682                         # markeredgecolor='white',
683                         # markeredgewidth=0.5,
684                         # label=f"${self.beams[ext]}_{{{fl + 1}}}$",
685                     )
686
687                     logging.debug(
688                         f"plot - RMS: {np.sqrt(np.mean(dev[ok] ** 2)):2.3f}"
689                     )
690
691         for ccd in range(self.ccds):
692             ccdrange = spectra[1][0][0].shape[-1] // self.ccds
693
694             # spectrum
695             # noinspection PyTypeChecker
696             ok = np.where(
697                 (lines['wav'] >= wavelengths[1][0][0].data[ccdrange * ccd]) &
698                 (lines['wav'] <= wavelengths[1][0][0].data[ccdrange * (ccd+1)])
699             )
700             # noinspection PyTypeChecker
701             axs[0, ccd].plot(
702                 lines['wav'][ok],
703                 lines['flux'][ok] * 0,
704                 'x',
705                 color='C4',
706                 label="\\textsc{salt}\nModel" if ccd == 0 else None,
707             )
708             # noinspection PyTypeChecker
709             for x in lines['wav'][ok]:
710                 axs[0, ccd].axvline(x, ls='dashed', c='0.7')
711
712         axs[0, 0].set_ylabel("Rel. Intensity ($\\%$)")
713         axs[1, 0].set_ylabel(
714             "Closest Peak ($\\Delta\\lambda$)"
715         )
716         # for ax in axs[:, 0]:
717         #     ax.legend(loc='upper left', ncols=(fl + 1) * (ext + 1) + 1)
718         leg = fig.legend(
719             loc='center',
720             ncol=min(8, len(spectra[0]) + 1),
721             columnspacing=0.5,
722             bbox_to_anchor=(
723                 np.mean((
724                     plt.rcParams['figure.subplot.left'],
725                     plt.rcParams['figure.subplot.right']
726                 )),
727                 np.mean((
```

```
                    plt.rcParams['figure.subplot.bottom'],
                    plt.rcParams['figure.subplot.top']
                ))
            ),
        )
        leg.set_draggable(True)
        for ax in axs[1, :]:
            ax.grid(axis='y')

        axs[-1, 0 if self.ccds == 1 else 1].set_xlabel(
            f"Wavelength ({self.wav_unit})"
        )

        # plt.tight_layout()

        plt.show()

        # Save results
        if self.save_prefix:
            fig.savefig(fname=self.save_prefix)

        return

        # MARK: Process all listed images

    def process(self, arc: bool = False) -> None:
        files = self.fits_list
        if arc:
            files = self.arc_list

        logging.info(f"Processing '{self.beams}' lines.")

        spectra = [[], []]
        wavs = [[], []]
        peaks = [[], []]
        peak_props = [[], []]

        for fl in files:
            # Load data
            spec2d, wav2d, bpm2d = self.load_file_data(fl)

            # Mask traces in BPM
            bpm2d = self.mask_traces(
                spec2d,
                bpm2d,
                max_traces=0,
                bg_margin=15,
                h_min=0.05
            )
            m_spec2d = np.ma.masked_array(spec2d, mask=bpm2d)  # spec2d
            m_wav2d = np.ma.masked_array(wav2d, mask=bpm2d)  # wav2d

            # Initial spectra
            spec_i = np.mean(m_spec2d, axis=-2)
            wav_i = np.mean(m_wav2d, axis=-2)

            # Transform data
            t_spec2d, t_wav = self.transform(
                m_spec2d,
                m_wav2d,
                res_plot=self.can_plot
            )

            # Final spectra
            spec_f = np.mean(t_spec2d, axis=-2)
            wav_f = t_wav

            # Find peaks
            peaks_i, props_i = self.find_peaks(
                spec_i,
                **FIND_PEAK_PARAMS
            )
            peaks_f, props_f = self.find_peaks(
```

```
                spec_f,
                **FIND_PEAK_PARAMS
            )

            spectra[0].append([*spec_i])
            spectra[1].append([*spec_f])
            wavs[0].append([*wav_i])
            wavs[1].append([*wav_f])
            peaks[0].append([*peaks_i])
            peaks[1].append([*peaks_f])
            peak_props[0].append([*props_i])
            peak_props[1].append([*props_f])

        # Plot results
        self.plot(spectra, wavs, peaks, peak_props, arc=arc)

        if arc:
            return
        elif self.arc_list:
            self.process(arc=True)

        return


# MARK: Main function
def main(argv) -> None:
    """main function."""

    return


if __name__ == "__main__":
    main(sys.argv[1:])
```

Appendix C

Proceedings

Development of STOPS and it's application to spectropolarimetric observations was presented at conferences, with the following proceedings included here.

- HEASA 2021 - Cooper, van Soelen, and Britto (2022)
- HEASA 2022 - Cooper and van Soelen (2023)

PROCEEDINGS OF SCIENCE

Development of tools for the SALT/RSS spectropolarimetry reductions: application to the blazar 3C 279

Justin Cooper,[a,*] **Brian van Soelen**[a] **and Richard J. Britto**[a]

[a] *University of the Free State,*
205 Nelson Mandela Drive, Bloemfontein, South Africa

E-mail: CooperJ@ufs.ac.za, VanSoelenB@ufs.ac.za

Blazars represent a subset of AGN with relativistic jets, where the direction of the jet lies very close to our line of sight. The highly Doppler boosted emission from the blazar's jet results in high apparent luminosities, and blazars display variability on periods from less than one day up to years. At optical wavelengths, the observed emission of the blazar is a superposition of the polarised non-thermal synchrotron emission, arising from the jet, and the unpolarised thermal emission, arising from the accretion disc, broad line region, torus and host galaxy. Polarimetry observations can serve as an important tool for diagnosing the emission from blazars. The RSS spectrograph, on SALT, can operate in spectropolarimetry mode and is currently being used to undertake spectropolarimetric observations of transient blazar sources. We present additional tools developed to work in conjunction with the current SALT spectropolarimetry reduction pipeline, POLSALT, that aims to streamline the reduction of the SALT polarisation data, including the testing of the wavelength calibration of the individual O and E beams. This was applied to observations of 3C 279 during 2017.

**** High Energy Astrophysics in Southern Africa (HEASA2021) ****
**** 13 - 17 September, 2021 ****
**** Online ****

[*] Speaker

PoS(HEASA2021)056

1. Introduction

Active Galactic Nuclei (AGN) are the centres of galaxies powered by accretion onto a supermassive black hole. The accretion can power relativistic jets which produce non-thermal emission over multiple wavelengths [1]. Blazars are a subclass of AGN where the direction of the jet lies very close to our line of sight. The highly Doppler boosted emission from the jet results in high apparent luminosities.

At optical wavelengths the observed emission is a superposition of polarised non-thermal synchrotron emission, arising from the jet, and unpolarised thermal emission, arising from the disc, broad line region, torus, and host galaxy [2].

The Robert Stobie Spectrograph (RSS) on the Southern African Large Telescope (SALT) [3] [4] is capable of long-slit spectropolarimetry and has been used to observe blazars in flaring and quiescent states. Data reduction of these observations is processed using the SALT spectropolarimetry reduction package POLSALT.[1] POLSALT allows for the full reduction, from pre-reduction to the extraction of the target spectra, and the measuring of the polarisation. However, it does not allow for much flexibility with the wavelength calibrations, nor does it provide tools to confirm that the wavelength calibrations lead to similar wavelength calibrated spectra for the O and E beams.

In order to streamline the data reduction we are developing additional tools to work in conjunction with POLSALT. We present the overview of this pipeline and demonstrate its application to an observation of 3C 279 taken in 2017.

2. Pipeline Overview

The tools being developed are designed to work in conjunction with POLSALT and provide a method to perform the wavelength calibrations using conventional IRAF methods [5]. They also allow easy comparisons to be made between the wavelength solutions of the O and E beam, to determine their quality and reliability.

The workflow for reductions is depicted in figure 1. It summarises the steps followed to reduce spectropolarimetric data. Steps that are performed using POLSALT are indicated in blue; steps performed by the new tools are shown in orange, while the IRAF calibration is shown in green.

If the wavelength solutions are found with IRAF, the tools split the multi-extension FITS files into the correct format for IRAF and the IRAF wavelength calibration is performed. The files are then written back into multi-extension FITS files in the correct format for POLSALT to complete the extraction and measurement of polarisation.

The cross-correlation between the O and E beam spectra, named correlation in figure 1, and relative flux calibrations are optional, though correlation is suggested. Relative flux calibrations may be performed assuming a standard and published standard spectra can be acquired. We performed the relative flux calibrations using the ASTROPY [6, 7] and SCIPY[2] packages.

[1] https://github.com/saltastro/polsalt
[2] http://www.scipy.org/

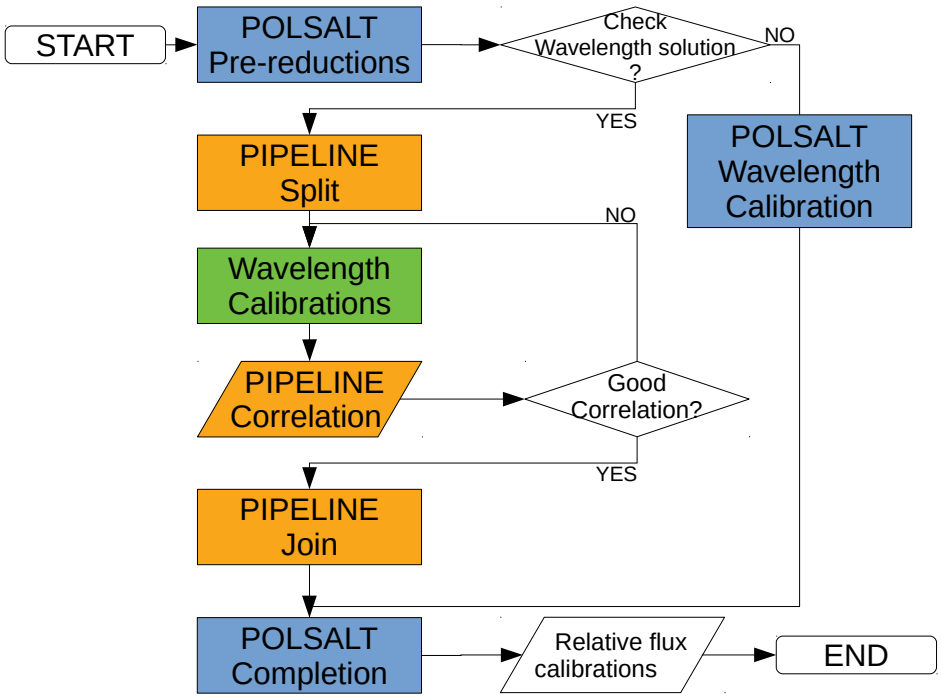

Figure 1: The flow diagram of the SALT RSS spectropolarimetry reductions steps.

2.1 Pre-reduction

The first step in the pipeline uses POLSALT and this performs the pre-reductions, the over-scan subtraction, gain and cross talk corrections, and mosaicing. After the pre-reduction is performed, the next step is to either undertake the wavelength calibration with POLSALT, or to split the files into the correct format for IRAF.

2.2 FITS split

Once all pre-reductions are complete, the tool SPLIT converts the multi-extension FITS files into multiple, single extension O or E beam FITS files. This is done as some IRAF tasks do not handle multi-extension FITS files well. The O and E beam frames are cropped to remove any non-exposed rows to accommodate the standard IRAF tasks and the FITS files saved with updated header information.

2.3 Wavelength calibration

If the POLSALT pipeline is used, the wavelength calibration is performed using the wavelength calibration tools which form part of PYSALT [8].

If the files have been formatted for IRAF, standard wavelength calibration methods are followed, using the NOAO package and the `identify`, `re-identify`, and `fitcoords` tasks. This allows greater control of the resultant wavelength solution.

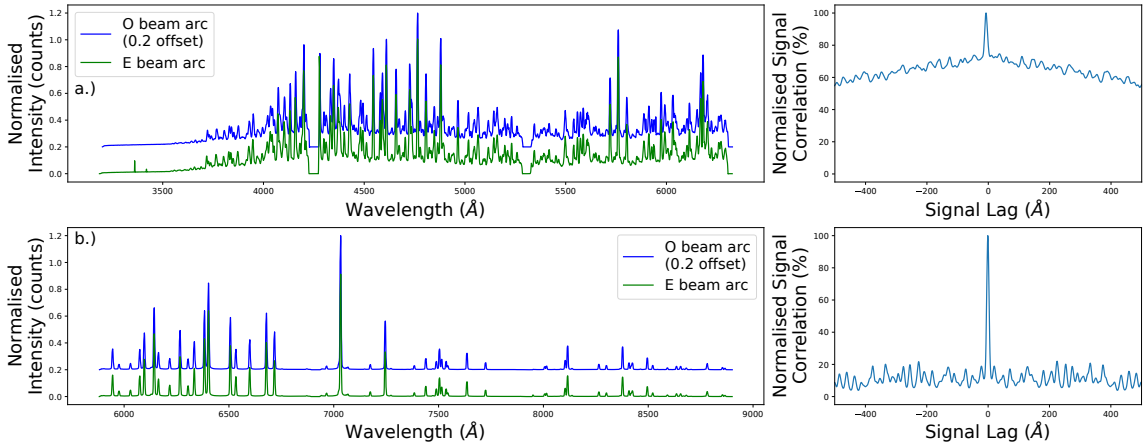

Figure 2: Comparison of the O and E beams for a.) ThAr and b.) Ne arc lamp spectra as well as the cross-correlation of their O and E beams.

2.4 Correlation

Our tool CORRELATE allows a comparison to be made between the O and E beam solutions, by performing a cross-correlation between the two arc or target observations, after the wavelength solution as been applied by IRAF. This is important as the polarisation is calculated from the difference between the O and E beam and, therefore, accurate wavelength solutions are required. The comparison between the O and E beams for a ThAr and Ne arc spectra and their cross-correlations, with a near zero lag, are shown in figure 2.a) and figure 2.b), respectively. Figure 2's Signal Lag plots show a clear peak at zero lag but also show an important distinction between noisy and quiet spectra in the non-peaking region.

2.5 FITS join

Once the IRAF wavelength calibrations are complete, the tool JOIN performs cosmic-ray cleaning using the LACOSMIC package [9], applies a wollaston correction which accounts for the physical shift of the spectra on the CCD, and then formats the single extension O and E beam FITS files into the multi-extension format required by POLSALT. This includes saving the wavelength solution found in IRAF as an additional extension. Currently only wavelength solutions fit with a Chebychev function are recognised but further development is planned to recognise Legendre functions.

2.6 Completion - extraction and polarisation measurement

After the wavelength solution is found, the final step is performed using POLSALT, which performs the curvature corrections, background subtraction, spectral extraction, and the raw and final stokes calculations. The binning and plotting also form part of the POLSALT completion.

3. Application to 3C 279

The blazar 3C 279 was observed in linear spectropolarimetry mode, on 2017 May 17, using the the PG0900 grating with two different grating angles (12.5° and 19.5°). The spectrophotometric

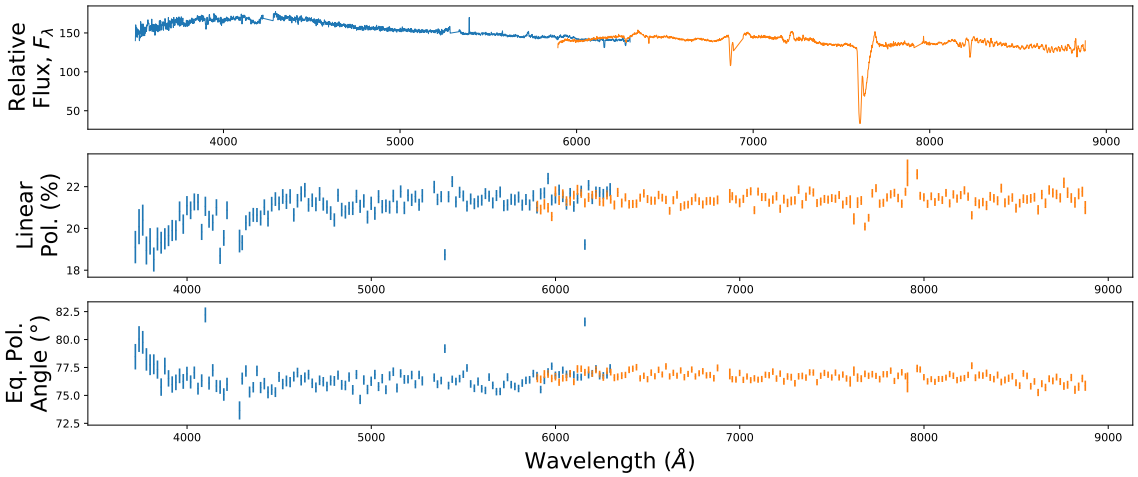

Figure 3: Reduced observations of 3C 279, taken with grating angle 12.5° (blue line) and 19.5° (orange line). Top: relative flux calibrated spectra. Middle: degree of linear polarisation. Bottom: Polarisation angle (relative to instrument).

standard star Hiltner 600 was observed on 2017 February 24, using the same configuration and was used for relative flux calibrations.

The target and standard were reduced following the steps discussed about. The flux correction was performed using ASTROPY and SCIPY python packages to correct the flux shape.

The results are shown in figure 3, indicating a good overlap between the observations taken at two different grating angles, with the polarisation measurements generally agree well where the observations overlap.

Figure 2 shows the comparison of the O and E beams for this observations. The cross-correlation is very close to zero lag, indicating the wavelength solution is similar for both the O and E beams.

4. Discussion and Conclusions

Creating an independent 2D wavelength solution for the O and E beams using IRAF allows for more flexibility in obtaining the wavelength solutions and provides a tool to directly compare the O and E beam solutions. This is useful for difficult cases, such as arc line identification for the PG0300 spectral grating, because there are fewer arc lines in some parts of the spectra and it is more complicated to create a consistent solution across the full wavelength range covered.

The cross-correlation plot cannot only be considered when deciding on whether to proceed onward with the reductions or to return to wavelength calibrations as depicted in figure 1. The comparison of the spectra is as important since the cross-correlation may show zero lag but lines in the spectra could still be mis-identified in both beams. The cross-correlation serves as a method to check the similarity of the wavelength solutions but not the accuracy of said solutions.

The tools developed create an alternative to the POLSALT wavelength calibration and add a method to check the consistency of the wavelength solutions, as can be seen with the application to 3C 279. These assist with the wavelength calibration, in particular for observations taken with

the PG0300 and PG0900 RSS gratings, that have been used for numerous observations of blazar sources.

Acknowledgments

The observational data presented was obtained with the Southern African Large Telescope (SALT) under the proposal 2016-2-LSP-001 (PI: D.A.H. Buckley). This work is based on the research supported in part by the National Research Foundation of South Africa (Grant Numbers: 116300).

References

[1] C.M. Urry and P. Padovani, *Unified Schemes for Radio-Loud Active Galactic Nuclei*, PASP **107** (1995) 803 [astro-ph/9506063].

[2] M. Böttcher, B. Van Soelen, R.J. Britto, D.A.H. Buckley, J.P. Marais and H. Schutte, *Salt spectropolarimetry and self-consistent sed and polarization modeling of blazars*, *Galaxies* **5** (2017) .

[3] E.B. Burgh, K.H. Nordsieck, H.A. Kobulnicky, T.B. Williams, D. O'Donoghue, M.P. Smith et al., *Prime focus imaging spectrograph for the southern african large telescope: optical design*, in *Instrument Design and Performance for Optical/Infrared Ground-based Telescopes*, vol. 4841, pp. 1463–1471, International Society for Optics and Photonics, 2003.

[4] H.A. Kobulnicky, K.H. Nordsieck, E.B. Burgh, M.P. Smith, J.W. Percival, T.B. Williams et al., *Prime Focus Imaging Spectrograph for the Southern African Large Telescope: operational modes*, in *Instrument Design and Performance for Optical/Infrared Ground-based Telescopes*, M. Iye and A.F.M. Moorwood, eds., vol. 4841, pp. 1634 – 1644, International Society for Optics and Photonics, SPIE, 2003, DOI.

[5] D. Tody, *The IRAF Data Reduction and Analysis System*, in *Instrumentation in astronomy VI*, D.L. Crawford, ed., vol. 627 of *Society of Photo-Optical Instrumentation Engineers (SPIE) Conference Series*, p. 733, Jan., 1986, DOI.

[6] Astropy Collaboration, T.P. Robitaille, E.J. Tollerud, P. Greenfield, M. Droettboom, E. Bray et al., *Astropy: A community Python package for astronomy*, A&A **558** (2013) A33 [1307.6212].

[7] Astropy Collaboration, A.M. Price-Whelan, B.M. Sipőcz, H.M. Günther, P.L. Lim, S.M. Crawford et al., *The Astropy Project: Building an Open-science Project and Status of the v2.0 Core Package*, AJ **156** (2018) 123 [1801.02634].

[8] S.M. Crawford, M. Still, P. Schellart, L. Balona, D.A.H. Buckley, G. Dugmore et al., *PySALT: the SALT science pipeline*, in *Observatory Operations: Strategies, Processes, and Systems III*, D.R. Silva, A.B. Peck and B.T. Soifer, eds., vol. 7737 of *Society of Photo-Optical Instrumentation Engineers (SPIE) Conference Series*, p. 773725, July, 2010, DOI.

[9] P.G. Van Dokkum, *Cosmic-ray rejection by laplacian edge detection*, *Publications of the Astronomical Society of the Pacific* **113** (2001) 1420.

PROCEEDINGS OF SCIENCE

SALT Spectropolarimetric Pipeline Comparisons

J. Cooper[a,*] **and B. van Soelen**[a]

[a] *University of the Free State, Physics Dept.,*
PO Box 339, Bloemfontein, 9300

E-mail: Justin.jb78@gmail.com, vanSoelenB@ufs.ac.za

Blazars are active galactic nuclei (AGN) with jets aligned very closely to our line of sight. The optical emission of blazars is often dominated by the polarised, non-thermal emission arising in the jets, with an underlying unpolarised, thermal emission component arising from the host galaxy, dusty torus, and accretion disk components.

Coupled with multi-wavelength observations, optical spectropolarimetry of blazars during both flaring and quiescent states can be used to disentangle the polarised and unpolarised components in their spectral energy distributions, providing better constraints for the non-thermal particle distribution. To this end, spectropolarimetry of blazars during different states of activity was taken with the Southern African Large Telescope (SALT) using the Robert Stobie Spectrograph (RSS). For RSS spectropolarimetry, reductions are performed using the POLSALT pipeline. In order to streamline the spectropolarimetric reductions, we have implemented supplementary interactive tools which provides additional wavelength calibration to improve the accuracy of the wavelength calibration for the O & E beam.

Here we present a brief overview of the tools and the results for Hiltner 652, a spectropolarimetric standard, as well as results for the blazars 3C 279. The reduced, P_Q and P_U, Stokes parameters of Hiltner 652 show no major deviation from previously published results which reassures us that there is no interference introduced into the Stokes parameter calculations when wavelength calibrations are handled by our supplementary tools. The $\sim 6000-9000$ Å range of 3C 279 shows a notable dip in the normalized spectrum during a period of flaring when compared to epochs of enhanced activity. The degree of polarisation for 3C 279 of 13.2%, 9.5%, and 21.2% for the epochs 2017 March 28, 2017 March 31, and 2017 May 17, respectively, remains fairly constant across the observed wavelength ranges while still varying with the blazars' state of quiescence or flaring.

High Energy Astrophysics in Southern Africa 2022 - HEASA2022
28 September - 1 October 2022
Brandfort, South Africa

*Speaker

PoS(HEASA2022)056

1. Introduction

Blazars are a radio-loud sub-set of Active Galactic Nuclei (AGN), where the jet is aligned very closely to our line of sight and whose observed emission varies over time scales from hours to decades [1]. The optical emission observed from blazars is often dominated by the polarised, non-thermal emission arising in the jets, but there is also underlying non-polarised, thermal emission arising from the host galaxy, dusty torus, and accretion disk components [2]. When a blazar varies between flaring and quiescent states, the relative strength of the thermal component to the non-thermal component changes.

The Spectral Energy Distribution (SED) of blazars shows two clear components: a lower energy component produced through leptonic synchrotron processes (covering the radio to the UV/soft X-ray regimes) and a higher energy component (covering the X-ray to the γ-ray regimes) which can be produced through either leptonic or hadronic processes [3]. Optical spectropolarimetry observations, coupled with multi-wavelength observations during both flaring and quiescent states, can be used to disentangle the polarised and non-polarised components in the blazar's SED, providing better constraints for the non-thermal particle distribution [4, 5].

To this end, spectropolarimetric observations of blazars during different states of activity were taken using SALT [6] and the RSS [7]. RSS spectropolarimetry data is reduced with the dedicated POLSALT pipeline [8]. In order to facilitate the blazar observations we have developed supplementary tools to provide a more interactive approach to the wavelength calibration, allowing for improved accuracy for the O & E beam wavelength solutions [9]. Furthermore, spectropolarimetric standards, which were also observed with SALT and the RSS, were reduced alongside the blazar observations to test that the developed tools correctly performed the wavelength calibration. Here we present an overview of the pipeline as well as the preliminary results of a spectropolarimetric standard, namely Hiltner 652, and for the blazar 3C 279.

2. Pipeline Overview

RSS spectropolarimetry data is currently reduced using the POLSALT pipeline [8]. This python package allows for a full reduction from pre-reduction to extracted spectrum, and measured polarisation. However, the wavelength calibration component of the package does not allow for flexibility, nor provide a tool to confirm that the wavelength calibrations of the O & E beams are in agreement. This flexibility is most notably missed when performing calibrations of observations taken using the PG0300 grating[1] due to the very sparse spectral features of the Argon arc lamp used by SALT as well as second order contamination which differs between the O & E beams.

The developed tools work in conjunction with the existing pipeline and provide a method to perform the wavelength calibrations using conventional IRAF [10] methods. Figure 1 shows the typical workflow for data reductions of spectropolarimetric SALT data. Items in blue refer to processing steps completed entirely using POLSALT while items in orange refer to processing steps completed using the developed tools. The single green item refers to the wavelength calibration

[1]This grating has been decommissioned and replaced by the PG0700, and is not available for general use as of November 2022.

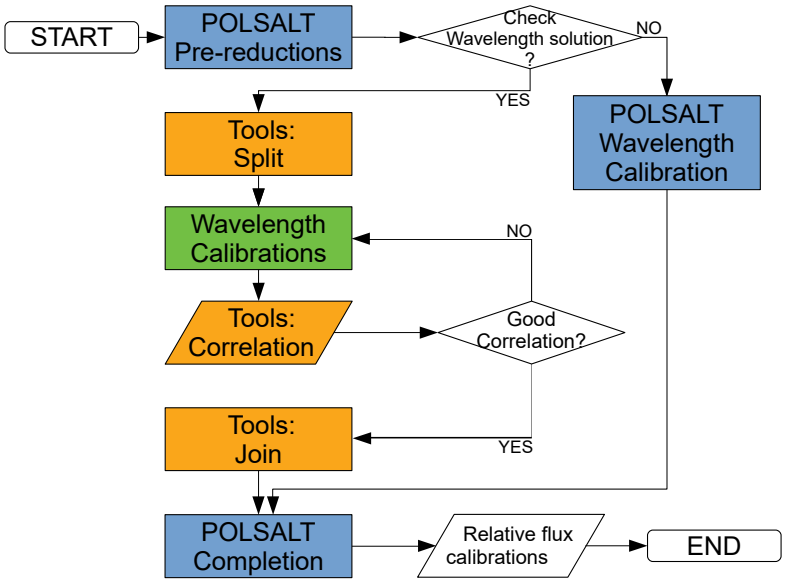

Figure 1: A general workflow for data reductions using a combination of POLSALT and our developed tools.

Source	Observation date	Grating angle (°)	Slit width (")	Exposure time (sec)	Wavelength range (Å)
Hiltner 652	2022 June 10	12.878	2	48.5	3350 - 6440
3C 279	2017 March 28	12.5	1.5	480.8	3300 - 6300
3C 279	2017 March 28	19.625	1.5	480.8	5800 - 8800
3C 279	2017 March 31	12.5	1.5	480.8	3300 - 6300
3C 279	2017 March 31	19.625	1.5	480.8	5800 - 8800
3C 279	2017 May 17	12.5	1.5	720.8	3300 - 6300
3C 279	2017 May 17	19.625	1.5	720.8	5800 - 8800

Table 1: All spectropolarimetric observations taken with SALT and the RSS and used as part of development and testing of the supplementary tools.

done in IRAF. Additional tools to cross-check that the wavelength calibration is consistent across both beams have also been implemented.[2]

3. Observations

The spectropolarimetric observations were taken using the RSS mounted on SALT, in LINEAR mode. The spectropolarimetric standard, Hiltner 652, was observed in 2022 and the blazar 3C 279, was observed in 2017, as summarized in Table 1. All observations presented here were observed using the PG0900 and were reduced following the reduction workflow as described in Figure 1.

[2]A further, in-depth, discussion of the developed tools can be found at [9].

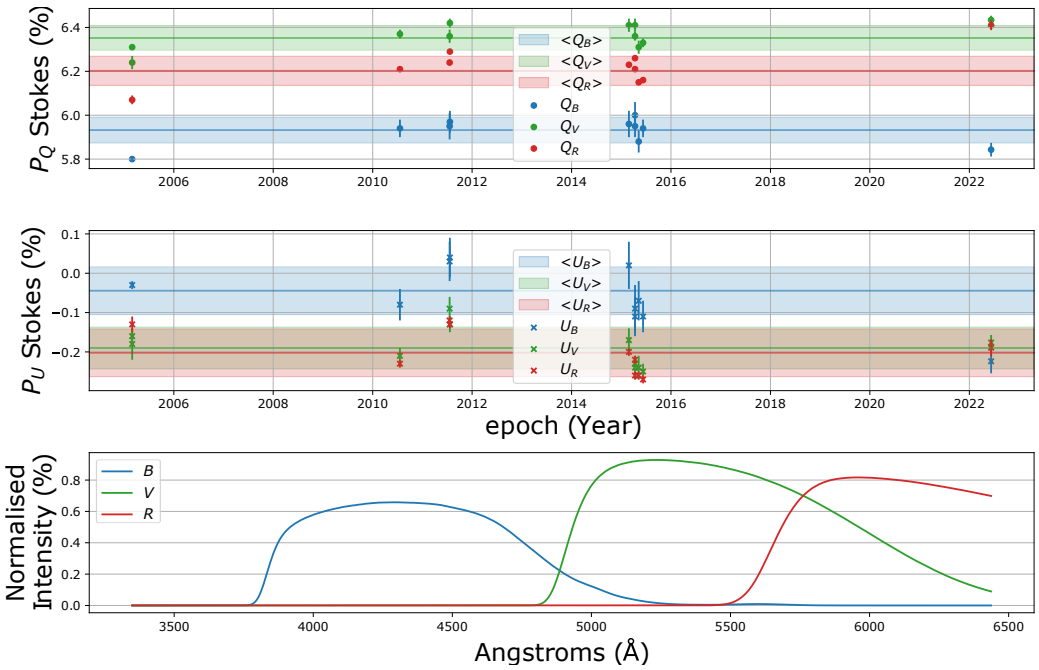

Figure 2: The reduced Q and U Stokes parameters for Hiltner 652 obtained with SALT in 2022 (post 2020) calculated by convolving the spectropolarimetry with the Johnson-Cousins filter pass-bands. This is compared to the published FORS1 [11] and FORS2 [12] observation results (top and middle panels). The average of the FORS reduced Stokes parameters as well as their standard deviation are plotted as the horizontal lines and shaded regions, respectively. Hiltner 652 was observed by SALT in 2022, by FORS1 from 1999 to 2006 (shown as average value at March 2005), and by FORS2 from 2010 to 2016. Finally, the Johnson-Cousins filter pass-band's used by POLSALT to calculate the stokes parameters in the different filters are shown in the bottom panel.

4. Results

The linear Stokes parameters, Q & U, normalized to the total intensity, referred to henceforth as the reduced Stokes parameters, P_Q & P_U, are relative quantities which are used to calculate the polarisation properties, and from which the fraction of linear polarisation may be easily calculated as $P_L = \sqrt{P_Q^2 + P_U^2}$ [13]. The reduced Stokes parameters of Hiltner 652, convolved against the Johnson-Cousins filter pass-bands, as performed by POLSALT, are shown in Figure 2 and are compared against published filtered reduced Stokes parameters obtained with FORS1 [11] and FORS2 [12]. The bottom panel of Figure 2 also shows the filter band-passes for the wavelength range covered by the SALT spectropolarimetry; note that the full R band is not covered by the observation setup.

The reduced Stokes parameters of Hiltner 652 fall within or near the 1σ level of the previously published reduced Stokes parameters over the course of multiple years. This shows that Hiltner 652 is not only a good standard for spectropolarimetric observations but also that using POLSALT with the supplementary wavelength calibrations correctly calculated the Stokes parameters.

The blazar 3C 279 was observed during periods of enhanced and flaring γ-ray activity for energies of $0.1 - 100$ GeV and were sourced from the Fermi Light Curve Repository (Fermi LCR)

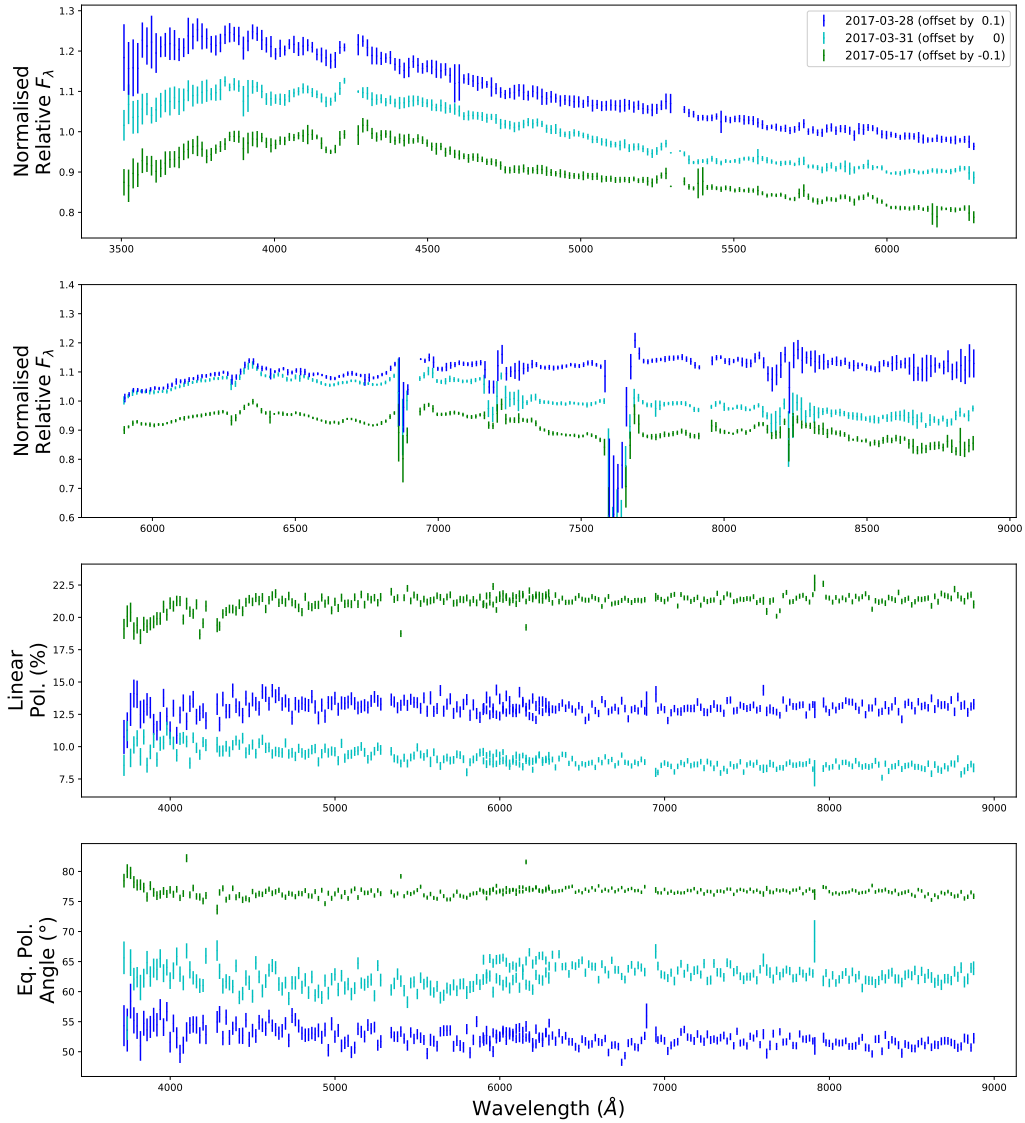

Figure 3: Optical spectropolarimetric observations of 3C 279 during two different periods of flaring. The relative flux calibrated spectra for the grating angles 12.5° (top), observed first at each epoch, and 19.625° (second from top), the degree of polarisation (third from top), and the polarisation angle (bottom).

[14]. 3C 279 was observed at fluxes of 1.58×10^{-6}, 2.87×10^{-6}, and 2.00×10^{-6}ph cm^{-2} s^{-1} as compared to a 'quiescent' median flux of 4.59×10^{-7}ph cm^{-2} s^{-1}.

Figure 3 shows the relative flux calibrated spectra normalized to the spectrum's mean (and offset as indicated), degree of polarisation, and polarisation angle for 3C 279. The relative flux was normalized to better compare how the shape of the spectrum changes during the differing γ-ray states. 3C 279 showed variable flux and polarisation during the three observations, with the polarisation changing by $\sim$ 12.23 % and the angle changing by $\sim$ 24.22°. The relative spectral shape remains similar over all three observations, however the second observation (2017-03-31) appears to show a slightly brighter spectrum in the blue. There is also a relatively good agreement

in the polarisation at the wavelength overlap for the different grating angles. The difference of the polarisation and degree of polarisation is on the order of 0.25 % and 1.25°, respectively.

5. Discussion and Conclusions

In this paper we have considered the observations of a spectropolarimetric standard, Hiltner 652, and a flaring blazar, 3C 279, to test our supplementary tools used for the reduction of spectropolarimetric data obtained with the RSS. The results serve to confirm that the supplementary tools' wavelength reductions, in combination with POLSALT, produces the correct polarisation behavior. Our results for Hiltner 652 agree well with the historical results obtained using the FOcal Reducer and low dispersion Spectrograph (FORS1 and FORS2) mounted at the Very Large Telescope (VLT).

For 3C 279, there is similarly good agreement between the polarisation for the observations taken at two grating angles where the wavelength ranges overlap. Some disagreement is found which may be due to the inherent nature of flaring blazars which cause the polarisation angle to drastically vary and the two observations at different grating angles are not taken simultaneously. Additionally, the disagreement may be due to a lower Signal-to-Noise Ratio (SNR) at the edges of the RSS, which would introduce a larger systematic error. The lower SNR could originate from either blaze effects, or from the extraction of the trace, which is currently limited to a rectangular aperture in the current POLSALT pipeline.

The results show that our supplementary wavelength calibrations for POLSALT increase the efficiency of the data reduction and produce acceptable results. This reduction procedure has been used for the reduction of a number of blazar observations undertaken as part of a long term monitoring campaign [15].

Acknowledgments

All observations taken in this study were obtained using the RSS mounted on SALT under the programme ID 2016-2-LSP-001 (PI DAH Buckley).

References

[1] C.M. Urry and P. Padovani, *Unified Schemes for Radio-Loud Active Galactic Nuclei*, *Publications of the Astronomical Society of the Pacific* **107** (1995) 803 [astro-ph/9506063].

[2] G. Ghisellini, F. Tavecchio, L. Foschini, G. Ghirlanda, L. Maraschi and A. Celotti, *General physical properties of bright Fermi blazars*, *Monthly Notices of the Royal Astronomical Society* **402** (2010) 497 [0909.0932].

[3] M. Böttcher, A. Reimer, K. Sweeney and A. Prakash, *Leptonic and hadronic modeling of fermi-detected blazars*, *The Astrophysical Journal* **768** (2013) 54.

[4] H.M. Schutte, M. Böttcher, J. Barnard, A. Dmytriiev, B. van Soelen, A. Falcone et al., *Modeling the Multi-wavelength Polarization and Spectral Energy Distributions of Blazars*, in *44th COSPAR Scientific Assembly. Held 16-24 July*, vol. 44, p. 1869, July, 2022.

[5] H.M. Schutte, R.J. Britto, M. Böttcher, B. van Soelen, J.P. Marais, A. Kaur et al., *Modeling the spectral energy distributions and spectropolarimetry of blazars—application to 4C+01.02 in 2016-2017**, *The Astrophysical Journal* **925** (2022) 139.

[6] E.B. Burgh, K.H. Nordsieck, H.A. Kobulnicky, T.B. Williams, D. O'Donoghue, M.P. Smith et al., *Prime Focus Imaging Spectrograph for the Southern African Large Telescope: optical design*, in *Instrument Design and Performance for Optical/Infrared Ground-based Telescopes*, M. Iye and A.F.M. Moorwood, eds., vol. 4841 of *Society of Photo-Optical Instrumentation Engineers (SPIE) Conference Series*, pp. 1463–1471, Mar., 2003, DOI.

[7] H.A. Kobulnicky, K.H. Nordsieck, E.B. Burgh, M.P. Smith, J.W. Percival, T.B. Williams et al., *Prime focus imaging spectrograph for the Southern African large telescope: operational modes*, in *Instrument Design and Performance for Optical/Infrared Ground-based Telescopes*, M. Iye and A.F.M. Moorwood, eds., vol. 4841 of *Society of Photo-Optical Instrumentation Engineers (SPIE) Conference Series*, pp. 1634–1644, Mar., 2003, DOI.

[8] S. Crawford and K. Nordsieck, "Polsalt." https://github.com/saltastro/polsalt, 2020.

[9] J. Cooper, B. van Soelen and R. Britto, *Development of tools for SALT/RSS spectropolarimetry reductions: application to the blazar 3C279*, in *High Energy Astrophysics in Southern Africa 2021*, p. 56, May, 2022, DOI.

[10] D. Tody, *The IRAF Data Reduction and Analysis System*, in *Instrumentation in astronomy VI*, D.L. Crawford, ed., vol. 627 of *Society of Photo-Optical Instrumentation Engineers (SPIE) Conference Series*, p. 733, Jan., 1986, DOI.

[11] L. Fossati, S. Bagnulo, E. Mason and E. Landi Degl'Innocenti, *Standard Stars for Linear Polarization Observed with FORS1*, in *The Future of Photometric, Spectrophotometric and Polarimetric Standardization*, C. Sterken, ed., vol. 364 of *Astronomical Society of the Pacific Conference Series*, p. 503, Apr., 2007.

[12] A. Cikota, F. Patat, S. Cikota and T. Faran, *Linear spectropolarimetry of polarimetric standard stars with VLT/FORS2*, *Monthly Notices of the Royal Astronomical Society* **464** (2017) 4146 [1610.00722].

[13] E. Landi Degl'Innocenti, S. Bagnulo and L. Fossati, *Polarimetric Standardization*, in *The Future of Photometric, Spectrophotometric and Polarimetric Standardization*, C. Sterken, ed., vol. 364 of *Astronomical Society of the Pacific Conference Series*, p. 495, Apr., 2007, DOI [astro-ph/0610262].

[14] S. Abdollahi, M. Ajello, L. Baldini, J. Ballet, D. Bastieri, J.B. Gonzalez et al., *The fermi-lat light curve repository*, 2023. 10.48550/ARXIV.2301.01607.

[15] J. Barnard, B. van Soelen, J. Cooper, R. Britto, J.P. Marais, I. van der Westhuizen et al., *Optical Spectropolarimetry Observations of the BL Lac-type object PKS 0537-441 after a period of quiescence*, in *High Energy Astrophysics in Southern Africa 2021*, p. 9, May, 2022, DOI.